Relevance of inhibitory G protein-dependent signaling in prelimbic pyramidal neurons to cocaine-related behavior

A THESIS
SUBMITTED TO THE FACULTY OF
THE UNIVERSITY OF MINNESOTA
BY

Timothy Romans Rose

IN PARTIAL FULFILLMENT OF THE REQUIREMENTS
FOR THE DEGREE OF
DOCTOR OF PHILOSOPHY

Advisor: Kevin Wickman, PhD

January 2022

Acknowledgments

First and foremost, I would like to thank my advisor, Dr. Kevin Wickman. Your guidance, leadership, and utmost excellence in scientific research helped show me what I am capable of. Thank you for the opportunity to deepen my sense of awe and wonder of the brain. I also thank the members of my thesis committee, Dr. Anna Lee, Dr. Sade Spencer, and Dr. Patrick Rothwell for their insights and encouragement these past years.

I am ever grateful for the amazing community found in Dr. Wickman's lab. In my colleague, Dr. Ezequiel Marron, I found unwavering mentorship, friendship, and a selfless drive to help others. Thank you for shaping my worldview and inspiring me to be a better human being. I won't forget the companionship and camaraderie shared with Dr. Baovi Vo, Dr. Allison Anderson, and Margot DeBaker. Our conversations about life, science, career, food, and everything under the sun kept me grounded throughout the years. A deep thank you, also, to the rest of the Wickman lab, including Dr. Megan Tipps, Melody Truong, Eric Mitten, Michael Woods, Shirley Luo, Bushra Haider, Courtney Wright, and Mehrsa Zahiremami. Your diverse perspectives, as well as technical and emotional support, brought color into my life for the past 5 years.

To my friends and family, I thank you all for the years of encouragement and comfort you have given to me. Special thanks to my amazing wife (Amanda Low), who walked with me through the ups and downs, as well as some of the most challenging moments faced. I am grateful for the ever-present love and support from my parents and parents-in-law (Marlene Rose, John Rose, Boon Teck Low, Siew Ping Lim).

Lastly, I would like to thank my funding sources which supported this work. This includes grants from the National Institute of Health (NIH) to TRR (DA007234), KW (DA034696, AA027544, MH107399), and MET (AA025978), a Wallin Neuroscience

Discovery Fund Award to KW, and University of Minnesota Doctoral Dissertation Fellowships to TRR and BNV.

Abstract

Drugs of abuse share the ability to enhance DA levels within the mesocorticolimbic system. This increased DA neurotransmission triggers persistent adaptations throughout the brain that are believed to underlie the detrimental behaviors that define addiction. For example, chronic cocaine exposure causes a suppression of inhibitory G protein-dependent signaling mediated by the $GABA_B$ receptor ($GABA_BR$) and G protein-gated inwardly rectifying K^+ (GIRK/Kir3) channel in pyramidal neurons of the prelimbic cortex (PL), a cell population important for executive function. As GIRK-dependent signaling is crucial for tempering excitatory input in neurons, the loss of this “inhibitory brake" may drive neuronal hyperexcitability and foster the development of addiction-related behavior. The goal of this thesis is to examine the contribution of GIRK channels in PL pyramidal neurons to behaviors that may be relevant to addiction, and to further understand the regulatory mechanisms that control inhibitory signaling mediated by $GABA_BRs$ and GIRK channels.

To test the prediction that a loss of GIRK channel activity in pyramidal neurons promotes neuronal hyperexcitability, we employed a viral genetic approach to selectively ablate a critical GIRK channel subunit (GIRK1) in PL pyramidal neurons. GIRK channel ablation blunted $GABA_BR$-GIRK currents in, and elevated the excitability of, PL pyramidal neurons – electrophysiological outcomes that closely resemble the effects of repeated cocaine exposure. To examine the behavioral consequences of elevated PL pyramidal neuron excitability, we used complementary viral approaches to model the impact of acute (chemogenetic) and persistent (GIRK channel ablation) excitation of PL pyramidal neurons on PL-dependent behaviors, including acute cocaine-induced locomotion and trace fear conditioning. We found that GIRK channel ablation enhanced the motor-

stimulatory effect of cocaine, but did not impact baseline activity or trace fear learning. In contrast, selective chemogenetic excitation of PL pyramidal neurons increased baseline and cocaine-induced activity and disrupted trace fear learning. These effects were mirrored in male mice by selective excitation of PL pyramidal neurons projecting to the ventral tegmental area, a brain region important for reward behavior. Collectively, these data show that manipulations enhancing the excitability of PL pyramidal neurons, and specifically those projecting to the VTA, recapitulate behavioral hallmarks of repeated cocaine exposure in mice.

Withdrawal from prolonged cocaine exposure has been correlated with negative affective behaviors, as well as formation of persistent drug-related memories that drive drug-seeking behavior. Therefore, we next modeled the impact of viral-mediated GIRK, or $GABA_BR$, ablation in PL pyramidal neurons on mood-related behaviors and cocaine conditioned place preference (CPP). While GIRK ablation did not impact anxiety- or depression-related behavior, the manipulation impaired the extinction of cocaine CPP in male mice. In contrast, $GABA_BR$ ablation was without effect. Since an impairment in extinction may result in prolonged drug-seeking behavior, we next assessed whether strengthening GIRK channel activity could enhance the extinction of cocaine CPP. As predicted, overexpression of GIRK2 in PL pyramidal neurons facilitated extinction of cocaine CPP in male mice. Together, these findings highlight a unique, sex-specific role for GIRK channels in PL pyramidal neurons in tempering cocaine conditioned responding.

Despite established links between GIRK channel plasticity and disease, the basic mechanisms that regulate GIRK-dependent signaling in PL pyramidal neurons are not fully understood. One important regulator of GIRK channel activity is the regulator of G protein signaling (RGS) protein, and specifically RGS6 and RGS7 (RGS6/7). RGS6/7 facilitate the termination of inhibitory G protein-dependent signaling, and are thus critical for

maintaining the high temporal resolution of $GABA_BR$-GIRK signaling. While both RGS6/7 are expressed in the PFC, little is known about their functional roles in the PL. After establishing that RGS6/7 are coexpressed in most PL pyramidal neurons, we next examined their contribution to synaptically-evoked and baclofen-activated $GABA_BR$-GIRK currents using constitutive $RGS6^{-/-}$ and $RGS7^{-/-}$ mice. We found that RGS6/7 differentially regulate GIRK channel activity; RGS6 regulates the amplitude, while RGS7 regulates the kinetics and sensitivity, of GIRK-dependent signaling. These shed light on the functional compartmentalization mechanisms that are critical for ensuring high temporal resolution of neuronal inhibitory G protein-dependent signaling.

Overall, the work in this thesis suggests that GIRK-dependent signaling in PL pyramidal neurons represents an “inhibitory brake” on cellular excitability that is critical for excitation/inhibition balance and optimal behavioral function. Although the weakening of this inhibition following repeated cocaine exposure may promote neuronal hyperexcitability and addiction-related behavior, therapeutic interventions that restore inhibitory tone may confer resilience to these effects.

Table of Contents

List of Figures

List of Abbreviations

AC	Adenylyl cyclase
AKAP	A-kinase anchoring protein
AMPK	AMP-activated protein kinase
ACC	Anterior cingulate cortex
BLA	Basolateral amygdala
BK	Big conductance Ca^{2+}-activated K^+
CaMKII	Ca^{2+}/calmodulin-dependent protein kinase II
CR	Calretinin
ChR2	Channelrhodopsin-2
CCK	Cholecystokinin
CNO	Clozapine-N-oxide
CPP	Conditioned place preference
cAMP	Cyclic AMP
DA	Dopamine
D1R	Dopamine 1 receptor
D2R	Dopamine 2 receptor
DAT	Dopamine transporter
GPR158	G protein-coupled receptor 158
GPCR	G protein-coupled receptors
GIRK	G protein-gated inwardly rectifying K^+
GB1	$GABA_{B1}$
GB1b	$GABA_{B1b}$
GB1a	$GABA_{B1a}$
GB2	$GABA_{B2}$
GAD	Glutamate decarboxylase
GRK	GPCR kinase
GAP	GTPase-accelerating protein
IL	Infralimbic cortex
KCTD	K^+ channel tetramerization domain
LTP	Long-term potentiation
MSNs	Medium spiny neurons
mGluR1	Metabotropic glutamate receptor 1
MIB2	Mind bomb-2
NEM	N-ethylmaleimide
NMDAR	N-methyl-D-aspartate receptor
NET	Norepinephrine transporter
NAc	Nucleus accumbens

OFC	Orbitofrontal cortex
PV	Parvalbumin
PTX	Pertussis toxin
PDZ	Postsynaptic density 95/disc-large/zona occludens
PFC	Prefrontal cortex
PKA	Protein kinase A
PKC	Protein kinase C
PP2A	Protein phosphatase 2A
RGS	Regulator of G protein signaling
SA	Self-administration
SERT	Serotonin transporter
7TM	Seven-transmembrane
SST	Somatostatin
SNX27	Sorting nexin 27
SUD	Substance use disorder
VIP	Vasoactive intestinal peptide
VTA	Ventral tegmental area
VFT	Venus flytrap
VMAT2	Vesicular monoamine transporter 2
VGCC	Voltage-gated Ca^{2+} channels

Chapter 1: Introduction

Chapter 1 contains work that was previously published in Current Topics in Behavioral Neurosciences in 2020.

Rose TR & Wickman K. Mechanisms and regulation of neuronal $GABA_B$ receptor-dependent signaling. *Curr Top Behav Neurosci*. 2020. PMID: 32808092.

1.1 Addiction: Clinical manifestation

In the United States, approximately 8-10% of people 12 years of age or older are addicted to drugs [1]. Drug abuse places a tremendous financial burden on society, costing Americans more than $740 billion annually from increased healthcare costs, lost productivity, and crime [2]. Substance use disorder (SUD) is a complex mental disorder that is characterized by chronic and compulsive drug seeking despite harmful consequences. SUDs exist across a spectrum, ranging from mild to severe depending on the number of diagnostic criteria met. “Addiction” describes the most severe form of a SUD.

The symptoms associated with SUDs fall into four major categories: impaired control, social impairment, risky use, and pharmacological criteria [3]. Impaired control includes cognitive deficits in decision making and behavioral inhibition, in addition to craving, an intense urge to consume the drug [3]. Pharmacological criteria include tolerance, which is defined by a diminished effect with continued use of the same dose of drug [3]. Tolerance can often lead to an escalation of drug consumption (e.g., binge) to achieve the desired effect. Another pharmacological criteria is withdrawal, which describes a set of negative emotional states and physical symptoms that occur following cessation from heavy drug use [3]. Substances are often taken to relieve or avoid the effects of withdrawal.

Addiction can be represented as a three-stage cycle: binge/intoxication, withdrawal/negative affect, and preoccupation/anticipation [1,3]. Symptoms grow more severe as an individual continues their substance use, in part due to profound changes in brain function that impair inhibitory control.

Binge/Intoxication is the first stage where an individual consumes a substance and experiences its rewarding effects. Addictive drugs engage the reward circuitry to evoke feelings of pleasure, which are positively reinforcing and promote repeated drug use. As drug use continues, the rewarding feelings initially tied to consumption shift to become associated with environmental stimuli that precede, or predict, consumption [1]. Over time, exposure to these drug-associated cues begins to trigger an intense desire, or urge, to take the drug. Tolerance to the drug's initial effects further encourages higher levels of drug consumption.

Withdrawal/negative affect is the second stage where an individual experiences negative emotional states and symptoms of physical illness when they stop taking the drug. These negative feelings during withdrawal are believed to be caused by 1) a reduced sensitivity of the brain's reward system to natural rewards and 2) an increased sensitivity of the brain's stress system to stressful stimuli. The desire to escape negative withdrawal symptoms can be a powerful motivator of continued drug use.

Preoccupation/anticipation is the third stage where an individual seeks substances again after a period of abstinence. This stage is characterized by dysfunction of the brain's prefrontal cortex (PFC), or the region that controls executive function – the ability to make decisions and regulate one's emotions, thoughts, and actions. Impaired executive function weakens the ability of an individual to resist strong urges to take drugs, and to voluntarily reduce drug-taking behavior. When combined with exposure to drug

cues or stressful environments, this often results in the resumption of drug-seeking behavior (i.e., relapse), and the cycle of addiction continues.

Although addiction can be devastating to those afflicted, only a minority of individuals who use drugs will ultimately become addicted. Susceptibility differs because people differ in their vulnerability to various genetic, environmental, and social factors. Risk factors for addiction include family history, early exposure to drug use, exposure to highly stressful environments, and mental illness (e.g., anxiety, depression). It is estimated that 10% of those that use addictive drugs will develop the most severe characteristics of addiction [1].

Although there is no cure for addiction, it can be managed through treatment, allowing individuals to stop using drugs, resume productive lives, and avoid relapse. Treatment often involves a combination of behavioral therapy and medication. Behavioral therapy involves strategies that are designed to enhance the salience of natural rewards, manage negative emotional states, improve executive function, and avoid drug-associated environmental cues [1]. Addiction medications can be indispensable in helping to control craving or withdrawal symptoms, or in countering the intoxicating effects of drugs. Medications are generally specific for the type of substance consumed: methadone, buprenorphine, and naltrexone can help manage opioid-use disorder [4]; naltrexone, acamprosate, and disulfiram can help treat alcohol dependence [5]; nicotine replacement products, bupropion, and varenicline can help treat nicotine addiction [6]. Despite established evidence of their success, these current addiction medications still lack consistent and long-term efficacy, and/or have undesirable side effects [3,7]. Furthermore, for those with addiction to psychostimulants, such as cocaine and methamphetamine, there are no FDA-approved medications. The current lack of effective treatments underlines the importance of understanding the biological basis of addiction.

1.2 Addiction: Preclinical models

Preclinical (i.e., animal) models of addiction are designed to recapitulate core features of human addiction. Such features include impaired executive function, withdrawal, behavioral sensitization in response to repeated drug exposure, cue-induced drug-seeking behavior, craving, relapse, and persistent drug-taking despite negative consequences (i.e., compulsive drug consumption). These animal models of addiction are crucial for elucidating the neurobiological mechanisms that underlie addiction-related behaviors, and for generating insights that drive the development of safer and more effective therapies.

1.2.1 Locomotor activity and behavioral sensitization

Exposure to many different classes of drugs of abuse (e.g., psychostimulants, opioids, nicotine, ethanol) results in a characteristic increase in locomotor activity that is caused by increased dopamine (DA) levels in the striatum [8]. Subsequent exposures to the same drug, or in some cases a different drug, lead to a potentiation of the locomotor response, a phenomenon known as “sensitization” or “cross-sensitization,” respectively. Although the face validity of behavioral sensitization in humans is challenging to demonstrate [8], this model offers a platform for studying common neurobiological pathways that are engaged by repeated exposure to many different drugs of abuse. While this model lacks the volitional aspect of drug-taking, experimenter-administered drug delivery allows for precise control over the dose of drug delivered, and the ability to rapidly induce sensitization with just a few injections makes this a reliable, high-throughput approach.

1.2.2 Conditioned place preference

Conditioned place preference (CPP) is commonly used to measure the motivational or rewarding properties of drugs of abuse. In the standard CPP paradigm, rodents are exposed to a chamber with two distinct contexts, often distinguished by tactile (e.g., bar or wire mesh flooring) and visual (e.g., patterns on walls) cues. After assessing a baseline preference for either context, the animals are given an injection with vehicle (e.g., saline) and confined to one context. Several hours later or the following day, they are given a drug injection and confined to the other context. After a few pairings, the rodents are then allowed to freely explore either context and the time spent in each is measured. Increased time spent in the drug-paired context, as compared to their baseline preference, serves as a measure of the rewarding valence of the drug. Other variants of this task incorporate extinction and reinstatement components. In extinction studies, the association between the context and the rewarding stimulus is diminished/overwritten by repeatedly pairing the context with no drug treatment. Thus, extinction learning results in a marked reduction in placed preference. Following extinction, the place preference can be reinstated by exposure to a low dose of drug or stress (e.g., restraint stress, footshock). Importantly, this reinstatement of conditioned place preference shares characteristics with relapse.

Similar to behavioral sensitization, the development of a drug-induced CPP is widely observed across different drugs of abuse [8]. The ability to test for a drug-induced place preference while the animal is in a “drug-free” state provides for cleaner assessment of the rewarding valence and enduring neurobiological changes induced by prior drug exposure. Taken together, the CPP paradigm serves as a useful model of cue-induced drug-seeking behavior observed in human patients with addiction.

1.2.3 Self-administration

Self-administration (SA) is considered the gold standard preclinical model for assessing the rewarding and reinforcing properties of drugs of abuse. In SA sessions, a rodent performs an action (e.g., lever press or nose port entry) in order to receive an intravenous infusion of a drug. Rodents will quickly increase their drug-taking until they reach a steady-state level of drug consumption. Similar to the CPP paradigm, drug SA can be extinguished and then reinstated by exposure to low dose of drug, drug-paired cue (e.g., light or sound that predicts drug delivery), or stress. The motivation of an animal to work for a drug can also be assessed by progressively increasing the number of responses required to receive the drug, which yields the "break point," or maximum number of responses an animal makes to receive the reward. Other iterations of SA pair drug reward with a punishment (e.g., footshock) to assess continued drug-taking despite negative consequences. Overall, the SA paradigm models many features of human addiction, including binge drug consumption, increased motivation for drug-taking behavior, compulsive drug consumption, and relapse.

1.2.4 Mesocorticolimbic dopamine system

The mesocorticolimbic dopamine (DA) system, also known as the "reward system," plays an integral role in reinforcing patterns of behavior that are necessary for obtaining rewards. This system mediates the rewarding and reinforcing properties of natural rewards (e.g., food, water, sex), as well as drugs of abuse. Addictive drugs exert their rewarding and reinforcing effects through activation of the mesocorticolimbic DA system [9]. While many brain regions are involved in reward processing, three important areas include the ventral tegmental area (VTA), nucleus accumbens (NAc), and prefrontal cortex (PFC).

1.2.5 Ventral tegmental area

The VTA is a heterogeneous midbrain structure that plays a fundamental role in motivational processing through its connections with different brain regions. Afferent inputs to the VTA include the striatum, dorsal raphe nucleus, lateral hypothalamus, and PFC, among others [10-12]. The VTA also sends efferent projections to limbic structures, such as the NAc, amygdala, and hippocampus, as well as cortical structures including the PFC, cingulate cortex, and orbitofrontal cortex [11,12]. The diversity of VTA inputs and outputs shape behavior by regulating aspects of reward, cognition, movement, and aversion [11,13].

The VTA contains multiple cell types, including dopaminergic (65%), GABAergic (30%), and glutamatergic neurons (5%) [14,15]. These neuron populations can participate in local microcircuits together, as well as project to distal brain regions [15,16]. Among these three subpopulations, VTA DA neurons stand out for their central role in reward-related behavior. Indeed, VTA DA neuron activity is critical for reward, reinforcement, motivation, and salience attribution [9]. However, DA neurons have also been implicated in aversion [14]. This behavioral divergence can be at least in part explained by the presence of distinct VTA DA neuron subpopulations. For example, activation of the mesolimbic dopamine pathway (i.e., lateral DA neurons that project to the lateral NAc shell) can drive reward and reinforcement, while the mesocortical dopamine pathway (i.e., medial DA neurons that project to the PFC) has been linked with aversion, among other important functions [9,17]. In addition to differences in projection target, DA neurons can also differ in their firing patterns and expression of certain receptors and ion channels [17]. Such attributes further contribute to the diversity of DA neuron subtypes and their functional roles.

1.2.6 Nucleus accumbens

The NAc is a limbic structure that can be divided into two subregions (shell and core) that possess overlapping but distinct functions and connectivities. The NAc shell plays an important role in positive reinforcement and incentive salience and is thought to govern immediate responding to salient stimuli [18,19]. The NAc core integrates motivation with motor action and is believed to control conditioned reinforcement [18,19]. The shell receives dopaminergic input from the VTA and glutamatergic input from the infralimbic subregion of the PFC and the medial orbitofrontal cortex, while the core receives glutamatergic input from the prelimbic subregion of the PFC [18]. Both the shell and core also receive input from the basolateral amygdala, ventral hippocampus, mediodorsal thalamus, and dorsal raphe [19]. With regards to efferent output, the shell primarily projects to the VTA and ventromedial ventral pallidum, while the core projects to the substantia nigra and dorsolateral ventral pallidum [18].

The vast majority (95%) of neurons in the NAc are GABAergic medium spiny neurons (MSNs), while the remainder are local interneurons [20]. MSNs can be divided into two types based on dopamine receptor expression, releasable peptides, and projection targets [21]. Dopamine 1 receptor (D_1R)-, dynorphin-, and substance P-expressing MSNs, also known as direct pathway MSNs, directly project to the midbrain, including the SN pars reticulata and VTA. Dopamine 2 receptor (D_2R)- and enkephalin-expressing MSNs, form the indirect pathway, projecting to the ventral pallidum. However, this dichotomy is complicated by the fact that a small portion of MSNs express both D_1Rs and D_2Rs, and some D_1R MSNs project to the ventral pallidum [22]. Nonetheless, activation of the direct pathway generally stimulates reward-related behaviors while activation of the indirect pathway often promotes aversive behaviors [19,20]. By integrating dopaminergic signaling, through D_1Rs or D_2Rs, with glutamatergic, GABAergic, and other neuromodulatory inputs from a variety of brain regions [23], NAc MSNs are well positioned to transform emotional

and environmental information into behavioral action. Importantly, changes in glutamatergic signaling in the NAc, particularly in MSNs, have been observed following repeated exposure to drugs of abuse, and these adaptations are thought to contribute to the development of pathogenic drug-seeking behavior observed in addiction [23,24].

1.2.7 Prefrontal cortex

The PFC is a neocortical brain region that is most developed in primates – animals known for their diverse and flexible behavior. Its high level of connectivity with cortical and subcortical brain regions help to facilitate its coordination of a wide range of neural processes related to cognition, motivation, and emotional regulation [25]. Neurons in the rodent PFC are organized within five cellular layers – glutamatergic pyramidal neurons in superficial layers 2 and 3 (layers 2/3) and deep layers 5 and 6 (layer 5/6) make up ~85% of neurons and (primarily GABAergic) interneurons the remaining ~15% [26]. Superficial layers 2/3 receive most of the PFC inputs, and in turn, provide output to deeper layers 5/6. Pyramidal neurons in layers 5/6 represent the primary output neurons in the PFC, sending efferent projections to various cortical and subcortical regions [26,27]. Although the PFC contains multiple subregions – including the prelimbic cortex (PL), infralimbic cortex (IL), anterior cingulate cortex (ACC), and orbitofrontal cortex (OFC) – most of the following discussion will focus on the PL as it pertains to my thesis research.

Glutamatergic pyramidal neurons

Pyramidal neurons are the most prevalent cell type in the PL (~85%) [26]. They are often identified by characteristic morphological and electrophysiological features, including a pyramidal-shaped soma, a long apical dendrite, lack of spontaneous activity, and large size (apparent capacitance of > 100 pF) [28]. They can be further distinguished

by the presence of Ca^{2+}/calmodulin-dependent protein kinase II (CaMKII) [29], a protein that is important for neural plasticity [30]. Indeed, transgenic CaMKIICre(+) mice have been utilized to manipulate pyramidal neurons in the PL [31].

Despite possessing some shared morphological and electrophysiological features, PL pyramidal neurons have been increasingly found to be heterogeneous, differing with respect to other morphological and electrophysiological properties, the expression of receptors, and projection targets [27,32,33]. For example, PL pyramidal neurons that project to the VTA, NAc, or basolateral amygdala (BLA) are distinct subpopulations that differ in their cortical layer distribution and molecular expression patterns [34]. Distinct firing patterns [35,36] and differential expression of D_1Rs or D_2Rs [37] have also been observed among pyramidal neurons. Further adding to the diversity of PL pyramidal neuron function is a wide variety of afferent and local input. The most prominent afferent inputs come from the ventral hippocampus, amygdala, midline thalamus, VTA, raphe nuclei, and several cortical regions [38]. Efferent projections from the PL extend to the NAc, midline thalamus, BLA, insular cortex, claustrum, raphe nuclei, and VTA, among others [12,39].

The diversity and extensive connectivity of PL pyramidal neurons enables them to regulate a broad spectrum of behaviors related to cognition, reward, aversion, and affect [27,40-42]. Attempts at determining the role that the PL plays in reward-related behavior have relied on loss-of-function (lesioning or inactivating pyramidal neurons) or gain-of-function (exciting pyramidal neurons) approaches. Other studies record pyramidal neuron activity or glutamate release during behavior to infer the role of these neurons in behavioral processes. From these studies it is clear that PL pyramidal neurons encode relevant cues, contexts, and behavioral choices to guide reward-seeking behavior [36,43-45]. Indeed, activity in these neurons is necessary for cue-induced drug-seeking [46,47], particularly in neurons that project to the NAc core [48,49]. PL pyramidal neurons also play a role in the development

of locomotor sensitization induced by psychostimulants [50]. Interestingly, while some pyramidal neurons encode rewarding experiences, others encode aversive experiences, or even both rewarding and aversive experiences [51]. These data suggest that the valence and behaviors associated with pyramidal neurons are likely to be region- and subpopulation-specific.

GABAergic interneurons

Local GABA neurons make up roughly ~15% of neurons in the PL [26]. They can be identified by a round-shaped soma, small size (apparent capacitance of < 100 pF), and specific firing characteristics [52]. They can be further distinguished by the expression of glutamate decarboxylase (GAD), the enzyme responsible for converting glutamate into GABA. Indeed, GAD-GFP and GADCre mouse lines have been widely used to target and manipulate forebrain GABA neurons [31].

PL GABA neurons synapse onto adjacent pyramidal neurons to provide a major source of inhibitory input. This GABAergic neurotransmission tempers the excitability of pyramidal neurons and plays a fundamental role in excitation/inhibition balance. By integrating a variety of afferent inputs and providing inhibitory output to pyramidal neurons, GABA neurons orchestrate the firing patterns of pyramidal neuron ensembles to guide behavior [53-55].

Multiple PL GABA neuron subtypes have been classified based on their expression of molecular markers, including, parvalbumin (PV), somatostatin (SST), vasoactive intestinal peptide (VIP), cholecystokinin (CCK), and calretinin (CR) [27,51]. These GABA neuron subtypes differ in their laminar organization, afferent inputs, innervation of local pyramidal and/or GABA neurons, as well as their influence on behavior [53,56]. For example, PV neurons provide powerful inhibitory input to pyramidal neurons by synapsing in the

perisomatic region, while SST neurons preferentially innervate more distal dendrites [53]. In contrast, VIP neurons target both PV and SST neurons, thus disinhibiting pyramidal neurons. The diversity of GABA neuron subtypes and local microcircuits imparts computational complexity that is required for optimal PL performance.

1.3 Mechanisms of action of drugs of abuse

Although drugs of abuse vary in their chemical structure and molecular target(s) within the brain, they share the ability to enhance DA neurotransmission throughout the mesocorticolimbic system [9]. At first, the initial rewarding effects of drug exposure are associated with increased DA levels. Over time, however, prolonged drug use begins to reinforce environmental cues that predict the drug experience and trigger neuroadaptations in glutamatergic signaling that, in vulnerable individuals, may lead to addiction.

One class of drugs that have been well studied for their addictive properties are the psychostimulants, such as cocaine, methamphetamine and amphetamine. These drugs increase DA levels by disrupting the function of the dopamine transporter (DAT) and/or the vesicular monoamine transporter 2 (VMAT2). Cocaine, for example, directly blocks DAT, thereby leading to an accumulation of DA in downstream brain regions of the VTA [9]. While the motor-activating and rewarding properties of cocaine are largely attributable to the blockage of DAT [57], cocaine can also inhibit the serotonin transporter (SERT) and norepinephrine transporter (NET). In humans, cocaine is typically consumed through nasal insufflation (i.e., snorting), smoking, or by intravenous injection. The time course and level of cocaine concentrations in the plasma and brain, as well as the drug's subjective effects, depend on the route of administration [58]. Interestingly, the subjective "high" feeling typically precedes peak cocaine concentrations in the brain [58]. Once

consumed, cocaine is metabolized by hepatic and plasma enzymes, or eliminated through urination [59].

1.4 Inhibitory G protein receptor signaling

Addictive drugs alter communication between brain regions and cell types that make up the mesocorticolimbic system. Neuronal communication is initiated by electrical activity and calcium-induced release of neurotransmitters from presynaptic terminals. These neurotransmitters then bind to, and activate, receptors present on the postsynaptic neuron. Activation of ionotropic receptors (i.e., ion channels) can induce rapid excitatory or inhibitory effects mediated by the flow of ions across the membrane. Activation of metabotropic receptors (i.e., G protein-coupled receptors; GPCR) results in sustained excitatory, inhibitory, or modulatory effects that are mediated by the actions of second messengers (i.e., G proteins) on downstream effector proteins and ion channels. The integration of these signals determines whether a neuron will generate an action potential, release neurotransmitters, and thereby exert an influence on other neurons. While the actions of each of these receptors are essential for optimal neuronal communication and behavioral function, my dissertation focuses on inhibitory G protein signaling, and how it relates to drug addiction.

1.5 Inhibitory G protein-coupled receptors

GPCRs transduce extracellular signals (e.g., neurotransmitter binding) to intracellular signaling through heterotrimeric G proteins Gα, Gβ, and Gγ. The binding of a ligand to the receptor triggers a conformational change that promotes the exchange of GDP for GTP on Gα and the release of Gα and Gβγ. Gα and Gβγ are then free to modulate the activity of downstream effector enzymes and ion channels. GPCRs are classified

based on which Gα family they couple to, of which there are four: $G\alpha_s$, $G\alpha_{i/o}$, $G\alpha_q$, and $G\alpha_{12/13}$. In general, $G\alpha_s$ and $G\alpha_{i/o}$ bidirectionally modulate the activity of adenylyl cyclase, $G\alpha_q$ activates phospholipase C-β to release calcium from the endoplasmic reticulum, while $G\alpha_{12/13}$ activates small GTPase families [60]. Through their modulation of various effectors, GCPRs help regulate neuronal excitability, synaptic plasticity, and neurotransmitter release. The focus of my thesis research is on inhibitory signaling mediated by one specific type of GPCR, the $GABA_B$ receptor ($GABA_BRs$).

1.6 $GABA_BR$: Structure, function, regulation

1.6.1 Structure

Evidence from biochemical, electrophysiological, and behavioral studies have demonstrated that the $GABA_BR$ is an obligate heterodimer composed of the $GABA_{B1}$ (GB1) and $GABA_{B2}$ (GB2) subunits [61]. Crystal structures of $GABA_BR$ subunit domains have revealed that both GB1 and GB2 contain an extracellular Venus flytrap (VFT) domain, a seven-transmembrane (7TM) domain, and an intracellular carboxyl (C)-terminal domain [62]. The VFT domain of GB1 contains the orthosteric binding site for GABA, as well as other agonists and antagonists. While the GB2 VFT cannot bind ligands, it does enhance the agonist affinity for the GB1 VFT through direct interactions that stabilize the agonist-bound state [62]. The 7TM domain of GB2 facilitates coupling between the receptor and G proteins. While GB1 is not required for G protein coupling, the GB1 7TM domain enhances coupling efficiency [61]. The C-terminal domains of both subunits form a coiled-coil structure that facilitates heterodimerization and surface expression of $GABA_BRs$ [63].

1.6.2 Alternative splicing

The expression of multiple GB1 isoforms contributes to the diverse functions of $GABA_BRs$. There are 14 known isoforms of GB1 (GB1a-n), which can be generated by differential transcription or splicing of the mRNA [63]. GB1a and GB1b are the most abundant isoforms in the brain, and are the only isoforms that are highly conserved across vertebrate species [64]. Each isoform differs slightly in its spatial and temporal expression pattern in the rodent brain, but to a greater degree in subcellular localization. In general, GB1a is expressed presynaptically in axon terminals, while GB1b is expressed postsynaptically in dendritic spines [65]. However, GB1a can also be expressed postsynaptically in dendritic branches, although it is mostly excluded from dendritic spines [65,66]. In line with their distinct subcellular distribution, studies in hippocampal neurons from $GB1a^{-/-}$ and $GB1b^{-/-}$ mice revealed that presynaptic (GB1a/GB2) $GABA_BRs$ mediate inhibition of neurotransmitter release, while postsynaptic (predominantly GB1b/GB2) $GABA_BRs$ generate slow inhibitory postsynaptic currents [66].

GB1a is longer than GB1b (961 vs 841aa), as it contains two N-terminal protein interaction motifs, known as sushi domains [67]. Sushi domains are highly conserved among species, are present in several GPCRs, and mediate protein interactions in a wide array of adhesion proteins [68,69]. Interestingly, the two GB1a sushi domains (SD1 & SD2) are structurally distinct [70], which may help to explain the different protein interactions observed between domains [71,72]. In addition to stabilizing GB1a/GB2 receptors at the cell surface [73], the GB1a sushi domains are necessary and sufficient for axonal transport. Sushi domain mutations prevent GB1a from reaching axon terminals, and fusing the sushi domains to metabotropic glutamate receptor 1 (mGluR1) enables the somatodendritic protein to traffic down axons [74]. Thus, sushi domains act as axonal targeting signals, interacting with proteins to facilitate presynaptic transport.

1.6.3 Oligomerization

At the cell surface, $GABA_BRs$ can exist in an equilibrium between heterodimers, tetramers, and higher-order oligomers in both heterologous systems and native neurons [75]. $GABA_BR$ heterodimers assemble by random collision into higher-order oligomers through weak and transient GB1-GB1 interactions [76]. Destabilizing oligomers using competitors of the GB1-GB1 interaction, or a GB1 mutant, revealed different G protein coupling efficiencies depending on the oligomeric state of the $GABA_BR$ – suggesting a negative functional cooperativity among heterodimers within larger oligomers [77].

1.6.4 Neuronal $GABA_BR$-dependent signaling

$GABA_BRs$ are expressed throughout the brain and are positioned within neurons at both postsynaptic (dendritic spines & shafts) and presynaptic (axon terminals) sites [78]. In general, $GABA_BR$ activation inhibits neurons through G protein-dependent modulation of enzymes and ion channels. For example, activation of postsynaptic $GABA_BRs$ evokes a slow hyperpolarization of the postsynaptic membrane via activation of G protein-gated inwardly rectifying K^+ (Kir3/GIRK) channels [79]. Activation of presynaptic $GABA_BRs$ suppresses neurotransmitter release primarily through inhibition of voltage-gated Ca^{2+} channels (VGCC) and reduced Ca^{2+} influx [75]. Presynaptic $GABA_BRs$ function as either autoreceptors on GABAergic terminals, or heteroreceptors on terminals releasing other neurotransmitters. Thus, presynaptic $GABA_BRs$ may be activated by GABA released from GABAergic terminals, or spillover of GABA from neighboring terminals, to suppress neurotransmitter release [75]. By blocking the release of different types of neurotransmitters, $GABA_BRs$ can have excitatory or inhibitory influences at the circuit level.

1.6.5 GABABR coupling to G proteins

Heterotrimeric G proteins mediate signaling by coupling GPCRs to enzymes, ion channels, and other effector proteins. The heterotrimeric G protein is comprised of three distinct subunits (α,β,γ); 35 subunits (16 Gα, 5 Gβ, 14 Gγ) have been identified in humans [80]. Inactive heterotrimeric G proteins (Gαβγ) associate with $GABA_BRs$ through direct interactions with GB2 and K^+ channel tetramerization domain (KCTD) proteins [81]. Selective coupling of heterotrimeric G proteins to $GABA_BRs$ is primarily determined by the Gα subunit. Studies using *N*-ethylmaleimide (NEM), antisense knockdown, and G protein toxins helped reveal that prototypical $GABA_BRs$ couple to pertussis toxin (PTX)-sensitive G proteins, including most members of the $G\alpha_i$ and $G\alpha_o$ ($G\alpha_{i/o}$) families [82]. Interestingly, different $G\alpha_{i/o}$ families may facilitate the coupling of $GABA_BRs$ to different effectors. In both heterologous and native systems, for example, adenylyl cyclase was predominantly regulated by $G\alpha_i$, while GIRK channels and VGCCs were largely regulated by $G\alpha_o$ [83]. While less is known regarding the contribution of specific Gβ and Gγ subunits to $GABA_BR$-effector coupling, Gβ2γ3 was identified as a mediator of $GABA_BR$-GIRK signaling in neurons [84]. In addition, Gβ1, Gβ2, and Gγ2 co-immunopurified with native neuronal $GABA_BRs$, suggesting their potential involvement in $GABA_BR$ signal transduction as well [85].

1.6.6 $GABA_BR$-mediated regulation of effectors

Adenylyl cyclase

Adenylyl cyclase catalyzes the synthesis of cyclic AMP (cAMP), a key second messenger that regulates diverse cellular processes [86]. Ten adenylyl cyclase isoforms are expressed throughout the mammalian brain – nine transmembrane isoforms (AC-I – IX) and one soluble isoform (AC-X) [86]. While all transmembrane isoforms can be stimulated by direct interactions with $G\alpha_s$, $G\alpha_{i/o}$ proteins directly inhibit AC-I, AC-III, AC-V, AC-VI, AC-

VIII, and AC-IX. The Gβγ dimers also inhibit AC-I, but can stimulate AC-II and AC-IV [87]. Thus, $GABA_BRs$ can bidirectionally regulate adenylyl cyclase activity through "typical" $G\alpha_{i/o}$- or Gβγ-mediated inhibition, or "atypical" Gβγ-mediated stimulation.

Several early studies had shown that $GABA_BR$ agonists inhibit basal or forskolin-stimulated adenylyl cyclase activity in neurons via PTX-sensitive G proteins [88]. Others later found that $GABA_BRs$ can stimulate adenylyl cyclase-induced cAMP production during co-activation of $G\alpha_s$-coupled receptors by norepinephrine, isoprenaline, histamine, or vasoactive intestinal polypeptide [89]. This atypical Gβγ-mediated stimulation of adenylyl cyclase (AC-II & AC-IV) requires the presence of active $G\alpha_s$, thus demonstrating a form of G protein crosstalk between $GABA_BRs$ and $G\alpha_s$-coupled GPCRs that augments cAMP production [90]. The bidirectional regulation of cAMP levels by the $GABA_BR$ was confirmed *in vivo* using microdialysis in freely moving rats [91].

The typical $GABA_BR$-mediated inhibition of adenylyl cyclase leads to a reduction in cAMP levels and protein kinase A (PKA) activity that can influence several downstream processes. For example, presynaptic reductions in cAMP can inhibit vesicle fusion and spontaneous neurotransmitter release [92]. Postsynaptic reductions in PKA activity can alleviate an A-kinase anchoring protein (AKAP)-dependent tonic inhibition of TREK2 channels [93], decrease the Ca^{2+} permeability of NMDARs [94], enhance the magnitude of tonic $GABA_AR$ currents [95], and influence gene expression [96]. Taken together, the regulation of adenylyl cyclase by the GABABR is poised to influence diverse cellular processes across short and long timeframes – by modifying neuronal excitability and synaptic transmission, altering levels of intracellular secondary messengers (cAMP, Ca^{2+}), and regulating gene expression.

Voltage-gated Ca^{2+} channels

VGCCs are regulated by many $G\alpha_{i/o}$-coupled GPCRs, including $GABA_BRs$. VGCCs are typically closed at resting membrane potentials but are opened by membrane depolarization, leading to Ca^{2+} influx. Ca^{2+} influx depolarizes the cellular membrane, facilitates synaptic vesicle release, and as a secondary messenger, regulates diverse physiological processes [97]. VGCCs are composed of pore-forming subunits encoded by 10 mammalian genes. Seven genes encode the high-voltage-activated Ca^{2+} channel subfamily including L-type ($Ca_V1.1$ to 1.4), P/Q-type ($Ca_V2.1$), N-type ($Ca_V2.2$), and R-type ($Ca_V2.3$) channels, while three genes encode low-voltage-activated T-type ($Ca_V3.1$-3.3) channels [97]. In general, $GABA_BRs$ inhibit N- and P/Q-type channels in most neurons, and L-, T-, and R-type channels in select neuron populations [97,98].

$GABA_BR$ activation inhibits N- and P/Q-type channels in presynaptic terminals of both glutamatergic and GABAergic neurons, as well as R-type channels in some glutamatergic terminals [97,99]. Inhibition of presynaptic VGCCs reduces Ca^{2+} influx and decreases the probability of neurotransmitter release. $GABA_BRs$ inhibit VGCCs through direct interactions between Gβγ and the channel. Mechanistically, Gβγ binding to VGCCs slows channel activation kinetics and induces a positive shift in the voltage dependence to inhibit Ca^{2+} influx [100]. Gβγ-mediated inhibition can be relieved by strong depolarization or eventual dissociation of Gβγ from the channel [97]. $GABA_BRs$ can also inhibit several VGCC subtypes in dendrites and spines [101,102]. Postsynaptic $GABA_BR$-VGCC signaling prevents dendritic Ca^{2+} spikes to reduce cellular excitability and limit the actions of Ca^{2+} as a secondary messenger [98,103].

$GABA_BRs$ and VGCCs have been proposed to form signaling complexes that facilitate tight functional coupling through membrane-delimited Gβγ interactions. FRET experiments revealed that GB1a/GB2 receptors associate with Gβγ and N-type channels in hippocampal pyramidal neuron boutons, suggesting the formation of signaling

complexes that facilitate $GABA_BR$/VGCC-mediated presynaptic inhibition [104]. In line with this, a high-resolution proteomics approach showed that native neuronal N-type channels assemble with GB1a/GB2 receptors [71]. Electrophysiological, biochemical, and ultrastructural evidence also support the existence of postsynaptic signaling complexes. $GABA_BRs$ co-assemble and co-cluster with P/Q-type channels in dendritic shafts of cerebellar Purkinje neurons [105], and co-cluster with L-type channels in dendrites of hippocampal somatostatin interneurons to inhibit postsynaptic Ca^{2+} influx [103].

While the inhibitory influence of $GABA_BR$-VGCC signaling has been well established, under certain conditions it can also exert excitatory influence over neurons. At the microcircuit level, for example, presynaptic VGCC inhibition often suppresses the release of inhibitory neurotransmitters (e.g., GABA, Glycine), which disinhibit downstream neurons. Furthermore, $GABA_BR$-mediated inhibition of N-type channels and calcium influx in rat retinal neurons led to an indirect suppression of big conductance Ca^{2+}-activated K^+ (BK) channels, ultimately driving a net increase in neuronal excitability [106]. $GABA_BRs$ have also been reported to activate L-type channels via $G\alpha_q$ signaling in neonatal hippocampal neurons [107]. A similar activation of L-type channels through $GABA_BRs$ has been reported to occur following N-methyl-D-aspartate receptor (NMDAR) blockade [108]. Lastly, $GABA_BRs$ have been found to activate R-type channels on medial habenula neurons to facilitate Ca^{2+} influx and trigger neurotransmitter release into the interpeduncular nucleus [109].

GIRK channels

GIRK channels are homo- or heterotetramers formed by four subunits (GIRK1-4). GIRK1-3 show broad and overlapping expression throughout the CNS, while GIRK4 is primarily found in the heart [110,111]. While multiple GIRK channel subtypes are present throughout the rodent brain, the GIRK1/2 heterotetramer is generally considered the

prototypical neuronal GIRK channel [112]. GIRK channels are predominantly distributed within the somatodendritic compartment, at both perisynaptic and extrasynaptic sites [110]. There, they mediate the postsynaptic inhibitory effect of multiple neurotransmitters through $G\alpha_{i/o}$-coupled GPCRs, including the $GABA_BR$ [79].

$GABA_BR$-GIRK signaling has been characterized in many cell types throughout the brain [79,113]. $GABA_BRs$ activate GIRK channels through Gβγ dimers [114,115], whereby direct binding of Gβγ to GIRK channels enhances gating by stabilizing an interaction between the channel and phosphatidylinositol-4,5-bisphosphate (PIP_2), a co-factor required for channel gating [116]. Activation of GIRK channels evokes a slow hyperpolarizing conductance via K^+ efflux that can shunt excitatory input [117], inhibit back-propagation of action potentials, and block the generation of dendritic Ca^{2+} spikes [118]. The critical role of GIRK channels in tempering cellular excitability is evident in $GIRK2^{-/-}$ mice, which are hyperactive and susceptible to spontaneous seizures [119,120]. These behavioral phenotypes are similarly observed in $GB1^{-/-}$ and $GB2^{-/-}$ mice, underlining the importance of both forms of inhibitory signaling throughout the brain [121].

There is evidence that $GABA_BRs$, G proteins, and GIRK channels form macromolecular signaling complexes that enable specific and rapid signaling upon receptor activation [113]. $GABA_BRs$, $G\alpha_{i/o}$-type G proteins, and GIRK channels all associate with lipid rafts, suggesting that they may interact together [122,123]. $GABA_BRs$ and GIRK channels also co-cluster in the dendrites of rodent hippocampal neurons [124] and cerebellar neurons [105]. Immunoprecipitation experiments revealed $GABA_BR$/GIRK and $G\alpha_o$/GIRK co-assemblies in heterologous systems [125,126], and $GABA_BR$/GIRK co-assemblies in the mouse cerebellum [105,127]. Evidence in support of direct protein-interactions largely comes from biochemical assays in heterologous systems. BRET/FRET experiments revealed

close interactions (<100 Å) between $GABA_BRs$ and GIRK2 homotetramers, GIRK1/4 or GIRK1/3 heterotetramers, and $G\alpha_o$ proteins [125,127,128].

Some functional data also support the possibility of a pre-coupling of components in the form of a macromolecular complex. GIRK channels expressed in heterologous systems or native neurons can signal even in the absence of receptor activation, supporting the possibility that some signaling components are pre-coupled [129]. In addition, increased expression of $GABA_BRs$ in *Xenopus* oocytes reduced basal GIRK channel activation, perhaps via a downregulation of GIRK channel surface expression during constitutive $GABA_BR$ internalization, as has been similarly suggested in neurons [28,130,131]. This could indicate physical interactions among $GABA_BRs$ and GIRK channels, and perhaps a pre-coupling between components of this signaling cascade.

There is also evidence against the existence of pre-coupled macromolecular complexes, and in favor of a collision-coupling mode of $GABA_BR$-GIRK signaling. For example, increasing the surface expression of $GABA_BRs$ in *Xenopus* oocytes accelerated GIRK channel activation, which suggests that $GABA_BRs$ or G proteins can diffuse freely in the membrane to activate GIRK channels [129]. Furthermore, unlike the direct interactions reported in heterologous systems, native neuronal $GABA_BRs$ and GIRK channels did not co-immunopurify with one another in a high-resolution proteomics study [71]. Thus, the mode of coupling between components of this signalosome remains unclear. Taken together, these results suggest that a putative $GABA_BR$-G protein-GIRK complex may be dynamic, allowing for dissociation and reassociation of components. The formation of dynamic complexes, with low-affinity and/or transient interactions, could explain why $GABA_BRs$ and GIRK channels did not associate *in vivo* [71].

1.6.7 Regulation of neuronal $GABA_BR$-dependent signaling

Tight control over the timing and strength of $GABA_BR$-dependent signaling is crucial for establishing a proper inhibitory tone that balances excitation. Accordingly, signaling through $GABA_BRs$ is subject to regulation through an array of mechanisms.

Desensitization

Desensitization is a common regulatory mechanism of GPCR function to prevent overstimulation. For many GPCRs, desensitization involves direct phosphorylation of the receptor by GPCR kinase (GRK), followed by arrestin binding, and dynamin-dependent and clathrin-mediated endocytosis [132]. Internalized receptors accumulate in endosomal sorting compartments where they may either be dephosphorylated and recycled back to the cell surface or targeted to lysosomes for degradation [133].

While prolonged activation of $GABA_BRs$ induces desensitization of the receptor response, $GABA_BR$ desensitization does not involve receptor internalization via the classical GRK phosphorylation and arrestin recruitment pathway. Rather, surface stability of $GABA_BRs$ is regulated through a variety of phosphorylation-independent and phosphorylation-dependent mechanisms [134-136].

Phosphorylation

Unlike many GPCRs, $GABA_BR$ activity is not correlated with the overall phosphorylation state of the receptor, as phosphorylation of different residues influence $GABA_BR$ activity in distinct ways [87]. There are five known phosphorylation sites on $GABA_BRs$ that regulate endocytosis, surface stability, and desensitization. These include serine 867 (S867) and S917/923 on GB1, and S783 and S892 on GB2. Several kinases mediate phosphorylation at these sites.

CaMKII. CaMKII phosphorylates S867 on primarily GB1b, leading to the dynamin-dependent endocytosis of $GABA_BRs$ that couple to GIRK channels [137]. Glutamatergic signaling can downregulate the $GABA_BR$ [138], in part through activation of NMDARs that enhance CaMKII-mediated phosphorylation of S867 to promote $GABA_BR$ internalization [137]. Indeed, blockade of CaMKII activity, or phosphorylation of S867, was sufficient to prevent the glutamate-induced downregulation of $GABA_BRs$ in hippocampal neurons [137,138].

AMPK. AMP-activated protein kinase (AMPK) binds to the C-terminus of GB1, where it can phosphorylate two sites on GB1 (S917/923), and one site on GB2 (S783) [139]. Phosphorylation of S783 on GB2 reduced desensitization of $GABA_BRs$ and enhanced $GABA_BR$-GIRK coupling by stabilizing receptors at the plasma membrane. Interestingly, AMPK-mediated phosphorylation of S783 can be bidirectionally modulated by glutamatergic signaling through NMDARs. While transient NMDAR activation enhances AMPK activity and promotes S783 phosphorylation, prolonged NMDAR activation leads to the dephosphorylation of S783 [140]. Prolonged NMDAR activity activates protein phosphatase 2A (PP2A), which dephosphorylates S783 and targets $GABA_BRs$ for lysosomal degradation, thus reducing surface expression and $GABA_BR$ function [140]. Concurrent activation with $GABA_BRs$ prevents the NMDAR/PP2A-mediated reduction in $GABA_BR$ surface expression, likely via membrane hyperpolarization or decreased Ca^{2+} permeability of NMDARs [140]. Thus, glutamatergic and GABAergic signaling delicately control the phosphorylation state of $GABA_BRs$ to regulate intracellular trafficking and cell surface stability.

***PKA*.** PKA phosphorylates the cytoplasmic tail of GB2 at S892, leading to increased $GABA_BR$ surface stability and reduced slow desensitization in HEK-293 and hippocampal cells [141]. Prolonged activation of $GABA_BRs$ inhibits adenylyl cyclase to reduce PKA activity and S892 phosphorylation, which coincides with increased endocytosis-independent $GABA_BR$ degradation [142]. $GABA_BR$ degradation induced by chronic exposure to baclofen is attenuated by either PKA activation or co-stimulation of $G\alpha_s$-coupled β-adrenergic receptors [143]. Thus, PKA-induced phosphorylation of S892 and $GABA_BR$ surface stability are carefully controlled by G protein signaling cascades that modulate PKA activity.

***PKC*.** Protein kinase C (PKC) has been reported to phosphorylate GB1 at an unknown site in Chinese hamster ovary cells. Activation of $GABA_BRs$ enhances PKC recruitment to the plasma membrane, induces phosphorylation of GB1, and disrupts the direct interaction between NEM sensitive fusion (NSF) proteins and $GABA_BRs$ to facilitate agonist-induced, internalization-independent desensitization [144].

Ubiquitination

Ubiquitination is a posttranslational modification that involves covalent attachment of ubiquitin to a target protein, generally directing the protein to proteasomes or lysosomes for degradation [145]. Ubiquitination of the GB2 C-terminus promotes constitutive proteasomal degradation of $GABA_BRs$ in cultured cortical neurons, and inactivation of these sites increases cell surface receptor levels and enhances $GABA_BR$ signaling [146]. GB1 is also ubiquitinated at multiple sites by the ubiquitin ligase Mind bomb-2 (MIB2), which promotes lysosomal degradation of $GABA_BRs$ [147]. Interestingly, MIB2-induced ubiquitination may contribute to the glutamate- and CaMKII-induced down-regulation of $GABA_BRs$. Indeed, MIB2-induced GB1 ubiquitination is largely dependent on the

phosphorylation state of S867 on GB1; CaMKIIβ-induced S867 phosphorylation promotes, while S867 dephosphorylation inhibits, the ubiquitination of GB1 [148]. In addition to CaMKII, PKC has also been reported to promote ubiquitination, internalization, and degradation of $GABA_BRs$ [149].

KCTD proteins

The four KCTD proteins (KCTD8, 12, 12b, 16) assemble as homo- or heteromeric pentamers on the C-terminus of GB2, where they stabilize G proteins at the receptor and regulate the kinetics of G protein-dependent signaling [81]. KCTD proteins accelerate the onset of $GABA_BR$-GIRK currents, and KCTD12 and KCTD16 additionally increase agonist potency, as seen by a reduced EC_{50} value of baclofen-evoked GIRK currents [150]. KCTD12 and KCTD12b also induce fast desensitization of $GABA_BR$-GIRK currents by directly binding receptor-activated Gβγ dimers to uncouple Gβγ from GIRK channels [151]. Interestingly, PKA-mediated phosphorylation of S892 on GB2 can regulate KCTD12-induced fast desensitization. PKA activation in hippocampal neurons slows, while PKA inhibition accelerates, KCTD12-induced fast desensitization of $GABA_BR$-GIRK currents [152]. PKA fails to regulate desensitization in knock-in mice with a serine-892 to alanine mutation (S892A), demonstrating that phosphorylation of S892 slows KCTD12-induced fast desensitization *in vivo* [152]. In addition to regulating G protein signaling kinetics, KCTD proteins also scaffold effector channels and other proteins at the $GABA_BR$. For example, N-type Ca^{2+} channels, hyperpolarization-activated cyclic nucleotide-gated 2 (HCN2) channels, and 14-3-3 proteins associate with $GABA_BRs$ through direct interactions with KCTD16 [71].

RGS proteins

Regulator of G protein signaling (RGS) proteins are GTPase-accelerating proteins (GAPs) that facilitate termination of G protein signaling by promoting hydrolysis of GTP on active Gα to enable reassembly of the heterotrimeric G protein complex [153]. The mammalian RGS protein superfamily is divided into eight subfamilies (RZ, R4, R7, R12, RA, GED, GRK, SNX) based on amino acid sequence or structural similarity. Although some structural diversity among RGS proteins can explain the existence of non-canonical cell signaling roles, the RGS homology domain that is critical for accelerating GTPase activity is highly conserved among many members [154]. Several RGS proteins across subfamilies have been shown to regulate the kinetics of G protein-dependent signaling through $GABA_BRs$.

***R7 RGS/Gβ5*.** The R7 RGS protein family is comprised of four members (RGS6, RGS7, RGS9, RGS11) that play critical roles in fundamental neuronal processes, including vision, motor control, reward behavior, and nociception [155]. R7 RGS proteins form obligate heterodimers with G protein β5 (Gβ5) through interactions at their Gγ-like domains [156]. RGS/Gβ5 heterodimers can then form reversible complexes with adaptor proteins, such as R7-binding protein (R7BP) [157]. When palmitoylated, R7BP anchors the heterodimeric complex at the plasma membrane and prevents RGS protein degradation [158]. R7BP also facilitates the functional association of RGS/Gβ5 with GIRK channels to promote deactivation of G proteins [159,160]. Indeed, genetic ablation of either RGS6, RGS7, Gβ5, or R7BP prolongs deactivation kinetics of $GABA_BR$-GIRK currents [160-162]. Ablation of RGS7 or R7BP also enhanced the coupling efficiency of $GABA_BR$-GIRK signaling, increasing the potency of baclofen-induced GIRK currents [160].

In line with their functional association, biochemical, electrophysiological, and ultrastructural evidence support the existence of macromolecular complexes formed of RGS7/Gβ5, $GABA_BRs$, and GIRK channels in dendritic spines of hippocampal CA1 pyramidal neurons [124]. Insights from the RGS7-Gβ5-R7BP crystal structure further suggest that the orientation of the complex is compatible with macromolecular assemblies involving $GABA_BRs$ and GIRK channels [163].

In addition to forming complexes with R7BP, RGS7/Gβ5 can also assemble with G protein-coupled receptor 158 (GPR158) [164,165]. Formation of either complex is mutually exclusive, and facilitates trafficking of RGS7 to the plasma membrane [164]. The ability of RGS7 to negatively regulate $GABA_BR$ signaling through GIRK channels or P/Q/N-type channels is enhanced by R7BP, but opposed by GPR158 [166]. Interestingly, however, the RGS7/Gβ5-GPR158 complex has been reported to suppress homeostatic regulation of cAMP by $GABA_BRs$ [165]. Taken together, these data suggest that RGS7/Gβ5 dimers exist in two separate complexes at the plasma membrane that may differentially guide RGS7-mediated regulation toward effector systems.

***R4 RGS proteins*.** Two members of the R4 RGS subfamily (RGS2 and RGS4) have been implicated in negatively regulating $GABA_BR$-GIRK signaling in neurons. RGS2 reduces the coupling efficiency of $GABA_BRs$ with heteromeric GIRK2/3 channels in VTA dopamine neurons [167]. Evidence from immunoelectron microscopy and slice electrophysiology in GIRK subunit-specific knockout mice suggests that the effect of RGS2 on $GABA_BR$-GIRK signaling uniquely requires the GIRK3 subunit, and FRET analysis revealed direct interactions between RGS2 and GIRK3 [167].

RGS4 has been proposed to form a signaling complex with $GABA_BRs$ to terminate $GABA_BR$-GIRK signaling. Double immunohistochemistry and immunoprecipitation assays

revealed that RGS4 and $GABA_BRs$ associate together in the PFC and hypothalamus, and FRET analysis in transfected HEK-293 cells indicated direct interactions between RGS4 and both GB1 and GB2 [128,168]. RGS4 enhances GIRK channel deactivation rates within a second of agonist application *in vitro*, and RGS4 expression in GIRK-transfected CHO cells mimics the fast deactivation kinetics observed in hippocampal neurons and atrial myocytes [169]. In PFC pyramidal neurons, RGS4 has been reported to limit crosstalk between two $G\alpha_{i/o}$-coupled receptors, $GABA_BRs$ and A_2 adenosine receptors (A_2Rs). Within single dendritic spines, and through inhibition of PKA, $GABA_BR$ activation inhibits NMDARs while A_2R activation inhibits AMPARs [170]. RGS4 appears capable of limiting interference between the two receptors' neuromodulatory functions, as blocking RGS4 activity with either a small molecule inhibitor, or an intracellular anti-RGS4 antibody, enables crosstalk between pathways. This raises the intriguing possibility that RGS4 dysfunction in schizophrenia could disrupt pathway segregation and promote crosstalk that drives aberrant function [170].

1.6.8 Regulation of neuronal GIRK-dependent signaling

While many of the $GABA_BR$-specific regulatory mechanisms indirectly influence GIRK-dependent signaling, GIRK channels can be regulated directly in a variety of ways. For example, GIRK channels can be activated by Na^+, Mg^{2+}, or ethanol via Gβγ-independent mechanisms [171]. Unique structural elements in GIRK subunits also confer functional diversity to the channels. For example, specific residues in the pore and second transmembrane domain of GIRK1 potentiate basal and receptor-dependent GIRK channel activity [172]. GIRK1-containing channels also have a higher affinity for Gβγ than GIRK2/3 channels [173,174]. GIRK2 and GIRK4 have an endoplasmic reticulum export signal that is critical for plasma membrane expression, and GIRK2 has an internalization VL motif that

facilitates endocytosis [175]. The GIRK2c isoform and GIRK3 possess a postsynaptic density 95/disc-large/zona occludens (PDZ) binding motif that enables interaction with sorting nexin 27 (SNX27), a protein implicated in both forward trafficking and internalization [176]. GIRK3 also has a lysosomal targeting sequence that promotes degradation and reduces the number of GIRK3-containing channels [171].

Like $GABA_BRs$, GIRK channels are also regulated via phosphorylation. GIRK1 is phosphorylated by both PKA and PKC, which lead to either increased or decreased GIRK channel activity, respectively [177]. PP2A-mediated dephosphorylation of GIRK channels also decreases GIRK channel activity [177]. Additionally, neuronal activity and NMDAR activation can dephosphorylate GIRK2 at Ser-9, which enhances GIRK channel activity through increased forward trafficking [178]. Together, these phosphorylation pathways allow GIRK-dependent signaling to additionally be modulated by the activation of non-Gi/o GPCRs.

1.7 Drug-induced plasticity of $GABA_BR$-GIRK signaling

Experience-dependent plasticity of excitatory signaling (e.g., long-term potentiation; LTP) is widely regarded as one of the major mechanisms that underlies learning and memory. $GABA_BR$-GIRK signaling plays an essential role in the depotentiation of excitatory LTP [171], in addition to mediating inhibitory LTP [179]. Regulation of these synaptic plasticity processes undoubtedly contributes to the broad spectrum of behavioral abnormalities observed in constitutive $GABA_BR$ and GIRK subunit knockout mice [83,171]. Interestingly, exposure to addictive drugs or aversive experiences – potent modifiers of learning and memory – have been shown to alter inhibitory signaling mediated by $GABA_BRs$ and GIRK channels throughout the brain [171]. As addiction can be considered

a disorder of maladaptive learning, it is tempting to speculate that alterations in $GABA_BR$-GIRK signaling might contribute to addictive behaviors.

Several studies have described psychostimulant-induced adaptations in $GABA_BR$-GIRK signaling within the mesocorticolimbic system. In the VTA, for example, a single injection of cocaine (15 mg/kg, IP) led to a reduction of $GABA_BR$-GIRK signaling in both DA and GABA neurons – adaptations which lasted for 5 and 7 days, respectively [130,180]. Both adaptations coincided with decreased surface expression of $GABA_BRs$ and/or GIRK channels [130,180]. Other studies found that a single injection of methamphetamine similarly suppressed $GABA_BR$-GIRK signaling in VTA GABA neurons [130], and methamphetamine self-administration decreased $GABA_BR$-GIRK signaling in DA neurons in the VTA and substantia nigra [181].

In addition to midbrain neurons, $GABA_BR$-GIRK plasticity has also been reported in PL pyramidal neurons. In one study, for example, five once-daily injections of cocaine (15 mg/kg, IP) were found to reduce $GABA_BR$-GIRK signaling after a 24 withdrawal [28]. This adaptation persisted for up to 6 wk, and was dependent on D_1R activation, perhaps implicating mesocortical DA neurotransmission [28]. Additional evidence from ultrastructural and biochemical studies revealed a decrease in the surface expression of $GABA_BRs$ and GIRK channels, and a reduction in phosphorylated S783 on GB2 – findings that are congruent with a trafficking mechanism involving PP2A-mediated dephosphorylation of GB2 [28]. Follow-up behavioral studies modeled this adaptation in drug-naïve mice through a viral RNAi-mediated knockdown of Girk1 and Girk2 in the PL. Although the manipulation was not selective for pyramidal neurons, the knockdown of GIRK channels in the PL was sufficient to enhance the motor-stimulatory effect of cocaine and occlude the development of locomotor sensitization [28]. While these findings suggest that PL GIRK channel activity regulates behavioral sensitivity to cocaine, further investigation is warranted to understand

the behavioral consequences of these cocaine-induced plasticity mechanisms in PL pyramidal neurons.

1.8 Summary

Inhibitory signaling mediated by the $GABA_BR$ and GIRK channel is essential for cellular excitability and behavioral function, however, the strength of this inhibition is compromised in PL pyramidal neurons upon chronic cocaine exposure. The goal of my thesis work is to understand the contribution of GIRK channels in PL pyramidal neurons to behaviors that are relevant to addiction, and to better understand the regulatory mechanisms that control inhibitory signaling mediated by $GABA_BRs$ and GIRK channels. In **Chapter 2**, I first demonstrate that reduced GIRK channel activity in PL pyramidal neurons induces neuronal hyperexcitability. I next employ viral approaches to model the impact of acute (chemogenetic) and persistent (GIRK channel ablation) excitation of PL pyramidal neurons on behaviors that may be relevant to addiction, including acute cocaine-induced locomotion and trace fear conditioning. In **Chapter 3**, I extend these investigations to examine the contribution of the $GABA_BR$ and GIRK channel in PL pyramidal neurons to mood-related behaviors and cocaine CPP performance. Finally, in **Chapter 4**, I combine electrophysiological approaches with constitutive $RGS6^{-/-}$ and $RGS7^{-/-}$ mice to characterize the functional role(s) of RGS6 and RGS7 in the regulation of synaptically-evoked and baclofen-activated $GABA_BR$-GIRK currents. Altogether, work in this dissertation informs our basic understanding of how the GIRK channel in PL pyramidal neurons contributes to cellular excitability and behavior under normal and perhaps pathophysiological conditions.

Chapter 2: Impact of acute and persistent excitation of PL pyramidal neurons on motor activity and trace fear learning

Chapter 2 contains work that was previously published in The Journal of Neuroscience in 2020.

Rose TR*, Marron Fernandez de Velasco E*, Vo B, Tipps M, Wickman K. Impact of acute and persistent excitation of prelimbic pyramidal neurons on motor activity and trace fear learning. *J Neurosci*. 2020. 41(5):960-971. (*equal contributors)

Author contributions: K.W., T.R.R., E.M.F.d.V., and M.E.T. designed research; T.R.R., E.M.F.d.V., B.N.V., and M.E.T. performed research; K.W., T.R.R., E.M.F.d.V., B.N.V., and M.E.T. analyzed data; T.R.R. wrote the first draft of the paper; K.W., T.R.R., E.M.F.d.V., B.N.V., and M.E.T. edited the paper; E.M.F.d.V. contributed unpublished reagents/analytic tools. *T.R.R. and E.M.F.d.V. contributed equally to this work.

2.1 INTRODUCTION

The medial prefrontal cortex (mPFC) plays a crucial role in cognition and motivated behavior [182,183]. The mPFC provides glutamatergic input to several brain regions including the ventral tegmental area (VTA), basolateral amygdala (BLA), and nucleus accumbens (NAc) [184,185], and these projections have been linked to key facets of cocaine addiction [182,183,186]. For example, cocaine exposure increases glutamate release

in the NAc and VTA [187], and these increases and associated cocaine-induced neuroadaptations and drug-seeking behavior can be blocked by mPFC inactivation [46,50,188-190]. In addition, cocaine-induced adaptations in mPFC projections are critical for the development and expression of locomotor sensitization, a phenomenon sharing anatomic and neurochemical features with craving [186].

The mPFC consists of cingulate, prelimbic (PL), infralimbic (IL), and orbitofrontal cortices [182,183]. Numerous studies have highlighted the role of the PL in regulating addiction-related behaviors and cognition [183,191-195]. For example, PL lesions prevent the induction and expression of cocaine-induced locomotor sensitization, and PL inactivation decreases the reinstatement of cocaine-seeking behavior [196-198]. PL activity is also necessary for associative learning [42,199], which is dysregulated following repeated cocaine exposure [200]. In rodent trace fear conditioning studies, for example, persistent firing in the PL during the trace interval, the period separating the auditory cue and footshock delivery, is critical for fear learning [201-210]. Indeed, trace fear learning is prevented by optogenetic silencing of the PL during the trace interval [210].

The PL contains excitatory pyramidal neurons (~85%) and GABAergic interneurons (~15%) [211]. Pyramidal neurons, particularly those in layers 5 and 6, are primary projection neurons [184,185], while GABA neurons regulate pyramidal neuron excitability [212-214]. Prolonged contingent or non-contingent cocaine exposure triggers adaptations that increase PL pyramidal neuron excitability [28,215-221]. Repeated cocaine exposure also reduces GABAergic neurotransmission in PL pyramidal neurons via suppression of presynaptic GABA release [222], and blunting of postsynaptic $GABA_AR$- and $GABA_BR$-mediated signaling [28,217,222]. At present, the behavioral relevance of elevated PL pyramidal neuron excitability is not well-understood.

Previously, we reported that a cocaine sensitization regimen increased layer 5/6 PL pyramidal neuron excitability in mice, and that this adaptation correlated with reduced G protein-gated inwardly rectifying K^+ (GIRK/Kir3) channel activity [28]. Viral suppression of GIRK channel activity in the PL of drug-naïve mice increased the motor-stimulatory effect of cocaine. This manipulation was not selective for pyramidal neurons, however, and GABA neurons regulate pyramidal neuron excitability. Since psychostimulant exposure also suppressed GIRK-dependent signaling in VTA GABA neurons [130], we first asked whether layer 5/6 PL GABA neurons express GIRK channels, and if so, whether repeated cocaine exposure alters GIRK-dependent signaling in, or excitability of, these neurons. We then used neuron-specific viral approaches to probe the behavioral impact of manipulations that persistently or acutely enhance PL pyramidal neuron excitability.

2.2 MATERIALS AND METHODS

Animals. All experiments were approved by the University of Minnesota Institutional Animal Care and Use Committee. The generation of *Girk1*$^{-/-}$ (RRID:MGI:3041949), *Girk2*$^{-/-}$ (RRID:MGI:3852123), *Girk3*$^{-/-}$ (RRID:MGI:2676599), and *Girk1*$^{fl/fl}$ mice was described previously [120,223-225]. GAD67GFP mice were provided by Dr. Takeshi Kaneko [226]. CaMKIICre (B6.Cg-Tg(Camk2a-cre)T29-1Stl/J, RRID:IMSR_JAX:005359) and GADCre (B6N.Cg-*Gad2*$^{tm2(cre)Zjh}$/J, RRID:IMSR_JAX:010802) lines were purchased from The Jackson Laboratory (Bar Harbor, ME) and were maintained by backcrossing against the C57BL/6J strain. Cre(+) and/or Cre(-) offspring were used in some experiments. Male C57BL/6J mice were purchased for some studies. Mice were maintained on a 14:10 h light/dark cycle and were provided *ad libitum* access to food and water.

Chemicals. Baclofen, barium chloride, picrotoxin, and kynurenic acid were purchased from Sigma (St. Louis, MO). CGP54626, clozapine-N-oxide (CNO), and tetrodotoxin were purchased from Tocris (Bristol, UK). Cocaine was obtained through Boynton Health Pharmacy at the University of Minnesota.

Viral vectors. pAAV-hSyn-DIO-hM3Dq(mCherry) (RRID:Addgene_44361), pAAV-hSyn-DIO-hM4Di(mCherry) (RRID:Addgene_44362), and pAAV-hSyn-DIO-mCherry (RRID:Addgene_50459) were gifts from Dr. Bryan Roth. pAAV-CaMKIIα-hM3Dq(mCherry) and pAAV-CaMKIIα-mCherry plasmids were generated by the University of Minnesota Viral Vector and Cloning Core (VVCC; Minneapolis, MN) using standard cloning techniques and pAAV-CaMKIIα-hChR2(C128S/D156A)-mCherry (RRID:Addgene_35502, a gift from Dr. Karl Deisseroth) as the backbone. Similarly, pAAV-mDlx-hM4Di(mCherry), pAAV-mDlx-mCherry and pAAV-mDlx-tdTomato were generated using pAAV-mDlx-GCaMP6f-Fishell-2 (RRID:Addgene_83899, a gift from Dr. Gordon Fishell) as the source of the mDlx promoter/enhancer. pAAV-hSyn-Cre-GFP (RRID:Addgene_68544, a gift from Dr. Eric Nestler) was packaged into AAV2retro. AAV8-CaMKIIα-Cre(mCherry) was purchased from the University of North Carolina Vector Core (Chapel Hill, NC). All other viral vectors were packaged in AAV8 serotype by the University of Minnesota VVCC (Minneapolis, MN); all viral titers were between $3.5 \times 10^{12} – 2.2 \times 10^{14}$ genocopies/mL.

Intracranial viral manipulations. Intracranial infusion of virus (400 nL per side) in mice (7-8 wk) was performed as described [227], using the following coordinates (in mm from bregma: AP, ML, DV): PL (+2.50, ±0.45, -1.60), BLA (-1.50, ±3.35, -4.70), NAc (+1.50, ±1.00, -4.50), and VTA (-2.60, ±0.65, -4.70). After surgery, animals were allowed 3-4 wk

(chemogenetic studies) or 4-5 wk (Cre ablation or projection-specific chemogenetic studies) for full recovery and viral expression before electrophysiological or behavioral assessments. The scope and accuracy of targeting was assessed using fluorescence microscopy. Brightfield and fluorescent images were overlaid and evaluated using the *Mouse Brain Atlas* [228]. Targeting coordinates and viral loads yielded extensive coverage of the PL along the rostro-caudal axis, with limited spread into the anterior cingulate (cg), medial orbital, or IL cortices. Only data from mice in which >70% of viral-driven bilateral fluorescence was confined to the PL were included in the final analysis. To evaluate the targeting fidelity of AAV8/CaMKIIα- and AAV8/mDlx-based vectors, AAV8-CaMKIIα-mCherry or AAV8-mDlx-mCherry vectors were infused into the PL of GAD67GFP(+) mice. After a 2-wk period, brains were fixed with 4% paraformaldehyde, coronal sections (50 micron) were obtained by sliding microtome, and images of viral-driven mCherry and GFP fluorescence were acquired. Quantification of cells expressing mCherry, GFP, or both (overlap) was performed with ImageJ software [229].

Cocaine sensitization. GAD67GFP(+) mice (5-8 wk) underwent a cocaine sensitization paradigm, as described [28]. Briefly, mice were exposed to once-daily injections of cocaine (15 mg/kg IP) or saline over 5 consecutive days before electrophysiological assessments 1-2 d later.

Slice electrophysiology. Baclofen-induced somatodendritic currents were recorded in layer 5/6 PL neurons, as described [230]. For rheobase assessments, cells were held at 0 pA in current-clamp mode and given 1-s current pulses, beginning at -60 pA and increasing in 20 pA increments. Rheobase was identified as the injection step at which initial spiking was elicited. For PL GABA neuron recordings, rheobase was measured prior

to and after perfusion of baclofen (200 μM). For chemogenetic experiments, resting membrane potential and rheobase were assessed prior to and after bath perfusion of CNO (10 μM). Spontaneous inhibitory postsynaptic currents (sIPSCs) were recorded and analyzed, as described [227].

Behavioral testing. Adult mice (10-13 wk) were evaluated in open-field motor activity and trace fear conditioning tests. For motor activity studies, mice were acclimated to handling, injection, and open field chambers for 2-4 d prior to testing. For GIRK ablation experiments, distance traveled during the 60-min interval after saline injection on the final acclimation day was taken as baseline activity. Distance traveled after injection of cocaine (15 mg/kg IP) the next day was taken as cocaine-induced activity. For chemogenetic studies, CNO (2 mg/kg IP) was administered 30 min prior to saline injection and placement in the open field; distance traveled over the next 60-min was taken as baseline activity. Subsequently (2-4 d later), subjects were injected with CNO (2 mg/kg IP) 30 min prior to cocaine (15 mg/kg IP); distance traveled over the next 60-min interval was taken as cocaine-induced activity. In studies involving AAV8/mDlx-based vectors, separate cohorts of mice underwent baseline or cocaine-induced activity testing.

For trace fear conditioning studies, mice were acclimated to handling and testing room for 1-2 d prior to testing. The 6.5-min conditioning session (Day 1) involved 2 pairings of a 30-s auditory cue (65 dB white noise) and a 2-s footshock (0.5 mA), separated by a 30-s trace interval. For chemogenetic studies, CNO (2 mg/kg IP) was only administered once, 30 min prior to conditioning on Day 1. Cue recall was assessed on Day 3, with chambers reconfigured using a white plastic insert to cover the bar floor and a black tent insert to alter the size, shape, and color of the environment. Inserts were also cleaned with 0.1% acetic acid instead of ethanol to provide a distinct olfactory cue. Freezing was

monitored throughout the 15-min test period, divided into 5 x 3-min bins that included 2 x 3-min auditory cue presentations. For projection-specific manipulations, motor activity testing was performed 3-12 d after the trace fear conditioning study.

Experimental design and statistical analysis. Data are presented as the mean ± SEM. Statistical analyses were performed using GraphPad Prism 8 (GraphPad Software, Inc.; La Jolla, CA). Unless specifically noted, all studies involved balanced groups of males and females. While sex was included as a variable in preliminary analyses (student's *t* test, two-way ANOVA, three-way repeated measures ANOVA, mixed-effects model REML), no impact of sex was observed on any measure and data from males and females were pooled. Pooled data were analyzed by paired and unpaired student's *t* test, Mann-Whitney test, one-way ANOVA, two-way ANOVA, two-way repeated-measures ANOVA, and mixed-effects model REML, as appropriate. Pairwise comparisons were performed using Bonferroni's *post hoc* test, if justified. Within-subjects factors include test session (saline vs. cocaine, pre- vs. post-CNO treatment) and between-subjects factors include genotype (GAD67GFP:*Girk*$^{-/-}$, GAD67GFP), drug treatment (Ba^{2+}, CNO, cocaine, control), and viral treatment (Cre, DREADD, control vector), where appropriate. In **Fig. 2.3J**, CaMKIICre(+) mice were compared with CaMKIICre(-) littermate controls. Sample size (n or N) per group and statistical details of experiments are reported in the *Figure Legends* and *Results*. Data points that fell outside of the group mean by >2.5 standard deviations were excluded from analysis; this resulted in the exclusion of only one data point across the entire study. Differences were considered significant when $P<0.05$.

2.3 RESULTS

Impact of repeated cocaine on PL GABA neurons

We used GAD67GFP(+) mice to probe for the presence of GIRK channels in layer 5/6 PL GABA neurons, and to assess whether repeated cocaine evoked plasticity in GIRK-dependent signaling in these neurons. (**Fig. 2.1A**). The $GABA_BR$ agonist baclofen evoked an outward current in layer 5/6 PL GABA (GFP-positive) neurons that correlated with decreased input resistance; no sex difference was detected (t_{17}=0.73, P=0.47; unpaired student's *t* test). Baclofen-induced responses were suppressed by 0.3 mM external Ba^{2+}, consistent with GIRK channel activation (**Fig. 2.1B,C**; t_{17}=7.317, ****P<0.0001; unpaired student's *t* test). Indeed, layer 5/6 PL GABA neurons lacking GIRK1 or GIRK2 (but not GIRK3) exhibited diminished baclofen-induced currents (**Fig. 2.1D,E**; one-way ANOVA, significant effect of genotype **(**$F_{3,32}$=27.01, P<0.0001); Bonferroni's *post hoc* test: ****P<0.0001 (*Girk1*$^{-/-}$ vs. control), ****P<0.0001 (*Girk2*$^{-/-}$ vs. control), and P=0.097 (*Girk3*$^{-/-}$ vs. control)). GIRK1 or GIRK2 ablation did not impact rheobase (**Fig. 2.1F**; one-way ANOVA, no effect of genotype, $F_{2,25}$=0.97, P=0.39), but did blunt the baclofen-induced increase in rheobase (**Fig. 2.1G**; one-way ANOVA, significant effect of genotype, $F_{2,40}$=27.79, P<0.0001; Bonferroni's *post hoc* test: ****P<0.0001 (*Girk1*$^{-/-}$ vs. control), ****P<0.0001 (*Girk2*$^{-/-}$ vs. control)). Thus, layer 5/6 PL GABA neurons express a GIRK channel, formed by GIRK1 and GIRK2, that mediates approximately half of the $GABA_BR$-dependent somatodendritic current and suppression of excitability.

We next subjected GAD67GFP(+) mice to a cocaine sensitization regimen involving once-daily injections of cocaine (15 mg/kg IP) or saline over 5 consecutive days; this sensitization regimen was sufficient to provoke a suppression of $GABA_BR$-GIRK signaling in layer 5/6 PL pyramidal neurons [28]. Cocaine-treated GAD67GFP(+) mice displayed locomotor sensitization, as evidenced by a significant increase in distance traveled following the fifth cocaine injection, as compared to the first (t_6=5.138, **P=0.0021; paired student's *t* test). Subsequently (1-2 d later), we measured resting

membrane potential (RMP), rheobase, and baclofen-induced currents in layer 5/6 PL GABA neurons. Repeated cocaine had no impact on baclofen-induced current amplitude (**Fig. 2.1H,I**; t_{32}=0.960, P=0.34; unpaired student's t test), RMP (**Fig. 2.1J**; t_{31}=0.542, P=0.59; unpaired student's t test), or rheobase (**Fig. 2.1K**; t_{30}=0.9063, P=0.37; unpaired student's t test).

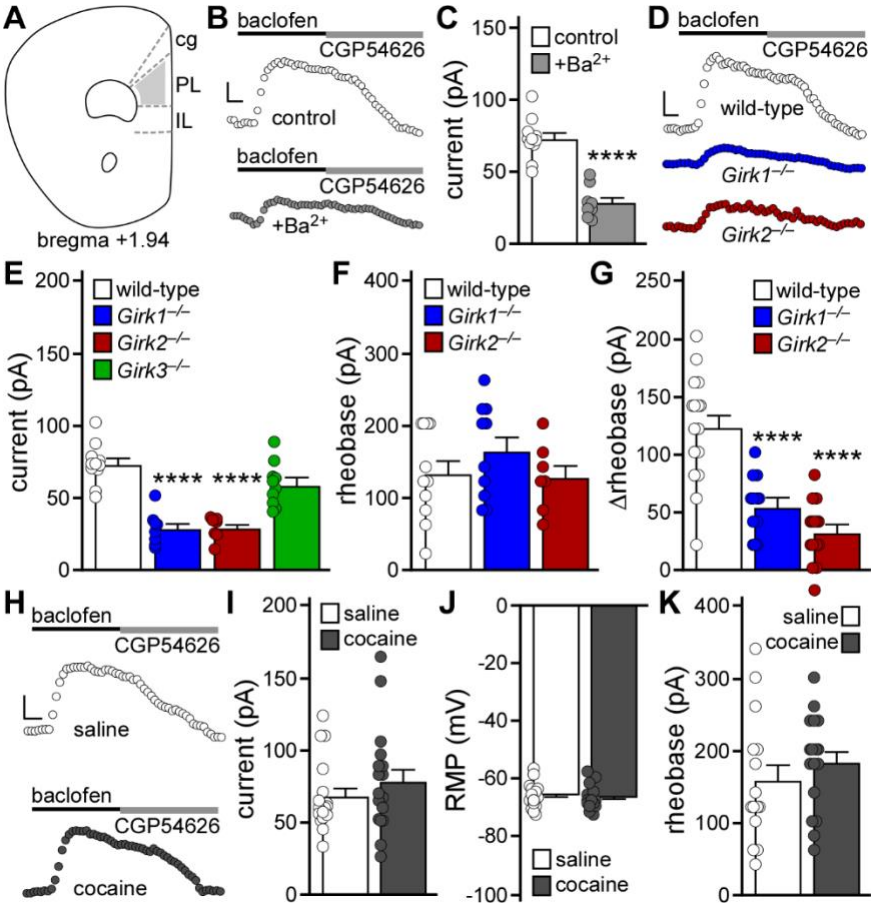

Figure 2.1. Impact of repeated cocaine exposure on layer 5/6 PL GABA neurons

A) Schematic highlighting the PL, and adjacent cingulate (cg) and infralimbic (IL) cortices. GFP-positive (GABA) neurons in layer 5/6 of the PL, in slices from GAD67GFP(+) mice, were targeted for analysis. **B)** Somatodendritic currents (V_{hold}=-60 mV) evoked by baclofen (200 µM) in GABA neurons from GAD67GFP(+) mice, in the absence and presence of external 0.3 mM Ba^{2+}. Currents were reversed by the $GABA_BR$ antagonist CGP54626 (2 µM). Scale: 25 pA/50 s. **C)** Baclofen-induced currents in GABA neurons from GAD67GFP(+) mice, in the absence (control) and presence of 0.3 mM Ba^{2+} (****P<0.0001; unpaired student's t test; n=8-11 recordings/group and N=2-4 male mice/group). **D)** Currents evoked by baclofen (200 µM) in GABA neurons from male GAD67GFP(+) (wild-type), GAD67GFP(+):*Girk1*$^{-/-}$ (*Girk1*$^{-/-}$), and GAD67GFP(+):*Girk2*$^{-/-}$ (*Girk2*$^{-/-}$) mice. Scale: 25 pA/50 s. **E)** Baclofen-induced currents in GABA neurons from GAD67GFP(+) and GAD67GFP(+):*Girk*$^{-/-}$ mice (****P<0.0001; one-way ANOVA with Bonferroni's *post hoc* test; n=7-11 recordings/group and N=2-4 male mice/group). Data used in the control group (wild-type) were the same as used in Fig. 2.1C control group. **F)** Baseline rheobase in GABA neurons from GAD67GFP(+) and GAD67GFP(+):*Girk*$^{-/-}$ mice (one-way ANOVA; n=7-11 recordings/group and 2-4 male mice/group). **G)** Change in rheobase induced by baclofen (200 µM) in GABA neurons from GAD67GFP(+) and GAD67GFP(+):*Girk*$^{-/-}$ mice (****P<0.0001; one-way ANOVA with Bonferroni's *post hoc* test; n=12-16 recordings/group and N=5-6 mice/group). No main effect of sex was detected ($F_{1,37}$=0.654, P=0.42; two-way ANOVA). **H)** Currents evoked by baclofen (200 µM) in GABA neurons

from GAD67GFP(+) mice, 1-2 d after repeated saline or cocaine treatment. Currents were reversed by the $GABA_BR$ antagonist CGP54626 (2 μM). Scale: 25 pA/50 s. **I)** Baclofen-induced currents in GABA neurons from GAD67GFP(+) mice, 1-2 d after repeated saline or cocaine treatment (unpaired student's *t* test; n=17 recordings/group and N=7 mice/group). No main effect of sex was detected ($F_{1,30}$=0.0004, *P*=0.98; two-way ANOVA). **J)** RMP in GABA neurons from GAD67GFP(+) mice, 1-2 d after repeated saline or cocaine treatment (unpaired student's *t* test; n=16-17 recordings/group and N=7 mice/group). No main effect of sex was detected ($F_{1,29}$=3.400, *P*=0.075; two-way ANOVA). **K)** Rheobase in GABA neurons from GAD67GFP(+) mice, 1-2 d after repeated saline or cocaine treatment (unpaired student's *t* test; n=15-17 recordings/group and N=7 mice/group). No main effect of sex was detected ($F_{1,28}$=0.075, *P*=0.79; two-way ANOVA).

GIRK channel ablation in PL pyramidal neurons

The lack of impact of repeated cocaine on layer 5/6 PL GABA neurons suggests that cocaine exerts a relatively selective impact on adjacent PL pyramidal neurons [28]. To probe the behavioral relevance of the GIRK neuroadaptation in layer 5/6 PL pyramidal neurons, we used a neuron-selective viral Cre approach and conditional *Girk1*$^{-/-}$ (*Girk1*$^{fl/fl}$) mice (**Fig. 2.2A**). The CaMKIIα promoter has been used extensively to drive transgene expression in PFC pyramidal neurons [231-234]. To evaluate the fidelity of pyramidal neuron targeting with our AAV8/CaMKIIα-based vectors, we infused AAV8-CaMKIIα-mCherry into the PL of GAD67GFP(+) mice. Only a small fraction (4%) of neurons co-expressed GFP and mCherry (**Fig. 2.2B**), suggesting that AAV8/CaMKIIα-based vectors primarily target pyramidal neurons in the PL.

AAV8-CaMKIIα-Cre(mCherry) or AAV8-CaMKIIα-mCherry vectors were infused into the PL of *Girk1*$^{fl/fl}$ mice. Following a 4-5 wk recovery period, we evaluated the impact of viral Cre and control treatment on mCherry-positive layer 5/6 PL neurons. Viral Cre treatment yielded smaller baclofen-induced currents in these neurons (**Fig. 2.2C,D**; t_{20}=4.33, ***P=0.0003; unpaired student's t test). While loss of GIRK channel activity had no impact on RMP (**Fig. 2.2E**; t_{21}=0.64, P=0.53; unpaired student's t test), rheobase was decreased (**Fig. 2.2F**; t_{21}=4.32, ***P=0.0003; unpaired student's t test), consistent with an increase in excitability.

To assess the behavioral consequences of the manipulation, *Girk1*$^{fl/fl}$ mice were infused with CaMKIIα-Cre(mCherry) or control vector, followed by open-field activity assessments. Suppression of GIRK channel activity in PL pyramidal neurons did not impact distance traveled following saline injection (baseline) but did enhance the motor-stimulatory effect of acute cocaine (15 mg/kg IP) (**Fig. 2.2G**; two-way repeated measures ANOVA, significant interaction between drug and viral treatment, $F_{1,15}$=7.71, P=0.014;

Bonferroni's *post hoc* test, **P*=0.011 (Cre vs. control vector, with respect to cocaine-induced locomotion)), recapitulating the behavioral impact of RNAi-based suppression of GIRK channel activity in PL neurons [28]. In a separate cohort, we tested the impact of the manipulation on trace fear conditioning, an associative learning task dependent on PL function [42,199,210]. Loss of GIRK channel activity in PL pyramidal neurons was associated with decreased cue fear recall, though the difference between Cre-treated and control subjects did not reach statistical significance (**Fig. 2.2H**; U=62.0, *P*=0.063; unpaired non-parametric Mann-Whitney test). Thus, loss of GIRK channel activity in PL pyramidal neurons enhanced the motor-stimulatory effect of cocaine but did not significantly impact baseline activity or trace fear learning.

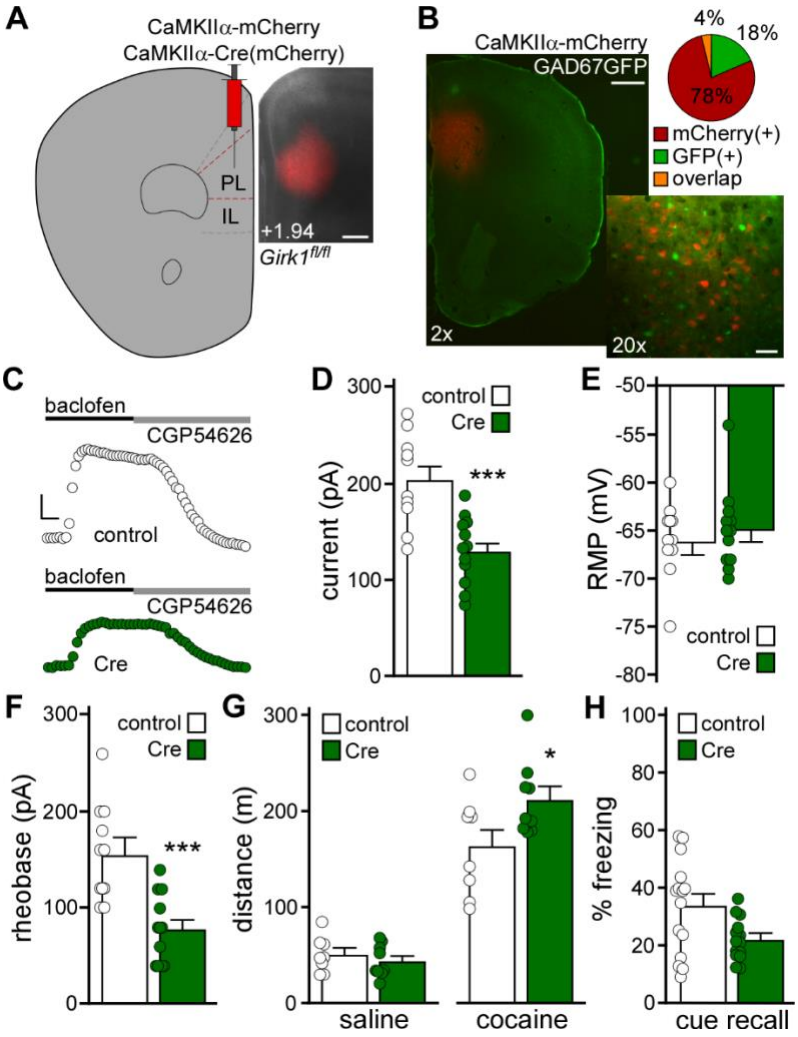

Figure 2.2 Viral Cre ablation of GIRK channels in PL pyramidal neurons

A) Example of viral targeting in a *Girk1*$^{fl/fl}$ mouse treated with AAV8-CaMKIIα-Cre(mCherry) vector. Scale: 325 microns. **B)** AAV8-CaMKIIα-mCherry labeling in the PL of a GAD67GFP(+) mouse, and a pie chart depicting percentage of fluorescent neurons expressing mCherry, GFP, or both (overlap) (n=935, 222, 45 neurons, respectively; N=3 mice). Scale: 500 microns (2x)/50 microns (20x). **C)** Currents evoked by baclofen (200 μM) in layer 5/6 PL pyramidal neurons from *Girk1*$^{fl/fl}$ mice treated with CaMKIIα-Cre(mCherry) or control vector. Currents were reversed by the $GABA_BR$ antagonist CGP54626 (2 μM). Scale: 50 pA/50 s. **D)** Baclofen-induced currents in layer 5/6 PL pyramidal neurons from *Girk1*$^{fl/fl}$ mice treated with CaMKIIα-Cre(mCherry) or control vector (***P<0.001; unpaired student's t test; n=10-12 recordings/group and N=3-6 mice/group). No main effect of sex was detected ($F_{1,18}$=0.15, P=0.71; two-way ANOVA). **E)** RMP in layer 5/6 PL pyramidal neurons from *Girk1*$^{fl/fl}$ mice treated with CaMKIIα-Cre(mCherry) or control vector (unpaired student's t test; n=11-12 recordings/group and N=3-6 mice/group). No main effect of sex was detected ($F_{1,19}$=0.079, P=0.78; two-way ANOVA).

F) Rheobase in layer 5/6 PL pyramidal neurons from *Girk1*$^{fl/fl}$ mice treated with CaMKIIα-Cre(mCherry) or control vector (***P<0.001; unpaired student's t test; n=11-12/group and N=3-6 mice/group). No main effect of sex was detected ($F_{1,19}$=1.11, P=0.31; two-way ANOVA). **G)** Saline- and acute cocaine-induced (15 mg/kg IP) motor activity in *Girk1*$^{fl/fl}$ mice treated with CaMKIIα-Cre(mCherry) or control vector (*P<0.05, two-way repeated measures ANOVA with Bonferroni's *post hoc* test; N=8-9 mice/group). No main effect of sex ($F_{1,13}$=0.061, P=0.81), or sex interactions, were detected (three-way repeated measures ANOVA). **H)** Trace fear conditioning in *Girk1*$^{fl/fl}$ mice treated with CaMKIIα-Cre(mCherry) or control vector. Percent freezing observed during cue recall test, conducted 2 d after trace fear conditioning (unpaired non-parametric Mann-Whitney test; N=14-15 mice/group). No main effect of sex was detected ($F_{1,26}$=3.271, P=0.082; two-way ANOVA). One outlier animal was excluded.

Chemogenetic excitation of PL pyramidal neurons

As repeated cocaine is associated with multiple adaptations that enhance mPFC pyramidal neuron excitability, we sought to complement the persistent viral Cre manipulation of GIRK channel activity with chemogenetic approaches to acutely enhance PL pyramidal neuron excitability. AAV8-CaMKIIα-hM3Dq(mCherry) or AAV8-CaMKIIα-mCherry vectors were infused into the PL of C57BL/6J mice (**Fig. 2.3A**). Following a 3-4 wk recovery, we tested whether chemogenetic excitation enhanced layer 5/6 PL pyramidal neuron excitability. Bath application of CNO (10 μM) significantly depolarized (**Fig. 2.3B**; ΔRMP, $t_{8.86}$=4.39, $^{**}P$=0.0018; unpaired student's *t* test with Welch's correction) and decreased the rheobase (**Fig. 2.3C;** Δrheobase, t_{12}=5.82, $^{****}P$<0.0001; unpaired student's *t* test) of hM3Dq(mCherry)-expressing, but not control, layer 5/6 PL pyramidal neurons.

We next examined the impact of chemogenetic excitation of PL pyramidal neurons on motor activity and trace fear conditioning. CNO pre-treatment elevated activity measured after both saline and cocaine injection in hM3Dq(mCherry)-expressing C57BL/6J mice, relative to controls (**Fig. 2.3D**; two-way repeated measures ANOVA, main effects of drug ($F_{1,16}$=63.29, *P*<0.0001) and viral ($F_{1,16}$=15.01, $^{\#\#}P$=0.0013) treatment, no interaction between drug and viral treatment ($F_{1,16}$=0.70, *P*=0.414)). Chemogenetic excitation of PL pyramidal neurons during trace fear conditioning was associated with lower freezing levels during the subsequent cue recall test (**Fig. 2.3E**; t_{23}=2.23, $^{*}P$=0.036; unpaired student's *t* test). In a parallel study, we used the well-characterized CaMKIICre line and Cre-dependent AAV vectors to drive expression of hM3Dq(mCherry) or mCherry in PL pyramidal neurons (**Fig. 2.3F**). In slice validation experiments, CNO (10 μM) depolarized (**Fig. 2.3G**; ΔRMP, t_7=6.34, $^{***}P$=0.0004; unpaired student's *t* test with Welch's correction) and decreased the rheobase (**Fig. 2.3H**; Δrheobase, $t_{14.26}$=5.58,

****P<0.0001; unpaired student's t test with Welch's correction) of hM3Dq(mCherry)-expressing layer 5/6 PL neurons. CNO pre-treatment elevated motor activity measured after both saline and cocaine injection in hM3Dq(mCherry)-expressing mice (**Fig. 2.3I**; mixed-effects model, main effects of drug ($F_{1,12}$=59.57, P<0.0001) and viral ($F_{1,15}$=18.32, ###P=0.0007) treatment, no interaction between drug and viral treatment ($F_{1,12}$=0.98, P=0.34)), and chemogenetic excitation of PL pyramidal neurons during trace fear conditioning decreased cue fear recall (**Fig. 2.3J**; t_{20}=3.23, **P=0.0042; unpaired student's t test). Thus, acute excitation of PL pyramidal neurons increased motor activity at baseline and following cocaine injection, and disrupted trace fear learning.

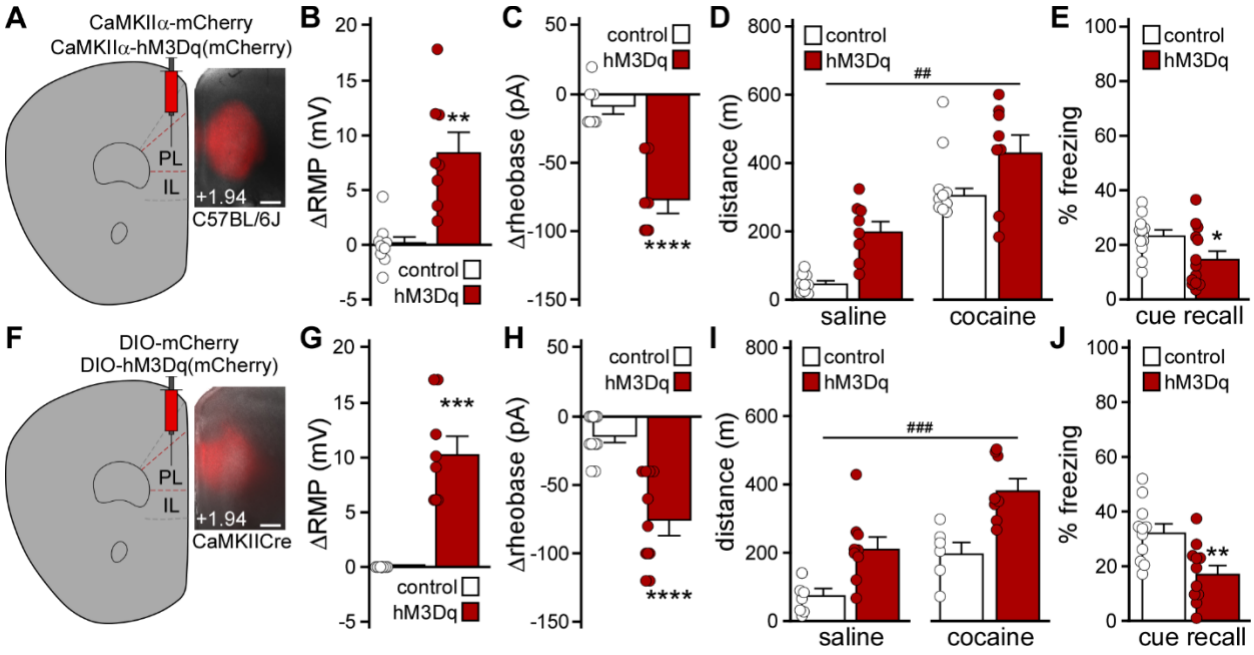

Figure 2.3. Impact of chemogenetic excitation of PL pyramidal neurons on behavior

A) Example of viral targeting in a C57BL/6J mouse treated with AAV8-CaMKIIα-hM3Dq(mCherry). Scale: 325 microns. **B)** Change in RMP induced by CNO (10 μM) in layer 5/6 PL pyramidal neurons from male C57BL/6J mice treated with AAV8-CaMKIIα-hM3Dq(mCherry) or control vector (***P*<0.01; unpaired student's *t* test with Welch's correction; n=8-9 recordings/group and N=3 mice/group). **C)** Change in rheobase induced by CNO (10 μM) in layer 5/6 PL pyramidal neurons from male C57BL/6J mice treated with CaMKIIα-hM3Dq(mCherry) or control vector (*****P*<0.0001; unpaired student's *t* test; n=7 recordings/group and N=3 mice/group). **D)** Saline- and acute cocaine-induced (15 mg/kg IP) motor activity in male C57BL/6J mice treated with CaMKIIα-hM3Dq(mCherry) or control vector, measured 30-min after CNO administration (2 mg/kg IP) ($^{\#\#}P$<0.01, main effect of viral treatment; N=8-10 mice/group). **E)** Trace fear conditioning in male C57BL/6J mice treated with CaMKIIα-hM3Dq(mCherry) or control vector. Percent freezing observed during cue recall test, conducted 2 d after trace fear conditioning in the presence of CNO (2 mg/kg IP) (**P*<0.05; unpaired student's *t* test; N=12-13 mice/group). **F)** Example of viral targeting in a CaMKIICre(+) mouse treated with AAV8-hSyn-DIO-mCherry. Scale: 325 microns. **G)** Change in RMP induced by CNO (10 μM) in layer 5/6 PL pyramidal neurons from CaMKIICre(+) mice treated with DIO-hM3Dq(mCherry) or control vector (****P*<0.001; unpaired student's *t* test with Welch's correction; n=8-11 recordings/group and N=3-5 mice/group). No main effect of sex was detected ($F_{1,15}$=1.94, *P*=0.18; two-way ANOVA).

H) Change in rheobase induced by CNO (10 μM) in layer 5/6 PL pyramidal neurons from CaMKIICre(+) mice treated with DIO-hM3Dq(mCherry) or control vector (****P<0.0001; unpaired student's t test with Welch's correction; n=11 recordings/group and N=3-5 mice/group). No main effect of sex was detected ($F_{1,18}$=0.82, P=0.38; two-way ANOVA). **I)** Saline- and acute cocaine-induced (15 mg/kg) motor activity in CaMKIICre(+) mice treated with DIO-hM3Dq(mCherry) or control vector, measured 30-min after systemic CNO administration (2 mg/kg IP) ($^{###}P$<0.001, main effect of viral treatment; N=6-9 mice/group). No main effect of sex ($F_{1,13}$=2.224, P=0.16), or sex interactions, were detected (mixed-effects model). **J)** Trace fear conditioning in CaMKIICre(+) (hM3Dq) and CaMKIICre(-) (control) mice treated with DIO-hM3Dq(mCherry) vector. Percent freezing observed during the cue recall test, conducted 2 d after trace fear conditioning in the presence of CNO (2 mg/kg IP) (**P<0.01; unpaired student's t test; N=11 mice/group). No main effect of sex was detected ($F_{1,18}$=1.48, P=0.24; two-way ANOVA).

Chemogenetic inhibition of PL GABA neurons

Prolonged cocaine exposure reduces GABAergic neurotransmission in PL pyramidal neurons [28,217,222], which should indirectly enhance PL pyramidal neuron excitability. Indeed, chemogenetic inhibition of layer 5/6 PL GABA neurons decreased the frequency of spontaneous inhibitory postsynaptic currents (sIPSCs) in adjacent pyramidal neurons (**Fig. 2.4A-C**; t_3=4.32, **P*=0.023; paired student's *t* test). To mimic reduced GABAergic input to PL pyramidal neurons in drug-naïve C57BL/6J mice, we used a viral chemogenetic approach involving the forebrain GABAergic neuron promoter/enhancer mDlx [235] to acutely inhibit PL GABA neurons (**Fig. 2.4D**). To test whether AAV8/mDlx-based vectors selectively targeted PL GABA neurons, we infused AAV8-mDlx-mCherry into the PL of GAD67GFP(+) mice. A large majority (76%) of PL neurons co-expressed GFP and mCherry, and a small fraction (7%) expressed only mCherry (**Fig. 2.4E**). Thus, AAV8/mDlx-based vectors afford relatively selective access to mouse PL GABA neurons. Notably, CNO hyperpolarized (**Fig. 2.4F**; ΔRMP, $t_{18.07}$=11.08, *****P*<0.0001; unpaired student's *t* test with Welch's correction) and increased the rheobase (**Fig. 2.4G**; Δrheobase, $t_{23.3}$=3.948, ****P*=0.0006; unpaired student's *t* test with Welch's correction) of hM4Di(mCherry)-expressing layer 5/6 PL GABA neurons in C57BL/6J mice.

We next examined the impact of chemogenetic inhibition of PL GABA neurons on motor activity and trace fear conditioning in C57BL/6J mice. CNO pre-treatment elevated motor activity measured after both saline and cocaine injection in hM4Di(mCherry)-treated subjects, compared to controls (**Fig. 2.4H**; two-way ANOVA, main effects of drug ($F_{1,28}$=37.99, *P*<0.0001) and viral ($F_{1,28}$=60.70, ####*P*<0.0001) treatment, no interaction between drug and viral treatment ($F_{1,28}$=0.416, *P*=0.52)), and chemogenetic inhibition of PL GABA neurons during trace fear conditioning was associated with decreased cue fear recall (**Fig. 2.4I**; t_{13}=2.20, **P*=0.047; unpaired student's *t* test). Thus, chemogenetic

inhibition of PL GABA neurons, like chemogenetic excitation of PL pyramidal neurons, increased motor activity at baseline and following cocaine injection, and disrupted trace fear learning.

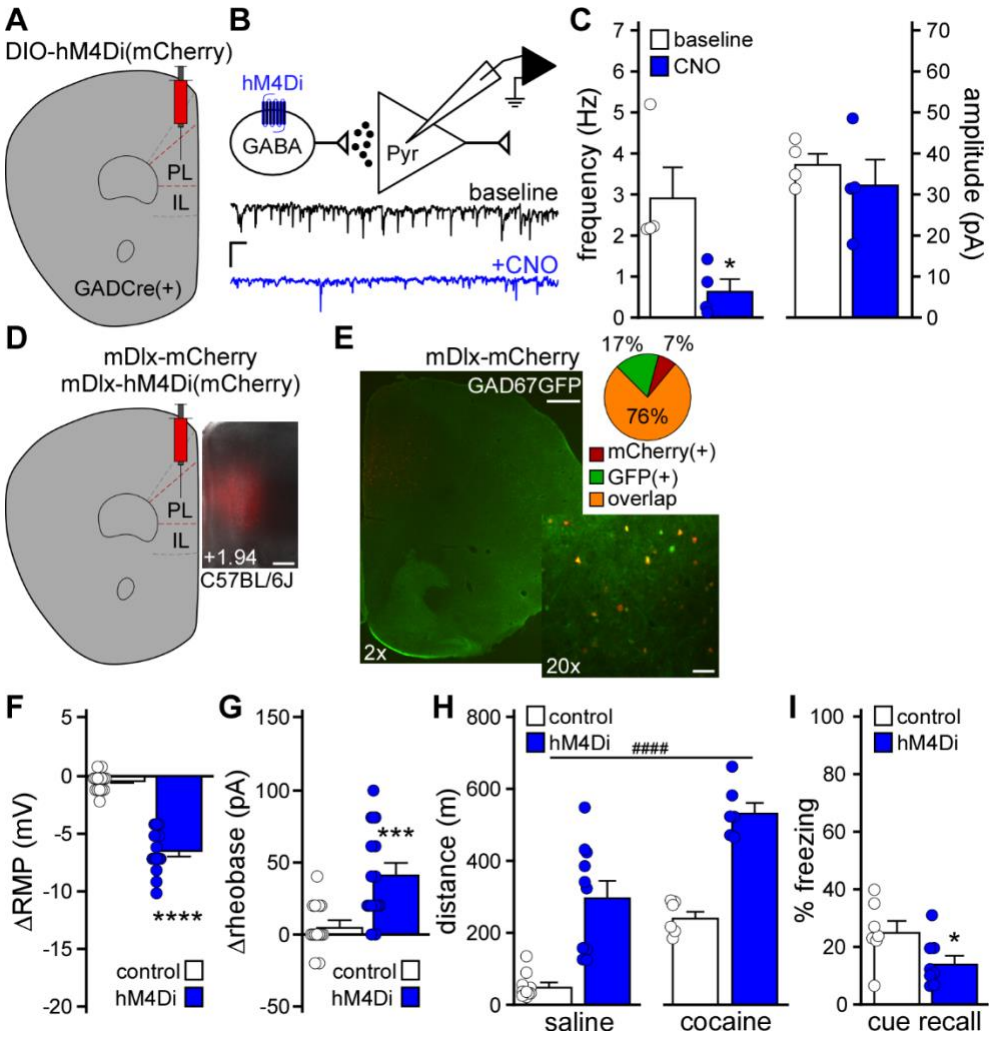

Figure 2.4. Impact of chemogenetic inhibition of PL GABA neurons on behavior

A) GADCre(+) mice were treated with intra-PL AAV8-hSyn-DIO-hM4Di(mCherry) vector. **B)** Spontaneous inhibitory postsynaptic currents (sIPSCs) were recorded in layer 5/6 PL pyramidal neurons from GADCre(+) mice treated with DIO-hM4Di(mCherry) vector (V_{hold}=-70 mV), before (baseline) and after bath application of CNO (10 μM). Scale = 20 pA/1 s. **C)** sIPSC frequency and amplitude in layer 5/6 PL pyramidal neurons, measured before and after CNO (10 μM) application in slices from GADCre(+) mice treated with DIO-hM4Di(mCherry) vector (*P<0.05; paired student's t test; n=4 recordings/group and N=2 male mice/group). **D)** Example of viral targeting in a C57BL/6J mouse treated with AAV8-mDlx-mCherry. Scale: 325 microns. **E)** AAV8-mDlx-mCherry labeling in the PL of GAD67GFP(+) mouse, and pie chart depicting percent of fluorescent neurons expressing mCherry, GFP, or both (overlap) (n=26, 62, 286 neurons, respectively; N=3 mice). Scale bars: 500 microns (2x)/50 microns (20x). **F)** Change in RMP induced by CNO (10 μM) in layer 5/6 PL GABA neurons from male C57BL/6J mice treated with mDlx-hM4Di(mCherry) or control vector (****P<0.0001; unpaired student's t test with Welch's correction; n=14 recordings/group and N=6 mice/group). **G)** Change in rheobase induced by CNO (10 μM) in layer 5/6 PL GABA neurons from male C57BL/6J mice treated with mDlx-

hM4Di(mCherry) or control vector (***P<0.001; unpaired student's t test with Welch's correction; n=14-16 recordings/group and N=6 mice/group). **H)** Saline- and acute cocaine-induced (15 mg/kg IP) motor activity in separate cohorts of male C57BL/6J mice treated with mDlx-hM4Di(mCherry) or control vector, measured 30-min after CNO administration (2 mg/kg IP) ($^{\#\#\#\#}P$<0.0001, main effect of viral treatment; N=6-10 mice/group). **I)** Trace fear conditioning in male C57BL/6J mice treated with mDlx-hM4Di(mCherry) or control vector. Percent freezing observed during the cue recall test, conducted 2 d after trace fear conditioning in the presence of CNO (2 mg/kg IP) (*P<0.05; unpaired student's t test; N=7-8 mice/group).

Chemogenetic excitation of distinct PL projections

We next used a projection-specific viral chemogenetic approach to manipulate PL neurons projecting to the BLA, NAc, or VTA [12,36,39,236]. These brain regions were selected because they receive glutamatergic input from the PL and regulate fear learning and/or motor activity [186,237-242]. We infused an AAV2retro-based [243] Cre vector (AAV2retro-hSyn-Cre-GFP) into the downstream target of interest, and a Cre-dependent vector (AAV8-hSyn-DIO-hM3Dq(mCherry) or AAV8-hSyn-DIO-mCherry) into the PL (**Fig. 2.5A,B,E,H**). The impact of chemogenetic excitation of each PL projection was first assessed using trace fear conditioning, 4-5 wk after surgery. While excitation of PL pyramidal neurons projecting to the BLA (**Fig. 2.5C**; t_{17}=0.543, *P*=0.59; unpaired student's *t* test) or NAc (**Fig. 2.5F**; NAc, t_{18}=1.109, *P*=0.28; unpaired student's *t* test) during trace fear conditioning did not affect cue fear recall, excitation of VTA-projecting PL pyramidal neurons disrupted cue fear learning (**Fig. 2.5I**; t_{19}=2.667, **P*=0.0152; unpaired student's *t* test).

We next assessed the impact of exciting each PL projection on motor activity. Chemogenetic excitation of BLA-projecting PL pyramidal neurons did not impact saline-induced activity, but did suppress cocaine-induced activity (**Fig. 2.5D**; two-way repeated measures ANOVA, significant interaction between drug and viral treatment ($F_{1,17}$=13.17, *P*=0.0021); Bonferroni's *post hoc* test, *****P* <0.0001 (DREADD vs. control vector, with respect to cocaine-induced locomotion)). Chemogenetic excitation of NAc-projecting PL pyramidal neurons had no effect on saline- or cocaine-induced motor activity (**Fig. 2.5G**; two-way repeated measures ANOVA, main effect of drug treatment ($F_{1,18}$=99.73, *P*<0.0001), no main effect of viral treatment ($F_{1,18}$=2.795, *P*=0.11) or interaction between drug and viral treatment ($F_{1,18}$=0.74, *P*=0.40)). Excitation of VTA-projecting PL pyramidal neurons enhanced activity measured after saline or cocaine injection (**Fig. 2.5J**; two-way repeated measures ANOVA, main effects of drug ($F_{1,19}$=40.65, *P*<0.0001) and viral

($F_{1,19}$=21.78, $^{###}P$=0.0002) treatment, no interaction between drug and viral treatment ($F_{1,19}$=1.986, P=0.17)). Thus, acute excitation of VTA-projecting PL pyramidal neurons recapitulated the motor activity and trace fear learning phenotypes seen with comprehensive excitation of PL pyramidal neurons.

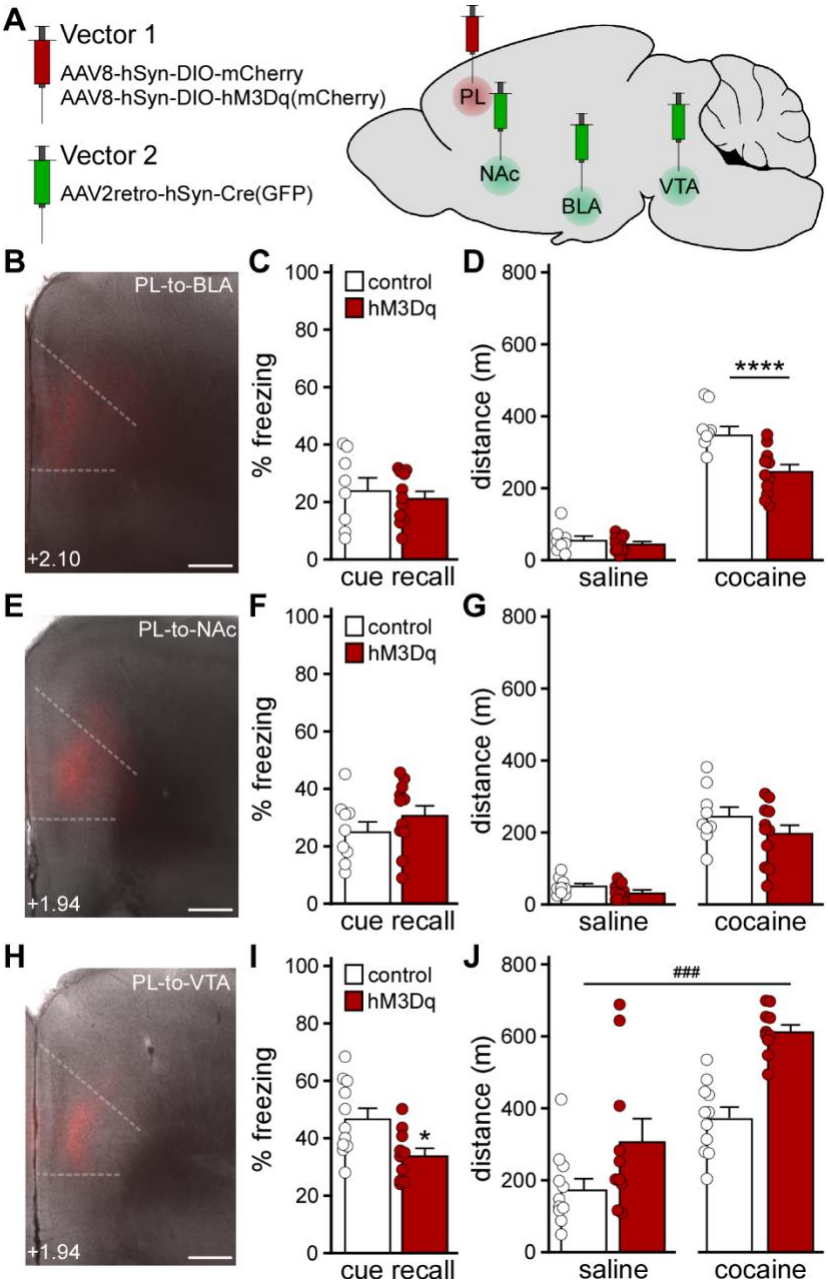

Figure 2.5. Impact of chemogenetic excitation of distinct PL projections on behavior

A) Projection-specific chemogenetic approach involving a Cre-dependent Vector 1 (AAV8-hSyn-DIO-hM3Dq(mCherry) or AAV8-hSyn-DIO-mCherry) infused into the PL, and AAV2retro-hSyn-Cre(GFP) was infused into the BLA, NAc, or VTA. **B)** Cre-dependent mCherry expression in the PL of a C57BL/6J mouse treated with intra-PL AAV8-hSyn-DIO-mCherry and intra-BLA AAV2retro-hSyn-Cre(GFP). Scale: 325 microns. **C)** Trace fear conditioning in male C57BL/6J mice treated with intra-PL DIO-hM3Dq(mCherry) or control vector, and intra-BLA AAV2retro-Cre(GFP). Percent freezing observed during the cue recall test, conducted 2 d after trace fear conditioning in the presence of CNO (2 mg/kg

IP) (unpaired student's *t* test; N=8-11 mice/group). **D)** Saline- and acute cocaine-induced (15 mg/kg IP) motor activity in male C57BL/6J mice treated with intra-PL DIO-hM3Dq(mCherry) or control vector, and intra-BLA AAV2retro-Cre(GFP), measured 30-min after CNO administration (2 mg/kg IP) (****P<0.0001, two-way repeated measures ANOVA with Bonferroni's *post hoc* test; N=8-11 mice/group). **E)** Cre-dependent mCherry expression in the PL of a C57BL/6J mouse treated with intra-PL AAV8-hSyn-DIO-mCherry and intra-NAc AAV2retro-hSyn-Cre(GFP). Scale: 325 microns. **F)** Trace fear conditioning in male C57BL/6J mice treated with intra-PL DIO-hM3Dq(mCherry) or control vector, and intra-NAc AAV2retro-Cre(GFP). Percent freezing observed during the cue recall test, conducted 2 d after trace fear conditioning in the presence of CNO (2 mg/kg IP) (unpaired student's *t* test; N=9-11 mice/group). **G)** Saline- and acute cocaine-induced (15 mg/kg IP) motor activity in male C57BL/6J mice treated with intra-PL DIO-hM3Dq(mCherry) or control vector, and intra-NAc AAV2retro-Cre(GFP), measured 30-min after CNO administration (2 mg/kg IP) (two-way repeated measures ANOVA; N=9-11 mice/group). **H)** Cre-dependent mCherry expression in the PL of a C57BL/6J mouse treated with intra-PL AAV8-hSyn-DIO-mCherry and intra-VTA AAV2retro-hSyn-Cre(GFP). Scale: 325 microns. **I)** Trace fear conditioning in male C57BL/6J mice treated with intra-PL DIO-hM3Dq(mCherry) or control vector, and intra-VTA AAV2retro-Cre(GFP). Percent freezing observed during the cue recall test, conducted 2 d after trace fear conditioning in the presence of CNO (2 mg/kg IP) (*P<0.05; unpaired student's *t* test; N=10-11 mice/group). **J)** Saline- and acute cocaine-induced (15 mg/kg IP) motor activity in male C57BL/6J mice treated with intra-PL DIO-hM3Dq(mCherry) or control vector, and intra-VTA AAV2retro-Cre(GFP), measured 30-min after systemic CNO administration (2 mg/kg IP) (###P<0.001, main effect of viral treatment; N=10-11 mice/group).

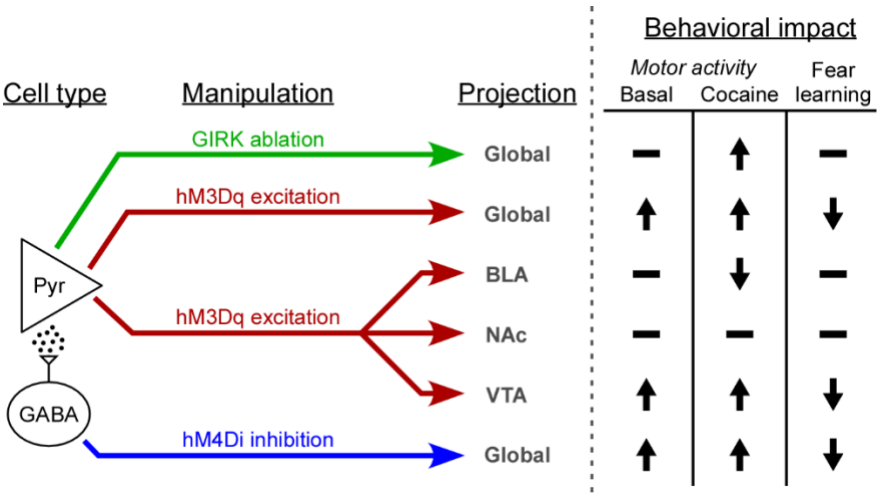

Figure 2.6. Behavioral impact of PL pyramidal neuron excitability manipulations

Schematic detailing the behavioral consequences of neuron- and/or projection-specific acute (chemogenetic) and persistent (GIRK ablation) manipulations that enhance PL pyramidal neuron excitability.

2.4 DISCUSSION

Previously, we reported that repeated cocaine exposure increased layer 5/6 PL pyramidal neuron excitability, likely due to a suppression of GIRK-dependent signaling [28]. The adaptations required D_1 dopamine receptor (D_1R) activation, implicating mesocortical dopaminergic neurotransmission. These adaptations were evident during early withdrawal (1-2 d after the last cocaine injection) and were not seen in adjacent layer 2/3 pyramidal neurons or layer 5/6 IL pyramidal neurons. Using an identical cocaine treatment regimen and timeline, we found that repeated cocaine does not impact GIRK-dependent signaling in, or excitability of, layer 5/6 PL GABA neurons. As some cocaine-induced adaptations are evident at earlier [213] or later [244] withdrawal timepoints, our cocaine treatment regimen may evoke adaptations in layer 5/6 PL GABA neurons outside the 1-2 d withdrawal window. It is also possible that repeated cocaine provokes adaptations in distinct interneuron sub-populations [213].

RNAi-based suppression of GIRK channel expression in the PL enhanced the motor-stimulatory effect of cocaine [28]. Here, we show that selective suppression of GIRK channel activity in PL pyramidal neurons recapitulates this phenotype. This finding aligns with other reports implicating the PL and $GABA_BR$-dependent signaling in locomotor sensitization. For example, PL lesions blocked the induction and expression of cocaine-induced locomotor sensitization [196-198], and baclofen infusion into the mPFC blocked acute cocaine-induced locomotion and induction of locomotor sensitization without affecting basal activity [43,245]. Collectively, these lines of evidence suggest that the cocaine-induced suppression of GIRK-dependent signaling in PL pyramidal neurons contributes to locomotor sensitization.

The mPFC regulates cognitive functions [42,199], including trace fear learning [206,209,210]. Persistent firing in the PL during the trace interval is critical for trace fear

learning [201-210], and optogenetic silencing of the PL either throughout the conditioning session, or during the trace interval, precludes fear learning [210]. Our chemogenetic data show that acute excitation of PL pyramidal neurons during conditioning can also disrupt fear learning. Disruptions in trace fear learning during conditioning may reflect impairments in attention and/or working memory [199], processes that are altered by psychostimulant exposure in humans [246-248], non-human primates [249], and rodents [250,251]. Alternatively, our chemogenetic manipulations, which likely impacted PL pyramidal neuron excitability during and shortly after conditioning, may also have disrupted memory consolidation [252].

Prolonged exposure to cocaine persistently elevates PL pyramidal neuron excitability [28,215,216,220,221] and reduces GABAergic neurotransmission in these neurons [28,217,222]. To mimic these adaptations in drug-naïve mice, we used three distinct approaches: viral Cre ablation of GIRK channels, chemogenetic excitation of PL pyramidal neurons, and chemogenetic inhibition of PL GABA neurons. While viral Cre ablation of GIRK channel activity in PL pyramidal neurons did not impact saline-induced motor activity, direct or indirect chemogenetic excitation of PL pyramidal neurons did. The outcomes were surprising given prior reports that chemogenetic excitation of PL pyramidal neurons did not alter open field activity [231,233]. These differences may relate to the scope of viral targeting, test duration, and/or behavioral testing history of subjects employed [253]. In line with our results, disinhibiting PL neurons by antagonizing $GABA_A$Rs or blocking GABA synthesis increased locomotion in 30-min open field tests [254,255]. Notably, neither of our chemogenetic manipulations, designed to mimic chronic cocaine-induced plasticity, occluded the acute motor-stimulatory effect of cocaine. Thus, acute cocaine exposure and acute PL pyramidal neuron excitation likely work through distinct/additive mechanisms to augment locomotion.

Chemogenetic excitation in PL pyramidal neurons enhanced key measures of neuronal excitability (rheobase and RMP), enhanced motor activity measured after saline or cocaine injection, and disrupted trace fear learning. In contrast, GIRK ablation increased PL pyramidal neuron excitability (rheobase but not RMP), enhanced cocaine-induced but not baseline activity, and evoked a non-significant decrease in trace fear learning. Why do persistent (GIRK ablation) and acute (chemogenetic) manipulations targeting PL pyramidal neurons yield overlapping but distinct behavioral outcomes? We speculate that ablation of GIRK channels, predominantly located in the somatodendritic compartment [123,256], preferentially impact somatodendritic physiology of PL pyramidal neurons, whereas chemogenetic excitation exerts a multi-faceted influence on intracellular signaling in somatodendritic/postsynaptic and axonal/presynaptic compartments [257]. Moreover, the persistent suppression of GIRK channel activity may promote compensatory adaptations not seen in acute chemogenetic models.

For our projection-specific manipulations, we targeted brain regions that receive glutamatergic input from the PL and regulate fear learning and/or motor activity (**Fig. 2.6**). The NAc has been implicated in fear learning [239] and the acute motor-stimulatory effect of cocaine [258], and mPFC inputs are involved in the development and expression of locomotor sensitization [186]. Nevertheless, we did not see any impact of exciting NAc-projecting PL pyramidal neurons on fear learning, or motor activity. Consistent with the latter finding, optogenetic stimulation of dorsal mPFC-to-NAc projections did not alter movement velocity in mice [36]. Similarly, despite evidence that activity in the PL and BLA are necessary for trace fear learning [210,240,242], we found that exciting BLA-projecting PL pyramidal neurons was without effect. This result is consistent with a study showing that optogenetic excitation of dorsal mPFC-amygdala projections did not affect cue fear learning in a delay fear conditioning model [259]. Interestingly, while exciting BLA-

projecting PL pyramidal neurons did not affect basal locomotion, in line with similar reports [259,260], this manipulation suppressed cocaine-induced activity. Taking into account previous reports showing that reversible inactivation of the BLA enhanced hyperactivity evoked by either cocaine [237] or amphetamine [261,262], our findings suggest that BLA neuron excitability is negatively correlated with cocaine-induced motor activity and subject to modulation via PL glutamate.

The VTA plays a significant role in motor activity and locomotor sensitization [186,241]. Chemogenetic inhibition of VTA DA neurons reduced basal and cocaine-induced locomotion [263], while exciting VTA DA neurons, or the VTA-to-NAc projection, elevated basal locomotion [241,263-266]. mPFC pyramidal neurons synapse onto VTA DA neurons [12,267,268] and activation of the mPFC [269,270] or intra-VTA infusion of glutamatergic agonists [271,272] induces burst-spiking of VTA DA neurons *in vivo*. mPFC stimulation also enhances DA release in the NAc [269,273,274], suggesting that exciting the PL projection to the VTA directly activates the mesolimbic DA pathway. Indeed, an excitatory monosynaptic projection from the mPFC to NAc-projecting VTA DA neurons has been reported [275]. VTA-projecting mPFC neurons exhibit cocaine-induced plasticity that facilitates glutamate release in the VTA and contributes to addictive behaviors, including behavioral sensitization [28,186]. We report here that acute stimulation of PL projections to the VTA enhances motor activity measured following saline or cocaine injection. The VTA also regulates aversive learning [238], and optogenetic inhibition of VTA DA neurons during footshock (but not auditory cue) presentation enhanced cue fear recall [276]. We show that acute excitation of VTA-projecting PL pyramidal neurons during trace fear conditioning disrupts cue fear recall. As the PL-to-VTA projection is subject to cocaine-induced plasticity [28], it is tempting to speculate that some of the dysregulation of

learning/memory processes seen following chronic cocaine exposure is linked in part to enhanced excitability of VTA-projecting PL pyramidal neurons [200].

In summary, we show that distinct manipulations of PL pyramidal neuron excitability in drug-naïve mice exert overlapping but distinct consequences on behaviors relevant to addiction. Our work further suggests that enhanced excitability of the glutamatergic PL projection to the VTA pre-sensitizes mice to the motor-stimulatory effect of cocaine and disrupts associative fear learning. As such, interventions that suppress the excitability of this microcircuit may prove useful for suppressing problematic behaviors linked to chronic cocaine intake.

Chapter 3: GIRK channel activity in prelimbic pyramidal neurons regulates the extinction of cocaine conditioned place preference in male mice

Contributions: T.R.R. designed research, performed research, analyzed data, and wrote the first draft of the paper; T.R.R., K.W., and E.M.F.d.V. edited the paper; E.M.F.d.V. contributed unpublished reagents/analytic tools.

3.1 INTRODUCTION

Chronic use of addictive drugs induces short- and long-term effects on plasticity throughout the mesocorticolimbic reward system. These drug-induced adaptations can provoke negative affective states, such as anxiety and depression, and promote the formation of long-term memories of the environmental stimuli associated with the drug use experience [200,277,278]. Over time, exposure to just the stimuli (e.g., context, cues) is sufficient to trigger physiological and psychological states that motivate continued drug use and relapse after abstinence [200,279,280]. From a therapeutic perspective, treating negative affective states and enhancing inhibitory control over drug conditioned responses is crucial for preventing relapse, but requires a deeper understanding of the underlying plasticity mechanisms and neural circuitry.

Past research has implicated the prefrontal cortex (PFC) in cue-induced drug seeking. In patients with substance use disorders, for example, the PFC is hyperactivated by exposure to drug-associated stimuli, and the level of hyperactivity correlates with drug

cravings [200]. In rodents, activity in the prelimbic (PL) subregion of the medial PFC (mPFC) is important for cue-induced drug seeking [46,47], particularly activation of PL pyramidal neurons that project to the NAc core [48]. PL pyramidal neurons encode reward-predictive cues [36], and undergo synaptic potentiation following drug exposure [281] that correlates with drug-seeking behavior [220,282]. These neurons also regulate affect-related behaviors and several cognitive functions relevant to addiction [283,284], including extinction learning [285,286], a process whereby the salience of a memory is reduced when a stimulus is repeatedly presented without reinforcement. Importantly, the extinction of drug reward memories is a learning process that could be targeted by behavioral and/or pharmacological interventions to prevent relapse [279]. The success of such approaches, however, depends on the elucidation of drug-induced plasticity mechanisms and neural correlates that underlie addiction-related behaviors. Given the strong overlap between functions regulated by the PL and those disrupted in addiction, considerable investigative effort has been directed at identifying drug-induced plasticity mechanisms in this brain region.

Prior work from our laboratory and others has shown that chronic cocaine exposure drives a persistent increase in the intrinsic excitability of PL pyramidal neurons [215,216,218-221,287,288]. This adaptation is attributable in part to a suppression of inhibitory G protein-dependent signaling mediated by $GABA_B$ receptors ($GABA_BR$) and G protein-gated inwardly rectifying K^+ (GIRK) channels [28,216]. Reduced GIRK channel activity in PL pyramidal neurons of drug-naive mice is sufficient to potentiate the motor-stimulatory effect of cocaine [31], yet the impact of this plasticity mechanism on other addiction-relevant behaviors remains unclear. Since GABAergic tone in the PL has been implicated in the regulation of affect-related behaviors [289-291], as well as the expression and extinction of cocaine-related memories [285,292], we sought to investigate whether reduced $GABA_BR$-GIRK signaling in PL pyramidal neurons influences affect- and cocaine reward-related

behaviors. Here, we employed complementary viral genetic approaches to selectively ablate the GIRK channel or $GABA_BR$ in PL pyramidal neurons, and then assessed the behavioral impact of these manipulations on tests of mood-related behaviors and cocaine conditioned place preference (CPP) and extinction. In parallel, we investigated the behavioral impact of acute chemogenetic excitation of, or GIRK channel overexpression in, PL pyramidal neurons. Our findings inform the neuronal populations and molecular mechanisms that mediate extinction learning in the PFC, and provide support for GIRK channels as therapeutic targets to disrupt cocaine-conditioned responding.

3.2 METHODS

Animals. All experiments were approved by the University of Minnesota Institutional Animal Care and Use Committee. The generation of *Girk1*$^{fl/fl}$ mice was described previously [225]. CaMKIICre (B6.Cg-Tg(Camk2a-cre)T29-1Stl/J, RRID:IMSR_JAX:005359) and Cre-dependent Cas9GFP (B6J.129(B6N)-Gt(ROSA)26Sortm1(CAG-cas9*,-EGFP)Fezh/J, RRID:IMSR_JAX:026175) knock-in lines were purchased from The Jackson Laboratory (Bar Harbor, ME) and were maintained by backcrossing against the C57BL/6J strain. Heterozygous CaMKIICre(+) and homozygous Cas9GFP(+/+) lines were crossed to yield CaMKIICre(+):Cas9GFP(+/+) mice. Male C57BL/6J mice were purchased from The Jackson Laboratory and used as wild-type controls in some studies. Mice were group housed, maintained on a 14:10 h light/dark cycle, and were provided ad libitum access to food and water.

Chemicals. Baclofen was purchased from Sigma Millipore (Burlington, MA), CGP54626 and clozapine-N-oxide (CNO) were purchased from Tocris Bioscience (Bristol, UK), and

cocaine hydrochloride was obtained through Boynton Health Pharmacy at the University of Minnesota (Minneapolis, MN).

Viral vectors. The Genome Engineering and iPSC Center of Washington University (St. Louis, MO) designed and tested a guide RNA (gRNA) sequence targeting the *Gabbr1* ($GABA_{B1}$; referred throughout as GB1) gene. Notably, this *Gabbr1* gRNA targeted a shared sequence near the N-terminus of the two most abundant isoforms – *Gabbr1a* and *Gabbr1b*. The target sequences for the *Gabbr1* gRNA, and a control gRNA targeting LacZ [293], were as follows: Gabbr1: 5'-ACGGCGTGCAGTATACATCG-3', LacZ: 5'-TGCGAATACGCCCACGCGAT-3'. Oligonucleotides containing gRNA sequences were purchased from Integrated DNA Technologies (Coralville, IA) and cloned into the following plasmids by the University of Minnesota Viral Vector and Cloning Core (Minneapolis, MN): pAAV-U6-gRNA(*Gabbr1*)-hSyn-NLSmCherry and pAAV-U6-gRNA(LacZ)-hSyn-NLSmCherry. pAAV-CaMKIIα-GIRK2c(eGFP), pAAV-CaMKIIα-hM3Dq(mCherry), and pAAV-CaMKIIα-mCherry plasmids were generated by the University of Minnesota Viral Vector and Cloning Core using standard cloning techniques and pAAV-CaMKIIα-hChR2(C128S/D156A)-mCherry (RRID:Addgene_35502, a gift from Karl Deisseroth) as the backbone, as described previously [31,294]. AAV8-CaMKIIα-Cre(mCherry) and AAV8-CaMKIIα-eGFP were purchased from the University of North Carolina Vector Core (Chapel Hill). All other viral vectors were packaged in AAV8 serotype by the University of Minnesota Viral Vector and Cloning Core; viral titers were between 0.2 and 4 × 10^{14} genocopies/ml.

Intracranial viral manipulations. Intracranial infusion of virus (400 nL per side) into the PL (+2.00 mm AP, ±0.45 mm ML, −1.60 mm DV) of mice (7-8 wk) was performed as

described previously [31,227]. The viral load and optimized coordinates yielded extensive coverage of the PL along anterior/posterior and medial/ventral axes, with limited spread into the adjacent anterior cingulate, medial orbital, and infralimbic cortices. After surgery, animals were allowed 2-3 wk (chemogenetic or GIRK2 overexpression studies) or 4-5 wk (GIRK1 or GB1 ablation studies) for full recovery and gene expression before behavioral and/or electrophysiological assessments. The scope and accuracy of viral targeting were assessed using fluorescence microscopy as previously described [31]. Brightfield and fluorescent images were overlaid and evaluated using the mouse brain atlas [228], and only data from mice in which >70% of viral-driven bilateral fluorescence was confined to the PL were included in the final analysis.

Slice electrophysiology. Somatodendritic currents evoked by baclofen (200 μM) were recorded in layer 5/6 PL pyramidal neurons from 11-13 wk old mice, as described previously [295]. Peak current amplitudes were analyzed using Clampfit v. 10.7 software (Molecular Devices; San Jose, CA). For rheobase assessments, cells were held at 0 pA in current-clamp mode and given 1 s current pulses, beginning at −60 pA and increasing in 20 pA increments. Rheobase was identified as the injection step at which initial spiking was elicited.

Elevated plus maze. Mice were acclimated to the testing room (1 h), and handling (5 min), 1 d prior to testing. On test day, mice were transferred to the testing room 1 h before evaluation. Mice were then placed in the center of a lit (~250 lux) maze (L/W/H: 75 ×10 × 53 cm), facing an open arm and away from the experimenter, and their subsequent activity was recorded for 5 min by video camera. Time spent in the open arms, closed arms, maze

center, and total distance traveled were extracted using ANY-maze 5.2 software (Stoelting Co; Wood Dale, IL). Data from animals that fell off the maze were excluded from analysis.

Forced swim test. FST studies were performed 2-3 d after EPM studies. Mice were transferred to the testing room 1 h before evaluation. Mice were then placed in a 4 L beaker filled with 1.5 L of 23-25°C water, and video was recorded for 6 min using a video camera and ANY-maze 5.2 software (Stoelting Co). The latency to first immobile bout, and percent time immobile during the final 4 min of testing, were analyzed by hand using ANY-Maze software.

Cocaine conditioned place preference. Cocaine CPP studies were performed 3-4 d after FST experiments (except for chemogenetic studies in which EPM/FST were not assessed). CPP was performed in two-compartment chambers (Med Associates; Fairfax, VT; L/W/H: 16.76 × 12.7 × 12.7 cm per compartment) housed within sound-attenuating cubicles. The chambers contained custom wall inserts that were constructed from polycarbonate sheets and designed to exhibit two visually distinct (vertical or horizontal striped walls) compartments using black and white electrical tape. Both compartments contained identical overhead lighting (single 2.8 W light bulb), but different flooring (wire mesh or metal rods) to permit tactile discrimination. Mice were acclimated to the testing room (30 min), and handling (5 min), 1-2 d before the CPP paradigm. On Day 1 (baseline testing), mice were placed in the chamber for 20 min with the door separating the compartments open; time spent in each compartment was recorded using Med-PC IV software (Med Associates). On Days 2-4 (conditioning), mice were subjected to two 20-min conditioning sessions, one in the morning (0800-1100) and one in the afternoon (1300-1600). In the morning session, mice were given a saline injection (IP) and confined

to the compartment that was preferred on Day 1. In the afternoon sessions, mice were given cocaine (15 mg/kg, IP) and confined to the opposite compartment. On Day 5 (preference testing), mice were placed in the chamber for 20 min with the door open; time spent in each compartment was recorded. On Days 8-9 (extinction training), mice underwent two 20-min extinction training sessions that mirrored the conditioning sessions on Days 2-4, with the exception that saline replaced cocaine in afternoon sessions. On Day 10 (extinction testing), mice were placed in the chamber for 20 min with the door open; time spent in each compartment was recorded. In chemogenetic studies, mice were injected with CNO (2 mg/kg, IP) 30 min prior to extinction testing on Day 10. In GIRK overexpression studies, mice underwent a modified CPP procedure involving only one day of extinction training (Day 8) prior to extinction testing (Day 9). For all studies, time spent in each compartment during testing on Day 1 (baseline), Day 5 (preference), and Day 9 or Day 10 (extinction) was analyzed. Preference scores were determined by calculating the ratio of time spent in the cocaine-paired side to total time spent in both sides. Movement during the extinction test was measured as the total number of beam breaks within both compartments. Only data from animals that formed a preference for the drug-paired side, designated by greater time spent in the drug-paired side than the saline-paired side during the Day 5 preference test, were included in analyses.

Experimental design and statistical analysis. Data are presented as the mean ± SEM. Statistical analyses were performed using GraphPad Prism 9 (GraphPad Software; San Diego, CA). Given prior reports of intrinsic sex differences in both mPFC and $GABA_BR$-GIRK physiology and function [295-299], data from male and female mice were analyzed separately in all studies. Electrophysiology, EPM, FST, and CPP movement data were analyzed by unpaired Student's *t* test, with or without Welch's correction, as necessary.

CPP preference scores were analyzed by one- or two-way repeated-measures ANOVA. Pairwise comparisons were performed using Bonferroni's *post hoc* test, if justified. Within-subjects factors include test day (baseline, preference, extinction) and between-subjects factors include viral treatment (Cre, *Gabbr1* gRNA, hM3Dq, GIRK2, control), where appropriate. Sample size (*n* or *N*) per group and statistical details of experiments are reported in the figure legends and Results. Differences were considered significant when $p < 0.05$.

3.3 RESULTS

Impact of PL pyramidal neuron-selective GIRK ablation on EPM and FST performance

Neurons in the mPFC track behavioral states in the EPM and FST [300,301], and optogenetic and chemogenetic manipulations targeting PL neurons modulate anxiety- and depression-related behaviors [283]. To probe the behavioral relevance of reduced GIRK channel activity in layer 5/6 PL pyramidal neurons, we used a PL pyramidal neuron-selective viral Cre approach and conditional Girk1$^{-/-}$ (*Girk1*$^{fl/fl}$) mice to selectively ablate GIRK1 (**Fig. 3.1A**), a critical subunit that contributes to channel formation in these neurons [28,295]. Throughout our study, we utilized the CaMKIIα promoter to selectively drive transgene expression in pyramidal neurons of the PL [31]. We previously reported that this manipulation reduced GIRK channel activity in, and increased intrinsic excitability of, layer 5/6 PL pyramidal neurons [31]. Importantly, both of these electrophysiological outcomes were similarly observed in PL pyramidal neurons from mice that were subjected to repeated cocaine exposure [28].

Girk1$^{fl/fl}$ mice received intra-PL infusions of CaMKIIα-Cre(mCherry) or CaMKIIα-mCherry vectors, and after a 4-5 wk recovery period, we evaluated the impact of viral Cre

or control treatment on EPM and FST (**Fig. 3.1B**). Viral Cre treatment did not impact total distance traveled (**Fig. 3.1C**; male: t(28) = 1.709, p = 0.099; female: t(27) = 0.883, p = 0.385; unpaired Student's t test) or percent time spent in the open arms of the EPM (**Fig. 3.1D**; male: t(28) = 0.906, p = 0.373; female: t(27) = 0.047, p = 0.963; unpaired Student's t test), nor did it impact latency to the first immobile bout (**Fig. 3.1E**; male: t(29) = 0.508, p = 0.615; female: t(28) = 1.579, p = 0.126; unpaired Student's t test) or percent time spent immobile in the FST (**Fig. 3.1F**; male: t(29) = 0.631, p = 0.533, unpaired Student's t test; female: t(19.45) = 0.151, p = 0.881, unpaired Student's t test with Welch's correction) in male or female mice. Thus, loss of GIRK channel activity in PL pyramidal neurons does not influence these measures of general locomotion, avoidance-like behavior, or behavioral despair in mice.

Impact of PL pyramidal neuron-selective GIRK ablation on cocaine CPP and extinction

GABAergic signaling in the PL has been implicated in the expression and extinction of context-evoked cocaine memories [285,292,302], and reduced GIRK channel function in PL pyramidal neurons enhanced behavioral sensitivity to the motor-stimulatory effect of cocaine [31]. To determine if decreased GIRK channel function in PL pyramidal neurons also influences cocaine reward-related learning, we examined the impact of PL pyramidal neuron-selective GIRK channel ablation on the acquisition and extinction of cocaine (15 mg/kg, IP) CPP (**Fig. 3.1A,B,G**).

Both Cre-treated and control male mice acquired place preference (**Fig. 3.1H**; two-way repeated-measures ANOVA, significant interaction between test day and viral treatment, F(2,40) = 5.688, p = 0.0067; Bonferroni's post hoc test: baseline vs preference: Cre [****p < 0.0001], control [***p = 0.0003]), with no difference between viral treatment

groups (**Fig. 3.1H**; Cre vs control vector: preference [p = 0.9196]). While extinction of place preference was observed in both groups (**Fig. 3.1H**; preference vs extinction: Cre [****p < 0.0001], control [****p < 0.0001]), extinction was diminished in male Cre-treated animals, as compared with controls (**Fig. 3.1H**; Cre vs control vector: extinction [**p = 0.0062]).

Acquisition and extinction of place preference were similarly observed in female Cre-treated (**Fig. 3.1I**; one-way repeated-measures ANOVA; significant effect of test day [F(1.947,9.737) = 21.05, p = 0.0003], Bonferroni's post hoc test: baseline vs preference [*p = 0.01], preference vs extinction [**p = 0.0065]) and control (**Fig. 3.1I**; one-way repeated-measures ANOVA; significant effect of test day [F(1.918,15.35) = 17.33, p = 0.0001], Bonferroni's post hoc test: baseline vs preference [**p = 0.0018], preference vs extinction [**p = 0.0076]) mice, but no differences were observed between viral treatment groups (**Fig. 3.1I**; two-way repeated-measures ANOVA; main effect of test day [F(2,26) = 33.39, ****p < 0.0001], no main effect of viral treatment [F(1,13) = 1.062, p = 0.322], no interaction between test day and viral treatment [F(2,26) = 0.8922, p = 0.422]). Thus, reduced GIRK channel activity in PL pyramidal neurons selectively impairs extinction of cocaine CPP in male, but not female, mice.

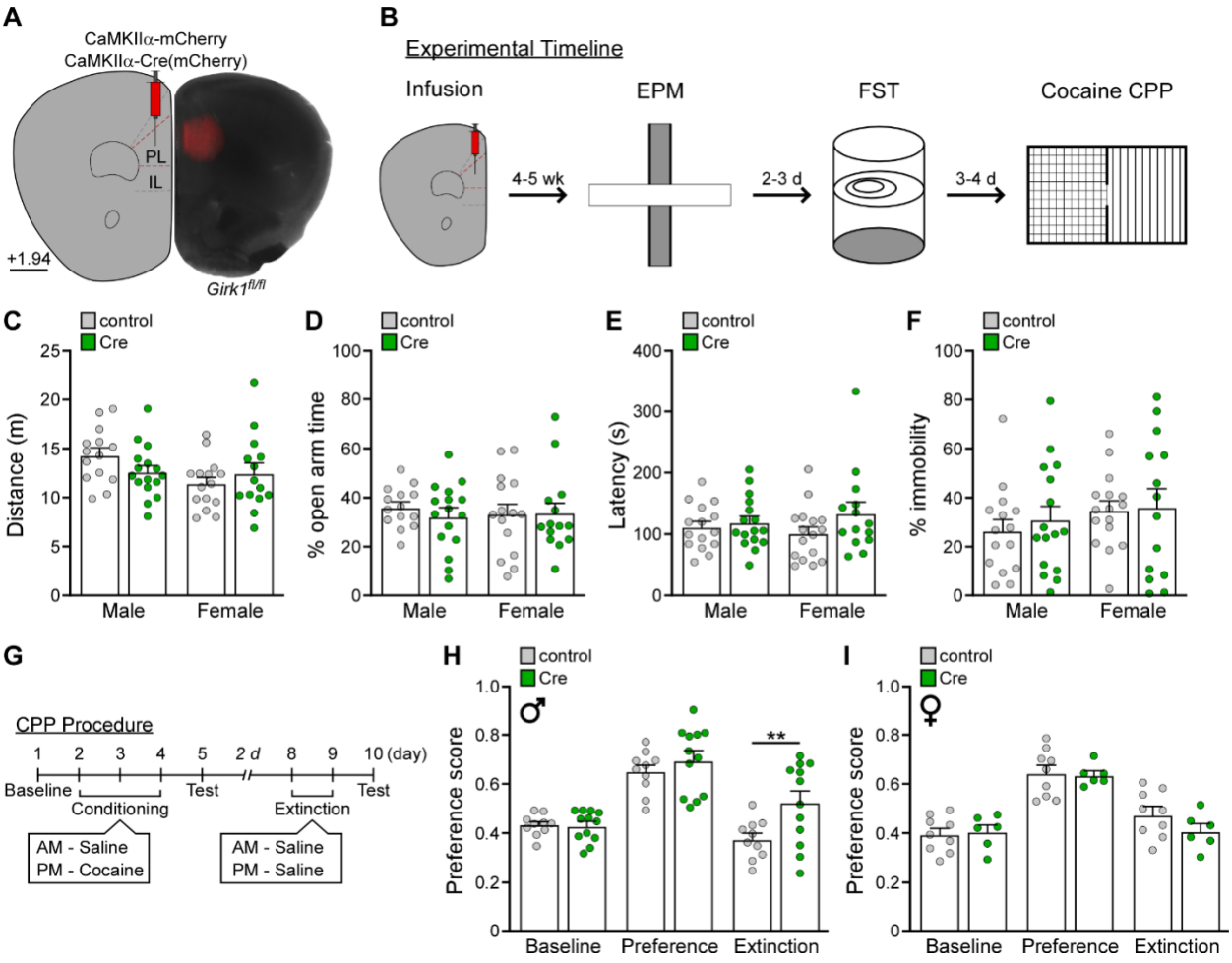

Figure 3.1. Impact of GIRK channel ablation in PL pyramidal neurons on affect- and reward-related behaviors

A) Example of viral targeting in a *Girk1*$^{fl/fl}$ mouse treated with AAV8-CaMKIIα-Cre(mCherry) vector. Scale: 650 microns. **B)** Schematic depicting the timeline of viral infusion and behavioral testing in EPM, FST, and cocaine CPP. **C)** Total distance traveled during the EPM test in *Girk1*$^{fl/fl}$ mice treated with CaMKIIα-Cre(mCherry) or control vector (male and female: unpaired Student's t test). N = 14-16 male mice/group, 14-15 female mice/group. **D)** Percent time spent in the open arms during the EPM test in *Girk1*$^{fl/fl}$ mice treated with CaMKIIα-Cre(mCherry) or control vector (male and female: unpaired Student's t test). N = 14-16 male mice/group, 14-15 female mice/group. **E)** Latency to first immobile bout during the FST test in *Girk1*$^{fl/fl}$ mice treated with CaMKIIα-Cre(mCherry) or control vector (male and female: unpaired Student's t test). N = 15-16 male mice/group, 14-16 female mice/group. **F)** Percent time spent immobile during the FST test in *Girk1*$^{fl/fl}$ mice treated with CaMKIIα-Cre(mCherry) or control vector (male: unpaired Student's t test; female: unpaired Student's t test with Welch's correction). N = 15-16 male mice/group, 14-16 female mice/group. **G)** Schematic outlining the cocaine (15 mg/kg, IP) CPP procedure. **H)** Preference scores during 20-min session during baseline, preference, and extinction testing in cocaine (15 mg/kg, IP) conditioned male *Girk1*$^{fl/fl}$ mice treated with CaMKIIα-Cre(mCherry) or control vector. **p < 0.01 (two-way repeated-measures ANOVA with

Bonferroni's post hoc test). N = 10-12 mice/group. **I)** Preference scores during 20-min session during baseline, preference, and extinction testing in cocaine (15 mg/kg, IP) conditioned female *Girk1*$^{fl/fl}$ mice treated with CaMKIIα-Cre(mCherry) or control vector (two-way repeated-measures ANOVA). N = 6-9 mice/group.

Impact of PL pyramidal neuron-selective $GABA_BR$ ablation on behavioral performance

While GIRK channels strongly couple to $GABA_BRs$ in PL pyramidal neurons [31], they also serve as inhibitory effectors for other G protein-coupled receptors [79]. Thus, as a complementary model of the cocaine-induced suppression of $GABA_BR$-GIRK signaling, we used a PL pyramidal neuron-selective viral CRISPR/Cas9 approach to selectively ablate $GABA_{B1}$ (GB1) (**Fig. 3.2A**), an obligate subunit of $GABA_BRs$. This approach involved the infusion of gRNA vectors targeting GB1 (U6-gRNA(*Gabbr1*)-hSyn-NLSmCherry), or bacterial β-galactosidase (U6-gRNA(LacZ)-hSyn-NLSmCherry) as control, into the PL of CaMKIICre:Cas9GFP mice, which selectively express Cas9 and eGFP in Cre(+) cells [293].

Vectors harboring *Gabbr1* or control gRNAs were infused into the PL of CaMKIICre:Cas9GFP mice, and following a 4-5 wk recovery period, we evaluated the impact of viral treatment on mCherry- and eGFP-positive layer 5/6 PL neurons. *Gabbr1* gRNA treatment abolished somatodendritic currents evoked by the $GABA_BR$ agonist baclofen in these neurons from male and female mice (**Fig. 3.2B,C**; male: $t(8.853) = 8.342$, ****$p < 0.0001$; female: $t(10.86) = 6.077$, ****$p < 0.0001$; unpaired Student's t test with Welch's correction). However, loss of $GABA_BR$ activity had no impact on RMP (**data not shown**; male: $t(10.85) = 1.440$, $p = 0.178$, unpaired Student's t test with Welch's correction; female: $t(9) = 0.4774$, $p = 0.645$, unpaired Student's t test) or rheobase (**Fig. 3.2D**; male: $t(16) = 1.552$, $p = 0.140$; female: $t(10) = 0.2749$, $p = 0.789$; unpaired Student's t test) in male or female mice. Interestingly, this lack of impact of $GABA_BR$ ablation on basal intrinsic excitability contrasts with the significant reduction in rheobase observed following GIRK channel ablation [31].

To examine the behavioral consequences of the manipulation, CaMKIICre:Cas9GFP mice were infused with *Gabbr1* gRNA or control, followed by assessments in the EPM, FST, and cocaine CPP paradigm (**Fig. 3.2I**). GB1 ablation did not impact total distance traveled (**Fig. 3.2E**; male: t(27) = 0.473, p = 0.640; female: t(23) = 0.631, p = 0.5346; unpaired Student's t test) or percent time spent in the open arms of the EPM (**Fig. 3.2F**; male: t(27) = 0.196, p = 0.8458; female: t(23) = 0.3503, p = 0.7293; unpaired Student's t test), nor did it impact latency to the first immobile bout (**Fig. 3.2G**; male: t(27) = 0.050, p = 0.9602; female: t(23) = 0.930, p = 0.3621; unpaired Student's t test) or percent time spent immobile in the FST (**Fig. 3.2H**; male: t(27) = 1.950, p = 0.062; female: t(23) = 0.700, p = 0.4908; unpaired Student's t test).

While both acquisition and extinction of place preference were observed in male *Gabbr1* gRNA-treated (**Fig. 3.2J**; one-way repeated-measures ANOVA; significant effect of test day [F(1.547,12.37) = 28.63, p < 0.0001], Bonferroni's post hoc test: baseline vs preference [***p = 0.0001], preference vs extinction [***p = 0.0006]) and control (**Fig. 3.2J**; one-way repeated-measures ANOVA; significant effect of test day [F(1.946,17.52) = 26.96, p < 0.0001], Bonferroni's post hoc test: baseline vs preference [***p = 0.0002], preference vs extinction [***p = 0.0004]) mice, no differences were observed between viral treatment groups (**Fig. 3.2J**; two-way repeated-measures ANOVA; main effect of test day [F(1.806,30.7) = 54.50, p < 0.0001], no main effect of viral treatment [F(1,17) = 2.395, p = 0.14], no interaction between test day and viral treatment [F(2,34) = 0.5695, p = 0.57]). Similarly, acquisition and extinction of place preference were observed in female *Gabbr1* gRNA-treated (**Fig. 3.2K**; one-way repeated-measures ANOVA; significant effect of test day [F(1.214,8.495) = 7.784, p = 0.0189], Bonferroni's post hoc test: baseline vs preference [*p = 0.0266], preference vs extinction [**p = 0.0032]) and control (**Fig. 3.2K**; one-way repeated-measures ANOVA; significant effect of test day [F(1.653,9.921) =

28.63, p = 0.0001], Bonferroni's post hoc test: baseline vs preference [**p = 0.0012], preference vs extinction [**p = 0.0074]) mice, and no differences were observed between viral treatment groups (**Fig. 3.2K**; two-way repeated-measures ANOVA; main effect of test day [F(2,26) = 23.12, p < 0.0001], no main effect of viral treatment [F(1,13) = 0.003, p = 0.96], no interaction between test day and viral treatment [F(2,26) = 0.206, p = 0.82]). Thus, reduced $GABA_BR$ activity in PL pyramidal neurons does not impact EPM, FST, or the acquisition and extinction of cocaine CPP in male or female mice.

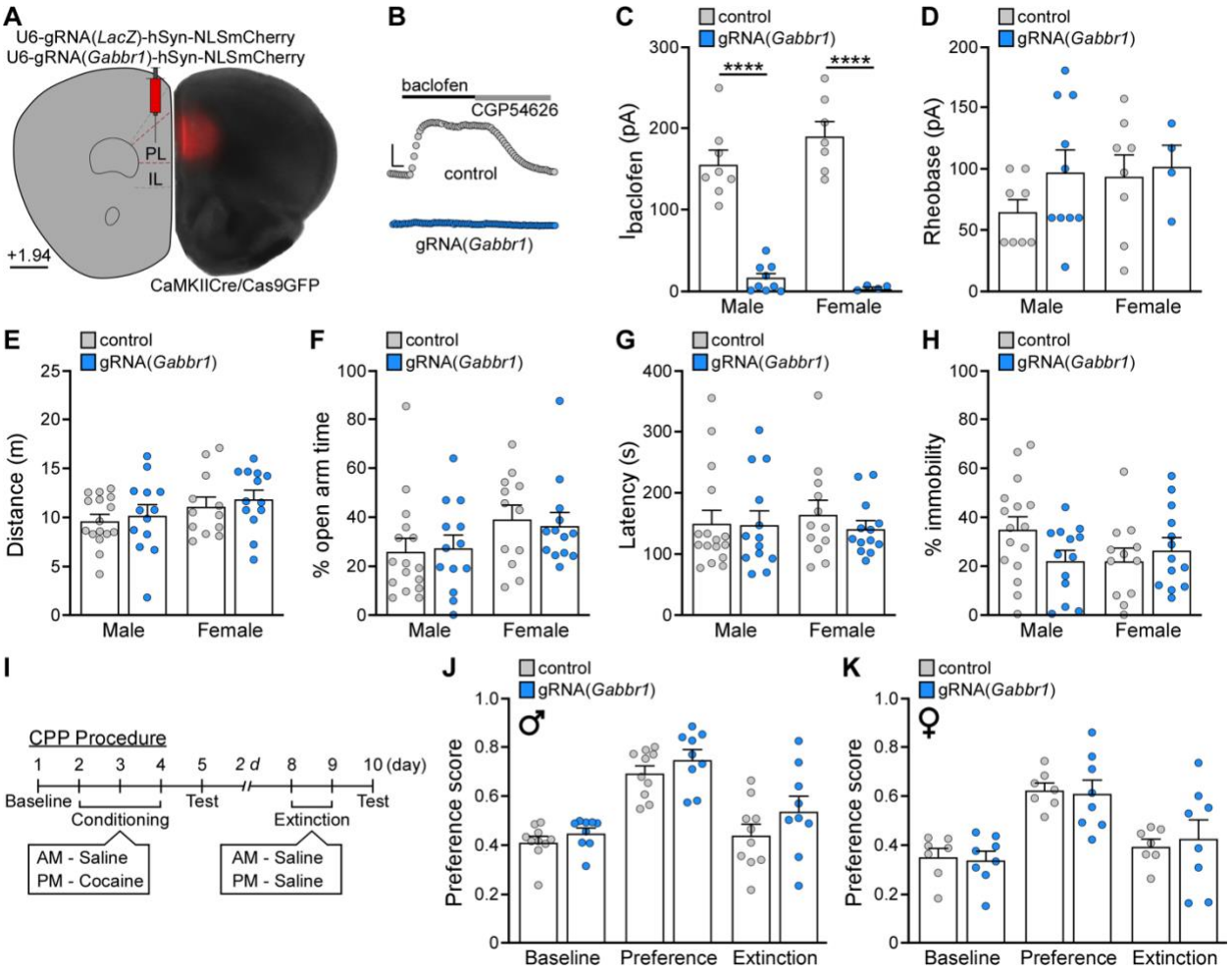

Figure 3.2. Impact of $GABA_BR$ ablation in PL pyramidal neurons on affect- and reward-related behaviors

A) Example of viral targeting in a CaMKIICre:Cas9GFP mouse treated with AAV8-U6-gRNA(*Gabbr1*)-hSyn-NLSmCherry vector. Scale: 650 microns. **B)** Currents evoked by baclofen (200 μM) in layer 5/6 PL pyramidal neurons from CaMKIICre:Cas9GFP mice treated with U6-gRNA(*Gabbr1*)-hSyn-NLSmCherry or control vector. Currents were reversed by the $GABA_BR$ antagonist CGP54626 (2 μM). Calibration: 100 pA/60 s. **C)** Baclofen-induced currents in layer 5/6 PL pyramidal neurons from CaMKIICre:Cas9GFP mice treated with U6-gRNA(*Gabbr1*)-hSyn-NLSmCherry or control vector. Male: ****$p < 0.0001$ (unpaired Student's t test with Welch's correction), n = 8-9 recordings/group and N = 3-4 mice/group. Female: ****$p < 0.0001$ (unpaired Student's t test with Welch's correction), n = 4-7 recordings/group and N = 2-3 mice/group. **D)** Rheobase in layer 5/6 PL pyramidal neurons from CaMKIICre:Cas9GFP mice treated with U6-gRNA(*Gabbr1*)-hSyn-NLSmCherry or control vector. Male: unpaired Student's t test, n = 8-10 recordings/group and N = 3-4 mice/group. Female: unpaired Student's t test, n = 4-8 recordings/group and N = 2-3 mice/group. **E)** Total distance traveled during the EPM test in CaMKIICre:Cas9GFP mice treated with U6-gRNA(*Gabbr1*)-hSyn-NLSmCherry or control vector (male and female: unpaired Student's t test). N = 13-16 male mice/group, 12-13 female mice/group. **F)** Percent time spent in the open arms during the EPM test in

CaMKIICre:Cas9GFP mice treated with U6-gRNA(*Gabbr1*)-hSyn-NLSmCherry or control vector (male and female: unpaired Student's t test). N = 13-16 male mice/group, 12-13 female mice/group. **G)** Latency to first immobile bout during the FST test in CaMKIICre:Cas9GFP mice treated with U6-gRNA(*Gabbr1*)-hSyn-NLSmCherry or control vector (male and female: unpaired Student's t test). N = 13-16 male mice/group, 12-13 female mice/group. **H)** Percent time spent immobile during the FST test in CaMKIICre:Cas9GFP mice treated with U6-gRNA(*Gabbr1*)-hSyn-NLSmCherry or control vector (male and female: unpaired Student's t test). N = 13-16 male mice/group, 12-13 female mice/group. **I)** Schematic outlining the cocaine (15 mg/kg, IP) CPP procedure. **J)** Preference scores during 20-min session during baseline, preference, and extinction testing in cocaine (15 mg/kg, IP) conditioned male CaMKIICre:Cas9GFP mice treated with U6-gRNA(*Gabbr1*)-hSyn-NLSmCherry or control vector (two-way repeated-measures ANOVA). N = 9-10 mice/group. **K)** Preference scores during 20-min session during baseline, preference, and extinction testing in cocaine (15 mg/kg, IP) conditioned female CaMKIICre:Cas9GFP mice treated with U6-gRNA(*Gabbr1*)-hSyn-NLSmCherry or control vector (two-way repeated-measures ANOVA). N = 7-8 mice/group.

Impact of PL pyramidal neuron-selective chemogenetic excitation on cocaine CPP and extinction

We found that two complementary models of reduced $GABA_BR$-GIRK signaling, GIRK and $GABA_BR$ ablation, differentially impacted the extinction of cocaine CPP in male mice. GIRK ablation also increased basal cellular excitability [31], while $GABA_BR$ ablation was without effect (**Fig. 3.2D**). Therefore, we hypothesized that increased PL pyramidal neuron excitability underlies the impairment of extinction in male mice. To test this hypothesis, we employed an acute chemogenetic approach (i.e., hM3Dq) to acutely increase the excitability of PL pyramidal neurons in male mice. We previously reported that this manipulation was sufficient to decrease the rheobase of, and depolarize RMP in, layer 5/6 PL pyramidal neurons [31].

Vectors encoding hM3Dq (CaMKIIα-hM3Dq(mCherry)) or control (CaMKIIα-mCherry) were infused into the PL of male C57BL/6J mice (**Fig. 3.3A**). After a 2-3 wk recovery period, we assessed the impact of CNO-induced hM3Dq activation on the extinction of cocaine CPP (**Fig. 3.3B**). CNO (2 mg/kg, IP) was administered 30 min before the extinction test.

Acquisition of CPP was observed in both hM3Dq-treated (**Fig. 3.3C**; one-way repeated-measures ANOVA; significant effect of test day [$F(1.544,13.89) = 24.45$, $p < 0.0001$], Bonferroni's post hoc test: baseline vs preference [****$p < 0.0001$]) and control (**Fig. 3.3C**; one-way repeated-measures ANOVA; significant effect of test day [$F(1.472,16.19) = 23.61$, $p < 0.0001$], Bonferroni's post hoc test: baseline vs preference [****$p < 0.0001$]) mice. However, extinction was also observed in both hM3Dq-treated (**Fig. 3.3C**; preference vs extinction [***$p = 0.0007$]) and control (**Fig. 3.3C**; preference vs extinction [**$p = 0.0088$]) mice, with no difference between viral treatment groups (**Fig. 3.3C**; two-way repeated-measures ANOVA; main effect of test day [$F(1.507,30.14) =$

46.42, p < 0.0001], no main effect of viral treatment [F(1,20) = 0.422, p = 0.52], no interaction between test day and viral treatment [F(2,40) = 0.898, p = 0.42]). While hM3Dq activation did not alter side preference during the extinction test, the manipulation did increase overall movement (**Fig. 3.3D**; t(11.41) = 4.957, ***p = 0.0004; unpaired Student's t test with Welch's correction). Thus, acute excitation of PL pyramidal neurons evokes hyperactivity, but does not impact extinction of cocaine CPP in male mice.

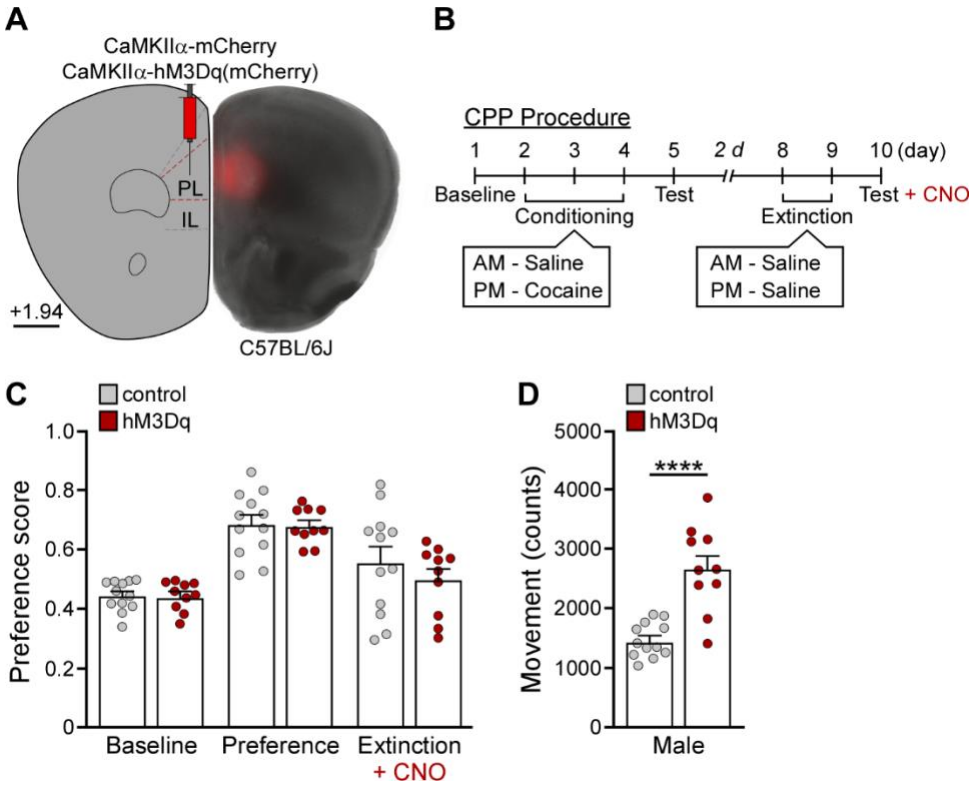

Figure 3.3. Impact of acute chemogenetic excitation of PL pyramidal neurons on reward-related behavior

A) Example of viral targeting in a wild-type (C57BL/6J) mouse treated with AAV8-CaMKIIα-hM3Dq(mCherry) vector. Scale: 650 microns. **B)** Schematic outlining the cocaine (15 mg/kg, IP) CPP procedure. Mice in this procedure were treated with CNO (2 mg/kg, IP) 30 min before the extinction test. **C)** Preference scores during 20-min session during baseline, preference, and extinction testing in cocaine (15 mg/kg, IP) conditioned male C57BL/6J mice treated with CaMKIIα-hM3Dq(mCherry) or control vector (two-way repeated-measures ANOVA). N = 10-12 mice/group. **D)** Total movement within both compartments during the extinction test conducted 30 min after pretreatment with CNO (2 mg/kg, IP) in male C57BL/6J mice treated with CaMKIIα-hM3Dq(mCherry) or control vector. ***p < 0.001 (unpaired Student's t test with Welch's correction). N = 10-12 mice/group.

Impact of PL pyramidal neuron-selective GIRK overexpression on EPM, FST, and cocaine CPP and extinction

Given that loss of GIRK channel activity in PL pyramidal neurons impaired extinction in male mice, we next investigated whether strengthening GIRK-dependent signaling in these neurons could accelerate extinction. To test this hypothesis, we employed a viral overexpression approach to upregulate GIRK2, a key neuronal GIRK channel subunit [79].

GIRK2 overexpression (CaMKIIα-GIRK2c(eGFP)) or control (CaMKIIα-eGFP) vectors were infused into the PL of male C57BL/6J mice (**Fig. 3.4A**), followed 2-3 wk later by behavioral and electrophysiological assessments. GIRK2 overexpression increased somatodendritic baclofen-evoked currents in GFP(+) PL neurons (**Fig. 3.4B,C**; t(7.229) = 7.301, ***p = 0.0001; unpaired Student's t test with Welch's correction). While increased GIRK channel activity had no impact on RMP (**data not shown**; t(14) = 0.236, p = 0.817; unpaired Student's t test), rheobase was increased (**Fig. 3.4D**; t(8.99) = 2.357, *p = 0.0429; unpaired Student's t test with Welch's correction), consistent with a reduction in basal intrinsic excitability.

GIRK2 overexpression did not impact total distance traveled (**Fig. 3.4E**; t(30) = 0.1851, p = 0.85; unpaired Student's t test) or percent time spent in the open arms of the EPM (**Fig. 3.4F**; t(30) = 0.5790, p = 0.57; unpaired Student's t test). While GIRK2 overexpression did not impact latency to the first immobile bout (**Fig. 3.4G**; t(19.50) = 1.555, p = 0.136; unpaired Student's t test with Welch's correction) in the FST, enhanced GIRK channel activity was associated with increased percent time spent immobile, although the difference between GIRK2-treated and control subjects did not reach statistical significance (**Fig. 3.4H**; t(30) = 2.004, p = 0.0541; unpaired Student's t test). The impact of this manipulation was next assessed in an abbreviated cocaine CPP procedure

(**Fig. 3.4I**), which involved a single extinction training session prior to the extinction test to reduce the level of extinction so that manipulation-induced enhancements in extinction could be detected (i.e., to prevent a floor effect). Both GIRK2-treated and control mice acquired CPP (**Fig. 3.4J**; two-way repeated-measures ANOVA, significant interaction between test day and viral treatment, $F(2,42) = 4.383$, $p = 0.0187$; Bonferroni's post hoc test: baseline vs preference: GIRK2 [***$p = 0.0002$], control [****$p < 0.0001$]), with no difference between viral treatment groups (**Fig. 3.4J**; GIRK2 vs control vector: preference [$p = 0.206$]). Although extinction of place preference was observed in both groups (**Fig. 3.4J**; preference vs extinction: GIRK2 [****$p < 0.0001$], control [**$p = 0.0038$]), extinction was enhanced in GIRK2-treated animals as compared to controls (**Fig. 3.4J**; GIRK2 vs control vector: extinction [**$p = 0.0051$]). Thus, strengthening GIRK channel activity in PL pyramidal neurons facilitates extinction of cocaine CPP in male mice.

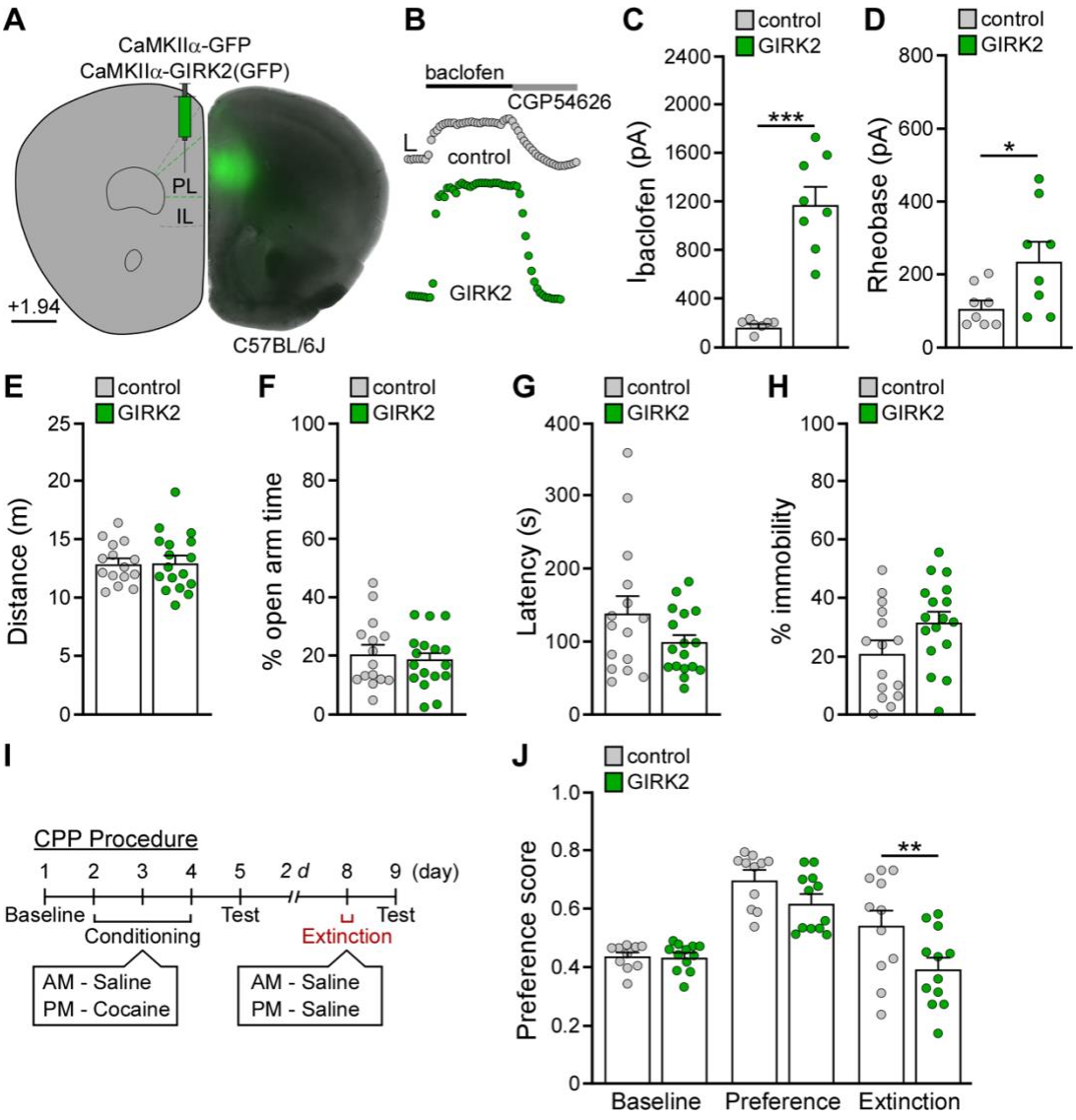

Figure 3.4. Impact of GIRK overexpression in PL pyramidal neurons on affect- and reward-related behavior

A) Example of viral targeting in a male wild-type (C57BL/6J) mouse treated with AAV8-CaMKIIα-GIRK2(GFP) vector. Scale: 650 microns. **B)** Currents evoked by baclofen (200 μM) in layer 5/6 PL pyramidal neurons from male C57BL/6J mice treated with CaMKIIα-GIRK2(GFP) or control vector. Currents were reversed by the $GABA_BR$ antagonist CGP54626 (2 μM). Calibration: 100 pA/50 s. **C)** Baclofen-induced currents in layer 5/6 PL pyramidal neurons from male C57BL/6J mice treated with CaMKIIα-GIRK2(GFP) or control vector. ***$p < 0.001$ (unpaired Student's t test with Welch's correction). n = 7-8 recordings/group and N = 3 mice/group. **D)** Rheobase in layer 5/6 PL pyramidal neurons from male C57BL/6J mice treated with CaMKIIα-GIRK2(GFP) or control vector. *$p < 0.05$ (unpaired Student's t test with Welch's correction). n = 8 recordings/group and N = 3 mice/group. **E)** Total distance traveled during the EPM test in male C57BL/6J mice treated with CaMKIIα-GIRK2(GFP) or control vector (unpaired Student's t test). N = 15-17 mice/group. **F)** Percent time spent in the open arms during the EPM test in male C57BL/6J

mice treated with CaMKIIα-GIRK2(GFP) or control vector (unpaired Student's t test). N = 15-17 mice/group. **G)** Latency to first immobile bout during the FST test in male C57BL/6J mice treated with CaMKIIα-GIRK2(GFP) or control vector (unpaired Student's t test with Welch's correction). N = 15-17 mice/group. **H)** Percent time spent immobile during the FST test in male C57BL/6J mice treated with CaMKIIα-GIRK2(GFP) or control vector (unpaired Student's t test). N = 15-17 mice/group. **I)** Schematic outlining the cocaine (15 mg/kg, IP) CPP procedure. Mice in this procedure underwent a single day of extinction training prior to the extinction test. **J)** Preference scores during 20-min session during baseline, preference, and extinction testing in cocaine (15 mg/kg, IP) conditioned male C57BL/6J mice treated with CaMKIIα-GIRK2(GFP) or control vector. **$p < 0.01$ (two-way repeated-measures ANOVA with Bonferroni's post hoc test). N = 11 mice/group.

3.4 DISCUSSION

Drug-induced adaptations in inhibitory metabotropic signaling pathways have been described throughout the mesocorticolimbic system [26,58]. We previously found that repeated cocaine exposure increased the excitability of PL pyramidal neurons, an adaptation driven in part by a suppression of $GABA_BR$-GIRK signaling [28]. Modeling the loss of GIRK channel activity in PL pyramidal neurons potentiated the motor-stimulatory effect of cocaine [28,31]. Here, we extended these findings by modeling the impact of these cocaine plasticity mechanisms on affect- and cocaine reward-related behaviors.

Withdrawal following chronic cocaine exposure has been correlated with increased anxiety- and depression-like behavior [303-305], as well as altered reactivity of the dorsal PL to anxiogenic stimuli [306]. Although these findings suggest a link between cocaine-induced dysfunction of the PL and negative affect, we observed that the ablation or overexpression of GIRK channels, or ablation of $GABA_BRs$, in PL pyramidal neurons did not alter behavior in the EPM or FST in male or female mice. The outcome was surprising given a recent report that GIRK ablation in PL pyramidal neurons increased open arm time in the EPM and immobility in the FST in male mice [296]. These different behavioral outcomes may relate to the scope of viral targeting and/or differences in the EPM or FST procedures, apparati, and analyses. Indeed, optogenetic and chemogenetic manipulations targeting overlapping but distinct PL subareas, projection neurons, and neighboring brain regions have yielded mixed results in preclinical models of anxiety- and depression-related behaviors [283,284,307]. Therefore, it remains unclear whether hypofunctional $GABA_BR$-GIRK signaling within specific PL pyramidal neuron subpopulations contributes to cocaine-induced behavioral alterations in affect-related behaviors.

Prolonged cocaine exposure has also been correlated with the disruption of multiple cognitive functions that are associated with the mPFC [200,308], including the

extinction of learned fear [309]. While GIRK ablation did not impact the acquisition of cocaine CPP, the manipulation impaired extinction in male, but not female, mice. Our finding aligns with a recent report demonstrating that chemogenetic inhibition of a local GABAergic interneuron population in the dorsal mPFC (dmPFC; including PL and anterior cingulate cortex) during extinction training impaired the extinction of cocaine CPP in male mice [285]. These results suggest that inhibitory activity in adjacent PL pyramidal neurons, including GIRK-dependent signaling, is necessary for the extinction of cocaine context-related memories in male mice. Interestingly, chronic exposure to stress delayed extinction of morphine- and nicotine-induced CPP in male rodents [310,311], and like cocaine, suppressed $GABA_BR$-GIRK signaling in PL pyramidal neurons in male and female mice [296,312]. Our results link these findings to suggest that PL GIRK plasticity in male mice might also contribute to the stress-induced persistence of drug reward-related memories. Whether reduced GIRK channel activity in PL pyramidal neurons impairs extinction by promoting the retrieval of cocaine-associated memories, and/or disrupting the formation of extinction memories, remains an important topic for future research.

The sex difference we observed in the extinction of cocaine CPP was not driven by differences in baseline GIRK channel function, or the efficacy of viral-mediated GIRK ablation, between male and female mice. Indeed, GIRK current amplitudes and intrinsic excitability in layer 5/6 PL pyramidal neurons are similar between young adult (60-70 d) male and female mice [295], and viral Cre-mediated ablation of the GIRK1 subunit had a similar efficacy on both electrophysiological measures (i.e., reduced GIRK currents and increased intrinsic excitability) between males and females [31,296]. However, this sex difference in extinction did align with prior preclinical studies that support a role for the PL in mediating sex differences in conditioned cocaine-seeking behavior [297], as well as extinction of learned fear [313,314]. Importantly, GIRK ablation in PL pyramidal neurons has

been reported to induce cognitive deficits in working memory and behavioral flexibility in male, but not female, mice [296]. Thus, it is possible that diminished behavioral flexibility in male mice may underlie the sex-specific impairment in extinction, perhaps by disrupting discrimination between an initial cocaine-associated memory and a newer extinction memory [315]. If this were true, it might suggest that GIRK channel plasticity in PL pyramidal neurons is sufficient to impair other forms of extinction, including the extinction of learned fear [313,316].

Since $GABA_BRs$ regulate GIRK channel function in PL pyramidal neurons [28,295], we hypothesized that manipulations that diminish $GABA_BR$ or GIRK channel function in these neurons would yield similar electrophysiological and behavioral outcomes. Unexpectedly, we found that $GABA_BR$ ablation did not recapitulate the increase in PL pyramidal neuron excitability or impairment in extinction observed following GIRK ablation. Although both approaches yield complementary models of reduced $GABA_BR$-GIRK signaling, key differences between the manipulations could explain their differential influence on physiology and behavior. For example, $GABA_BR$ ablation should disrupt signaling to all downstream effectors, while GIRK channel ablation should impair both Gβγ-independent (basal) and Gβγ-dependent signaling mediated through multiple inhibitory G protein-coupled receptors. Furthermore, $GABA_BRs$ and GIRK channels exhibit overlapping but distinct subcellular localizations. While both are expressed in somatodendritic compartments, $GABA_BRs$ are also expressed in axon terminals [83]. Therefore, ablation of the GB1 subunit, targeting both GB1a (predominantly presynaptic) and GB1b (postsynaptic) isoforms, should disrupt the inhibitory influence mediated through voltage-gated calcium channels and GIRK channels, respectively. Interestingly, constitutive $GB1a^{-/-}$ and $GB1b^{-/-}$ knockout mice exhibit differences in learning and memory processes [65,317], and only $GB1b^{-/-}$ mice have shown deficits in the extinction of conditioned aversive

taste memories [318]. Furthermore, reduced GB1b expression in the mPFC of aged rats strongly correlates with impaired behavioral flexibility, and intra-mPFC baclofen administration, which would predominantly target postsynaptic $GABA_BR$-GIRK signaling in layer 5/6 PL pyramidal neurons, enhanced behavioral flexibility [319]. Thus, the differential impact of GIRK1 or GB1 ablation on GPCR-effector signaling, and/or presynaptic inhibition, may underlie the distinct influence of each manipulation on neuronal excitability and/or extinction.

Given that GIRK, but not $GABA_BR$, ablation increased basal neuronal excitability [31], and that optogenetic stimulation of PL pyramidal neurons induced fear extinction deficits [316], we hypothesized that elevated excitability of PL pyramidal neurons during extinction testing drives the extinction impairment. However, we found that acute chemogenetic excitation of PL pyramidal neurons did not alter extinction in male mice – a result similarly observed following chemogenetic excitation of dmPFC pyramidal neurons during extinction training in male mice [285]. The interpretation of our result, however, may be confounded by the hyperactivity phenotype evoked by hM3Dq activation in PL pyramidal neurons [31]. In other words, hM3Dq-evoked hyperactivity may have masked an extinction impairment via an indiscriminate reduction in side preference, as has been suggested by others [320,321]. Alternatively, global chemogenetic activation simply may not affect extinction, because acute and broad excitation does not mimic the endogenous firing patterns and/or specific neuronal ensembles that may be required to overrule extinction of cocaine CPP. It is also possible that hyperexcitability of PL pyramidal neurons before the expression of extinction memories (i.e., before the extinction test) is what drives the deficit in extinction. Indeed, pharmacological and behavioral interventions that occur at various time points before the expression of extinction memory have been shown to

modulate extinction [315,322]. Thus, it remains unclear whether a more persistent increase in neuronal excitability underlies the extinction impairment observed following GIRK ablation.

Persistent and recurrent drug memories represent a major obstacle to sustained abstinence in humans and rodents [277,279,315], yet emerging evidence suggests that modulation of the extinction process may represent a promising strategy to selectively weaken drug memories and prevent relapse [315]. Since decreased GIRK channel activity in PL pyramidal neurons impaired the extinction of cocaine CPP in male mice, we sought to determine if strengthening GIRK-dependent signaling in these neurons would facilitate extinction. We found that overexpression of GIRK2 in PL pyramidal neurons enhanced extinction in male mice. This finding aligns with clinical and preclinical work to support the notion that postsynaptic inhibitory signaling in PL pyramidal neurons drives extinction learning. For example, GABAergic signaling in the human dorsal anterior cingulate cortex [323], as well as the homologous rodent PL [285,286,324], has been suggested to initiate extinction learning in male subjects. Preclinical studies have also shown that systemic delivery of baclofen accelerated the extinction of CPP evoked by methamphetamine and morphine in male rodents [310,325,326]. Furthermore, intra-mPFC baclofen restored behavioral flexibility in aged male rats [319], and intra-PL baclofen/muscimol reduced reward-seeking under extinction conditions in male rats [43,44]. Together with our findings, these results suggest that $GABA_BR$-GIRK signaling in PL pyramidal neurons serves as a key mediator of extinction learning in male mice.

In summary, we report here that GIRK channel activity in PL pyramidal neurons bidirectionally regulates the extinction of cocaine reward memories in male mice. Although the cocaine-induced weakening of this inhibitory influence may contribute to the persistence of drug-seeking behavior, therapeutic interventions that restore inhibitory tone may confer resilience to this effect.

Chapter 4: Distinct influence of R7 RGS proteins on $GABA_BR$-GIRK signaling in PL pyramidal neurons

Contributions: T.R.R., E.M.F.d.V., and K.W. designed research, T.R.R., E.M.F.d.V., and B.H. performed research, T.R.R. and E.M.F.d.V. analyzed data, T.R.R. wrote the first draft of the paper; T.R.R. and K.W. edited the paper.

4.1 INTRODUCTION

G protein-gated inwardly rectifying potassium (GIRK) channels are critical regulators of cellular excitability in the brain. Here, they mediate the postsynaptic inhibitory effect of multiple G protein-coupled receptors (GPCRs) to contribute to inhibitory neurotransmission and synaptic plasticity processes. GIRK channels have been shown to be crucial for a wide variety of neurological processes, and their dysregulation has been implicated in numerous neurological and psychiatric disorders [171]. Preclinical studies have described adaptations in GIRK channel activity that occur throughout the rodent brain following acute or prolonged exposure to drugs of abuse [28,130,180] or stressful experiences [131,296,312,327,328]. For example, chronic cocaine exposure suppressed inhibitory G protein-dependent signaling between $GABA_B$ receptors ($GABA_BRs$) and GIRK channels in pyramidal neurons in the prelimbic (PL) subregion of the prefrontal cortex (PFC) [28]. Follow-up work from our laboratory and others suggests that this hypofunctional $GABA_BR$-GIRK signaling contributes to cognitive and behavioral alterations associated with addiction, including an enhanced behavioral sensitivity to cocaine and cognitive inflexibility [31,296].

Despite established links between PL GIRK plasticity and addiction-related behavior, the basic mechanisms that control the strength, sensitivity, and duration of GIRK-dependent signaling in the PL are not well understood.

Regulators of G protein signaling (RGS) proteins facilitate the termination of signaling between G protein-coupled receptors (GPCRs) and their downstream effector enzymes and ion channels, such as GIRK channels. This is achieved by direct interactions between the RGS protein and the G alpha subunit to enhance the intrinsic GTPase activity of G alpha and promote the reassembly of the heterotrimeric G protein complex. In this way, RGS proteins ensure high temporal resolution of neuronal G protein-dependent signaling and reduce crosstalk between signaling pathways [153,170].

The R7 family of RGS proteins has received special attention for their important roles in regulating crucial neurological processes such as vision, cognition, motor activity, and reward [329]. Two members of the R7 RGS protein family, RGS6 and RGS7 (RGS6/7), have been found to accelerate the time course of $GABA_BR$-GIRK signaling in different brain regions: RGS6 in cerebellar granule cells and RGS7 in hippocampal pyramidal neurons. Indeed, constitutive ablation of RGS6 or RGS7 delays the deactivation of $GABA_BR$-GIRK currents in these neurons [160,162]. Interestingly, both RGS6/7 are also found in the rodent PFC [165,330,331], where their expression levels are differentially altered by chronic ethanol exposure [331,332]. At present, the specific expression patterns and functional roles of RGS6/7 within the PL subregion of the PFC are unclear.

The goal of this study was to determine if, and how, RGS6/7 might regulate $GABA_BR$-GIRK signaling in the PL. To first understand where RGS6/7 are expressed in the PL, we used multiplexed fluorescence *in situ* hybridization. We observed broad expression of RGS6/7 throughout the PL, including cortical layers 5 and 6 (layer 5/6), where most pyramidal neurons co-expressed both mRNA. We next employed

complementary electrophysiological approaches to assess the impact of constitutive RGS6 or RGS7 ablation on the kinetics, sensitivity, and amplitude of $GABA_BR$-GIRK currents in layer 5/6 PL pyramidal neurons. Interestingly, we found that RGS6/7 differentially regulate GIRK channel activity; RGS6 regulates the amplitude, while RGS7 regulates the kinetics and sensitivity, of GIRK-dependent signaling. Altogether, these findings suggest that RGS6/7 are co-expressed in PL pyramidal neurons, where they exert distinct regulatory influence over $GABA_BR$-GIRK signaling. Our results shed light on the functional compartmentalization mechanisms that are crucial for ensuring high temporal resolution of neuronal inhibitory G protein-dependent signaling.

4.2 METHODS

Animals. All experiments were approved by the University of Minnesota Institutional Animal Care and Use Committee. The generation of $RGS6^{-/-}$ and $RGS7^{-/-}$ mice was described previously [333,334]. C57BL/6J mice, bred on-site or purchased from the Jackson Laboratory (Bar Harbor, ME), were used as wild-type controls for these studies. Mice were maintained on a 14:10 h light/dark cycle and were provided *ad libitum* access to food and water.

Chemicals. Baclofen, barium chloride, picrotoxin, and kynurenic acid were purchased from Sigma Millipore (Burlington, MA). CGP54626 was purchased from Tocris Bioscience (Bristol, UK). ML297 was generously provided by Dr. Corey Hopkins.

Viral vectors. The pAAV-mDlx-ChR2(mCherry) plasmid was generated by the University of Minnesota Viral Vector and Cloning Core using standard cloning techniques and pAAV-mDlx-GCaMP6f-Fishell-2 (RRID:Addgene_83899, a gift from Gordon Fishell) as the

source of the mDlx promoter/enhancer. AAV8-mDlx-ChR2(mCherry) was packaged by the University of Minnesota Viral Vector and Cloning Core; viral titer was 7.29×10^{13} genocopies/ml.

Intracranial viral manipulations. Intracranial infusion of virus (400 nL per side) into the PL (2.50 mm AP, ±0.45 mm ML, −1.60 mm DV) of mice (7-8 wk) was performed as described previously [227]. After surgery, animals were allowed 2-3 wk for full recovery and viral expression before electrophysiological assessments.

Multiplexed fluorescence in situ hybridization. Multiplexed fluorescent in situ hybridization was performed using RNAscope as described (Wang et al., 2012). Male and female mice (8 wk) were briefly anesthetized with halothane and decapitated. Brains were rapidly extracted, and flash frozen in isopentane at -50°C for 20s. Frozen brains were wrapped in aluminum foil and stored at -80°C until use. Brains were equilibrated in the cryostat at -20°C for 2 hr before PL coronal sections (16 M) were collected and mounted onto Superfrost Plus slides (Thermo Fisher Scientific; Waltham, MA). After sectioning, slides were transferred to -80°C to await ISH processing. RNA ISH for CaMKIIα, RGS6, and RGS7 was performed according to the "RNAscope Multiplex Fluorescent Reagent Kit V2 Assay" user manual (Advanced Cell Diagnostics; Newark CA). Briefly, the -80°C slides were transferred to slide racks and the slices were fixed in 4% paraformaldehyde for 1 hr at 4°C. Slides were rinsed twice with PBS, followed by dehydration in 50%, 70%, and 100% ethanol. Slides were stored in fresh 100% ethanol at -20°C overnight. Slides were dried for 5 min at room temperature (RT) and a hydrophobic pen (ImmEdge Hydrophobic Barrier Pen; Vector Laboratories; Burlington, ON) was used to create a barrier around the slices to contain RNAscope reagents. Sections were incubated in hydrogen peroxide (10

min at RT), followed by incubation in protease solution (protease IV; 30 min at RT). Sections were next incubated in 1x target probes for specific RNAs (CaMKIIα, RGS6, RGS7) for 2 hr at 40°C using a hybridization oven (HybEZ hybridization system, Advanced Cell Diagnostics). Specific target probes used included: CaMKIIα-C2 probes (accession number NM_009792.3; target nt region, 896-1986), RGS6-C1 (accession number NM_001310478.2; target nt region, 587-1628), and RGS7-C3 (accession number NM_011880.3; target nt region, 333-1341). Following the hybridization step, sections were incubated with preamplifier and amplifier probes followed by incubation with fluorescently labeled probes with specific color-channel combinations: green, red, near infrared (Opal 520, Opal 620, Opal 690, respectively; Akoya Biosciences; Marlborough, MA). Sections were incubated with DAPI for 20s to stain nuclei (blue), and then mounted with glass coverslips using ProLong Gold Antifade (Thermo Fisher Scientific). Slides were dried for 30 min at RT before being stored at 2°C. Fluorescence images (20x & 40x) were acquired using a Keyence fluorescent microscope and overlaid using ImageJ software (National Institute of Health; Bethesda, MD). The ImageJ multipoint tool was used to quantify the number of putative CaMKIIα-positive cell bodies that express RGS6, RGS7, both or neither. Cells were deemed "positive" for expressing a given mRNA if they exhibited >5 puncta within and/or immediately around a central nucleus.

Slice electrophysiology. Somatodendritic currents evoked by baclofen (1.5 μM, 200 μM) or ML297 (10 μM) were recorded in layer 5/6 PL pyramidal neurons from 8-10 wk old mice, as described previously [295,335]. In some experiments, we performed concentration-response somatodendritic recordings involving low (1.5 μM) and saturating (1.5 μM) concentrations of baclofen to assess peak current amplitude and sensitivity. Peak current amplitude was measured from baseline current to peak baclofen response. Sensitivity was

analyzed as the percentage of peak current amplitude evoked by 1.5 μM baclofen to 200 μM baclofen. For rheobase assessments, cells were held at 0 pA in current-clamp mode and given 1 s current pulses, beginning at −60 pA and increasing in 20 pA increments. Rheobase was identified as the injection step at which initial spiking was elicited. For optogenetic slow IPSC (sIPSC) experiments, layer 5/6 PL pyramidal neurons within the virally-targeted area (visualized by mCherry fluorescence) were selected for whole-cell patch clamp recordings. sIPSCs were evoked by a single 4 ms blue light (470 nm, 3 mW/mm^2) pulse, and were measured at a holding potential (Vhold) of −70 mV and in the presence of kynurenic acid (2 mM) and picrotoxin (100 μM) to suppress ionotropic glutamate and $GABA_A$ receptors, respectively. sIPSCs were reversed by the $GABA_BR$ antagonist CGP54626 (2 μM). Current activation time, or time to peak amplitude, was measured from the start of the light pulse to peak amplitude. Current deactivation rates were extracted from a standard exponential fit of the trace corresponding to the return of current to baseline (Clampfit v. 10.7 software; Molecular Devices; San Jose, CA).

Experimental design and statistical analysis. Data are presented as the mean ± SEM. Statistical analyses were performed using GraphPad Prism 9 (GraphPad Software; San Diego, CA). Unless specifically noted, all studies involved balanced groups of males and females. While sex was included as a variable in preliminary analyses (two-way ANOVA), no impact of sex was observed on any measure and data from males and females were pooled. Pooled data were analyzed by unpaired Student's *t* test, one-way ANOVA, Brown-Forsythe one-way ANOVA, as appropriate. Pairwise comparisons were performed using Bonferroni's or Dunnett's *post hoc* test, if justified. Sample size (*n* or *N*) per group and statistical details of experiments are reported in the figure legends and Results. Differences were considered significant when $p < 0.05$.

4.3 RESULTS

Evidence for R7 RGS protein expression in the PL

Prior work from other laboratories has shown that both RGS6 and RGS7 are expressed at the mRNA and protein level in the PFC of rodents [165,330,331]. To better understand which cell types express RGS6/7 in the PL, we probed for both RGS6/7 alongside the pyramidal neuron marker, CaMKIIα, using multiplexed fluorescence *in situ* hybridization. Both RGS6/7 were widely detected throughout the PL (**Fig. 4.1**). We next narrowed in on the primary output regions of the PL, layers 5 and 6 (layer 5/6), where we quantified the percentage of putative pyramidal neurons that express RGS6, RGS7, both or neither mRNA. We found that the vast majority of layer 5/6 CaMKIIα-positive cells co-expressed both RGS6/7 (**Fig. 4.1**).

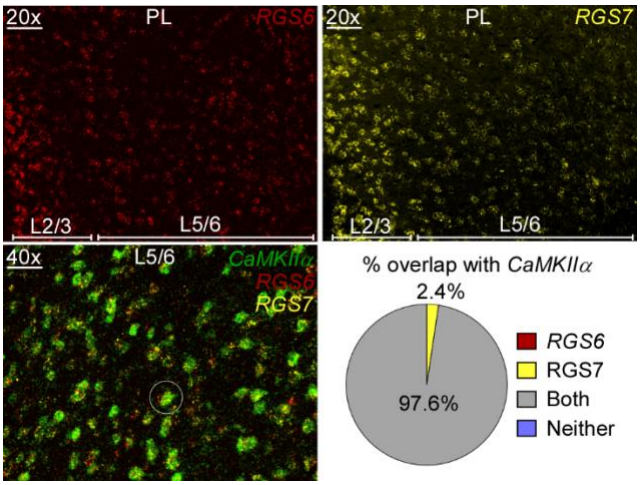

Figure 4.1. Expression of RGS6/7 in PL pyramidal neurons

Distribution of RGS6 and RGS7 mRNA within the PL; strong overlap with CaMKIIα mRNA in layer 5/6. White circle highlights a putative CaMKIIα-positive cell body that expresses both RGS6 and RGS7 mRNA. Pie graph depicts the percentage of CaMKIIα-positive cell bodies that express only RGS6, RGS7, both or neither mRNA (n = 0, n = 4, n = 165, and n = 0 neurons, respectively; N = 3 mice). Scale bars: 20x = 50 μm, 40x = 25 μm.

Impact of constitutive RGS6/7 ablation on synaptically-evoked $GABA_BR$-GIRK currents

We next wanted to investigate the functional roles of RGS6/7 in layer 5/6 PL pyramidal neurons. To determine if RGS6/7 influence the kinetics of synaptically-evoked $GABA_BR$-GIRK signaling in these neurons, we employed an optogenetic electrophysiological approach involving constitutive $RGS6^{-/-}$ and $RGS7^{-/-}$ mice, and wild-type (WT) controls. This approach involved the infusion of AAV8-mDlx-ChR2(mCherry) into the PL of adult $RGS6^{-/-}$, $RGS7^{-/-}$, or WT mice (**Fig. 4.2A**). The mDlx promoter/enhancer element allowed for the selective expression of channelrhodopsin-2 (ChR2), a blue-light activated non-selective cation channel, in PL GABA neurons [31]. Following a 2-3 wk recovery period, we evaluated the impact of constitutive RGS6/7 ablation on optically-evoked slow inhibitory postsynaptic currents (IPSCs) in layer 5/6 PL pyramidal neurons. A single 4 ms blue-light pulse evoked reliable slow IPSCs that were blocked by the $GABA_BR$ antagonist CGP54626 (2 μM) (**Fig. 4.2B**). While RGS6/7 ablation did not impact current amplitudes (**Fig. 4.2C,D**; one-way ANOVA, no effect of genotype, $F(2,38) = 0.969$, $p = 0.39$), RGS7 ablation prolonged current activation (**Fig. 4.2C,E**; one-way ANOVA, significant effect of genotype, $F(2,38) = 12.60$, $p < 0.0001$; Bonferroni's post hoc test: $p > 0.9999$ [control vs $RGS6^{-/-}$], ***$p = 0.0004$ [control vs $RGS7^{-/-}$]) and deactivation (**Fig. 4.2C,F**; Brown-Forsythe one-way ANOVA, significant effect of genotype, $F(2,17.92) = 16.45$, $p < 0.0001$; Dunnett's post hoc test: $p = 0.45$ [control vs $RGS6^{-/-}$], ***$p = 0.0008$ [control vs $RGS7^{-/-}$]). Thus, RGS7, but not RGS6, negatively regulates the temporal kinetics of synaptically-evoked $GABA_BR$-GIRK signaling in layer 5/6 PL pyramidal neurons.

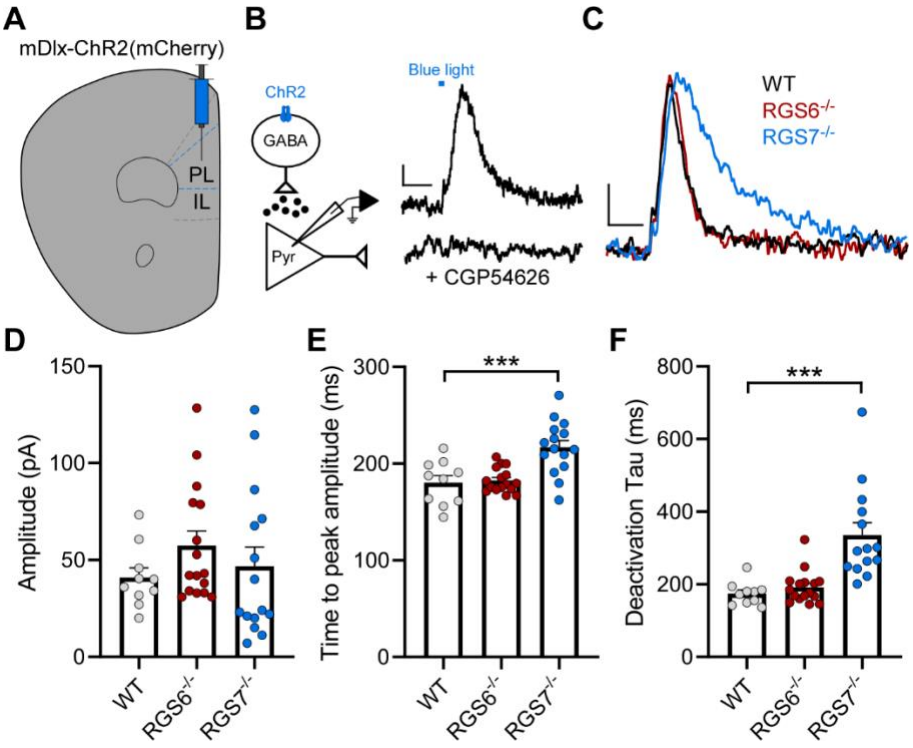

Figure 4.2. Impact of constitutive RGS6/7 ablation on optically-evoked slow IPSCs

A) Example of viral targeting in a C57BL/6J mouse treated with AAV8-mDlx-ChR2(mCherry) vector. **B)** Optically-evoked slow IPSCs were recorded in layer 5/6 PL pyramidal neurons from C57BL/6J mice treated with mDlx-ChR2(mCherry) vector (Vhold = −70 mV), before and after bath application of CGP54626 (2 μM). Calibration: 10 pA/250 ms. **C)** Optically-evoked slow IPSCs were recorded in layer 5/6 PL pyramidal neurons from C57BL/6J, RGS6$^{-/-}$, or RGS7$^{-/-}$ mice treated with mDlx-ChR2(mCherry) vector (Vhold = −70 mV). Calibration: 10 pA/1 s. **D)** Peak current amplitudes of optically-evoked slow IPSCs recorded in layer 5/6 PL pyramidal neurons from C57BL/6J, RGS6$^{-/-}$, or RGS7$^{-/-}$ mice treated with mDlx-ChR2(mCherry) vector (one-way ANOVA; n = 10-16 recordings/group and N = 5-6 mice/group). No main effect of sex was detected ($F(1,35) = 1.068$, $p = 0.31$; two-way ANOVA). **E)** Response onset timing determined as time to peak current amplitude in optically-evoked slow IPSCs recorded in layer 5/6 PL pyramidal neurons from C57BL/6J, RGS6$^{-/-}$, or RGS7$^{-/-}$ mice treated with mDlx-ChR2(mCherry) vector (***p = 0.0004; one-way ANOVA with Bonferroni's post hoc test; n = 10-16 recordings/group and N = 5-6 mice/group). No main effect of sex was detected ($F(1,35) = 2.491$, $p = 0.12$; two-way ANOVA). **F)** Deactivation time constant determined via single-exponential fitting of optically-evoked slow IPSCs recorded in layer 5/6 PL pyramidal neurons from C57BL/6J, RGS6$^{-/-}$, or RGS7$^{-/-}$ mice treated with mDlx-ChR2(mCherry) vector (***p = 0.0008; Brown-Forsythe one-way ANOVA with Dunnett's post hoc test; n = 10-16 recordings/group and N = 5-6 mice/group). No main effect of sex was detected ($F(1,34) = 0.3241$, $p = 0.57$; two-way ANOVA).

Impact of constitutive RGS6/7 ablation on baclofen-evoked $GABA_BR$-GIRK currents

To further characterize RGS6/7 function, we measured somatodendritic $GABA_BR$-GIRK currents evoked by low (1.5 μM) and saturating (200 μM) concentrations of the $GABA_BR$ agonist baclofen in layer 5/6 PL pyramidal neurons from RGS6$^{-/-}$, RGS7$^{-/-}$, or WT mice (**Fig. 4.3A**). GIRK channels in pyramidal neurons from RGS7$^{-/-}$, but not RGS6$^{-/-}$, mice were more sensitive to baclofen, as compared to WT controls (**Fig. 4.3B**; one-way ANOVA, significant effect of genotype, $F(2,42) = 59.82$, $p < 0.0001$; Bonferroni's post hoc test: $p = 0.24$ [control vs RGS6$^{-/-}$], ****$p < 0.0001$ [control vs RGS7$^{-/-}$]). In contrast, peak baclofen-evoked (200 μM) current amplitudes were larger in pyramidal neurons from RGS6$^{-/-}$, but not RGS7$^{-/-}$, mice (**Fig. 4.3C**; one-way ANOVA, significant effect of genotype, $F(2,42) = 8.301$, $p = 0.0009$; Bonferroni's post hoc test: **$p = 0.0076$ [control vs RGS6$^{-/-}$], $p = 0.81$ [control vs RGS7$^{-/-}$]). Since the baclofen-evoked response in these neurons consists of both GIRK and non-GIRK components [28], we utilized barium, an inwardly-rectifying K^+ channel blocker, to identify which component was increased upon elimination of RGS6. Baclofen-evoked currents recorded in the presence of external barium (0.3 mM) were similar in pyramidal neurons from RGS6$^{-/-}$ and WT mice (**Fig. 4.3D,E**; unpaired Student's t test, $t(24) = 0.128$, $p = 0.90$), which suggests that RGS6 ablation likely enhances the GIRK component of the composite baclofen response. To determine if the elevated GIRK current was caused by increased surface expression of the prototypical neuronal GIRK channel, comprised of GIRK1 and GIRK2 subunits [79], we employed ML297, a direct (By-independent) activator of GIRK1-containing GIRK channels [336]. ML297 (10 μM) evoked similar GIRK responses in pyramidal neurons from RGS6$^{-/-}$ and WT mice (**Fig. 4.3F,G**; unpaired Student's t test, $t(34) = 0.5625$, $p = 0.58$), which suggests that the enhanced GIRK current is likely mediated via a By-dependent

mechanism. Taken together, these findings suggest that RGS6 and RGS7 temper the strength and sensitivity, respectively, of baclofen-evoked $GABA_BR$-GIRK currents.

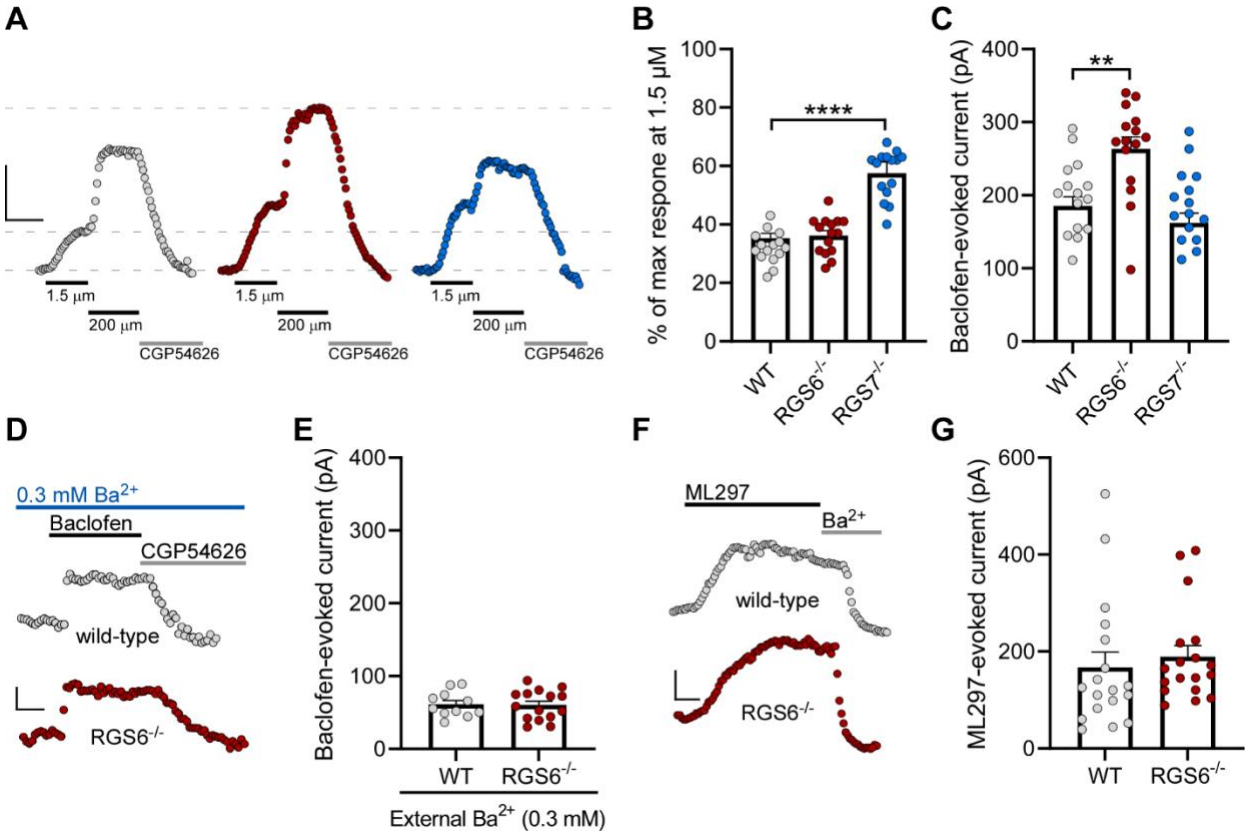

Figure 4.3. Impact of constitutive RGS6/7 ablation on somatodendritic GABABR-GIRK currents

A) Somatodendritic currents evoked by low (1.5 µM) and saturating (200 µM) concentrations of baclofen in layer 5/6 PL pyramidal neurons from C57BL/6J, RGS6$^{-/-}$, or RGS7$^{-/-}$ mice. Currents were reversed by the $GABA_BR$ antagonist CGP54626. Calibration: 100 pA/200 s. **B)** Sensitivity determined as percentage ratio of peak current amplitude evoked by a low (1.5 µM) versus saturating (200 µM) concentration of baclofen in layer 5/6 PL pyramidal neurons from C57BL/6J, RGS6$^{-/-}$, or RGS7$^{-/-}$ mice (****$p < 0.0001$; one-way ANOVA with Bonferroni's post hoc test; n = 15 recordings/group and N = 6-8 mice/group). No main effect of sex was detected ($F(1,39) = 0.4065$, $p = 0.53$; two-way ANOVA). **C)** Peak current amplitudes evoked by saturating (200 µM) concentrations of baclofen in layer 5/6 PL pyramidal neurons from C57BL/6J, RGS6$^{-/-}$, or RGS7$^{-/-}$ mice (**$p = 0.0076$; one-way ANOVA with Bonferroni's post hoc test; n = 15 recordings/group and N = 6-8 mice/group). No main effect of sex was detected ($F(1,39) = 0.9948$, $p = 0.32$; two-way ANOVA). **D)** Baclofen-evoked (200 µM) currents recorded in the presence of 0.3 mM external barium in layer 5/6 PL pyramidal neurons from C57BL/6J and RGS6$^{-/-}$ mice. Calibration: 25 pA/100 s. **E)** Peak baclofen-evoked (200 µM) current amplitudes in layer 5/6 PL pyramidal neurons from C57BL/6J and RGS6$^{-/-}$ mice (unpaired Student's t test; n

= 11-15 recordings/group and N = 4-5 mice/group). No main effect of sex was detected ($F(1,22) = 2.369$, $p = 0.14$; two-way ANOVA). **F)** Somatodendritic currents evoked by ML297 (10 μM) in layer 5/6 PL pyramidal neurons from C57BL/6J and RGS6$^{-/-}$ mice. Calibration: 50 pA/125 s. **G)** Peak ML297-evoked (10 μM) current amplitudes in layer 5/6 PL pyramidal neurons from C57BL/6J and RGS6$^{-/-}$ mice (unpaired Student's t test; n = 18 recordings/group and N = 8-9 mice/group). No main effect of sex was detected ($F(1,32) = 0.4626$, $p = 0.50$; two-way ANOVA).

4.4 DISCUSSION

Work from several laboratories has shown that RGS6/7 are expressed within the rodent PFC [165,330,331], however, the cellular expression profiles of each RGS protein in the PL were unclear. Here, we observed broad expression of RGS6/7 throughout the PL and found that the vast majority of layer 5/6 PL pyramidal neurons co-express both RGS6/7 mRNA. Upon confirming the presence of both RGS6/7 in PL pyramidal neurons, we probed for the functional role(s) of each protein in regulating synaptically-evoked and baclofen-activated $GABA_BR$-GIRK signaling.

Considering the GTPase-accelerating protein (GAP) activity of RGS6/7, ablation of either protein should be expected to prolong $GABA_BR$-GIRK signaling, as has been reported in different brain regions [160,162]. However, we observed that constitutive ablation of RGS7, but not RGS6, delayed the activation and deactivation of optically-evoked $GABA_BR$-GIRK currents in PL pyramidal neurons. Our finding aligns with a prior report demonstrating that constitutive ablation of RGS7, but not RGS6, delayed the activation and deactivation of electrically-evoked $GABA_BR$-GIRK currents in hippocampal pyramidal neurons [166]. Together, these results suggest that RGS7 serves as the dominant R7 RGS regulator of $GABA_BR$-GIRK signaling kinetics in both PL and hippocampal pyramidal neurons.

In addition to signaling kinetics, RGS6/7 have also been shown to regulate GPCR-GIRK coupling efficiency. Indeed, RGS7 ablation increased the sensitivity of $GABA_BR$-GIRK currents in hippocampal neurons [160], while RGS6 ablation increased the sensitivity of M2 muscarinic receptor-GIRK currents in sinoatrial pacemaking cells [337]. Here, we observed that constitutive ablation of RGS7, but not RGS6, increased the sensitivity of somatodendritic $GABA_BR$-GIRK currents in PL pyramidal neurons. Like before, these

results suggest that RGS7 plays a primary role in regulating $GABA_BR$-GIRK coupling efficiency in these neurons.

To our knowledge, neither RGS6 nor RGS7 have been reported to suppress the amplitude of $GABA_BR$-GIRK currents in neurons. Therefore, we were surprised to find that the loss of RGS6 increased the maximal amplitude of somatodendritic baclofen-evoked currents in layer 5/6 PL pyramidal neurons. This increased component of the baclofen-evoked current was barium-sensitive, consistent with a GIRK current, and was not caused by increased surface expression of the prototypical GIRK channel. These findings are congruent with a mechanism involving a reduction in canonical GAP function and enhancement in By-dependent GIRK channel activity. Interestingly, RGS6 ablation similarly increased the amplitude of whole-cell A_1 adenosine receptor-GIRK currents in sinoatrial pacemaking cells, without impacting GIRK channel expression, deactivation kinetics, or coupling efficiency [337]. Taken together, these results suggest that RGS6 can suppress GIRK current amplitudes in different cell types, perhaps via GAP activity and reduced steady-state levels of activated Gi/o and By.

In contrast to our findings with somatodendritic recordings, however, we found that RGS6 ablation did not affect the amplitude of optically-evoked $GABA_BR$-GIRK currents. These different findings may be explained by the different densities of $GABA_BRs$ and GIRK channels engaged by our two manipulations. In other words, optically-stimulated GABA release from local GABA neurons, as compared with saturating concentrations of baclofen, simply may not engage enough $GABA_BRs$ and GIRK channels on pyramidal neurons to detect differences in current amplitude upon RGS6 ablation. Alternatively, it is also possible that RGS6, $GABA_BRs$, and GIRK channels might functionally couple within distinct somatodendritic compartments that are not sufficiently engaged by local GABA

release [338]. Similar results have been observed in hippocampal neurons, where RGS7 and $GABA_BRs$ were found to associate together in the spines, but not shafts, of dendrites [124].

To conclude, we discovered that RGS6/7 are co-expressed in PL pyramidal neurons, where they exert distinct regulatory influences over $GABA_BR$-GIRK signaling; RGS6 regulates signaling amplitude, while RGS7 regulates signaling kinetics and coupling efficiency. These findings represent a novel example of how distinct R7 RGS proteins can differentially regulate the same signaling pathway within a neuron. Future investigations will be necessary to understand how RGS6/7 function shapes PL pyramidal physiology and behavior, under both normal and pathological conditions. Altogether, our results inform the compartmentalization mechanisms that are critical for ensuring high temporal resolution of neuronal inhibitory G protein-dependent signaling.

Chapter 5: Discussion

5.1 Summary of findings

My thesis research has contributed to the field's understanding of how the PL pyramidal neuron GIRK channel contributes to cellular excitability and addiction-related behavior. My findings suggest that GIRK-dependent signaling in these neurons represents an "inhibitory brake" on cellular excitability that is critical for excitation/inhibition balance and optimal behavioral function. Therefore, the weakening of this inhibition following repeated cocaine exposure may drive neuronal hyperexcitability and addictive behaviors. Because the adaptation in PL pyramidal neuron GIRK channel activity lasts for at least 6 wk, it is tempting to speculate that this plasticity mechanism may contribute to the persistent nature of drug seeking. As a whole, my thesis sheds light on the regulatory networks that control GIRK channel activity in PL pyramidal neurons, and underlines the critical contribution of GIRK-dependent signaling in these neurons to addiction-related behavior.

5.1.1 PL pyramidal neuron excitability impacts PL-dependent behaviors

Prolonged contingent or noncontingent cocaine exposure has been found to increase PL pyramidal neuron excitability through (direct) elevations in intrinsic excitability and (indirect) reductions in GABAergic neurotransmission [31]. In **Chapter 2** I modeled the cocaine-induced increase in PL pyramidal neuron excitability in drug-naive mice by using complementary chemogenetic manipulations that 1) acutely excite PL pyramidal neurons, and 2) disinhibit PL pyramidal neurons via reduced local GABA release. After validating that these manipulations effectively modeled the elevated intrinsic excitability of, and

reduced GABAergic neurotransmission in, PL pyramidal neurons, I assessed the impact of each manipulation on established PL-dependent behaviors, including acute cocaine-induced locomotion and trace fear conditioning. Since withdrawal from chronic cocaine intake is linked with heightened behavioral responding to cocaine and altered associative learning [200], I predicted that direct or indirect excitation of PL pyramidal neurons would enhance behavioral sensitivity to cocaine and disrupt associative learning.

Both manipulations induced similar behavioral outcomes. Activation of hM3Dq in pyramidal neurons, or hM4Di in GABA neurons, evoked hyperactivity at baseline, which was further augmented by cocaine. Given that DREADD-evoked hyperactivity did not occlude the acute motor-stimulatory effect of cocaine, it is likely that DREADD activation and acute cocaine exposure work through distinct mechanisms to enhance locomotion. Whether DREADD-evoked hyperactivity would occlude the development of locomotor sensitization, however, remains an important topic for future research. Both manipulations were also found to disrupt cue fear recall, which was assessed 2 d after trace fear conditioning in the presence of CNO. Importantly, trace fear learning is an associative learning task that relies on several cognitive functions associated with the PL, including working memory and attention [199]. Thus, deficits in cue fear recall may reflect the impairment of working memory and/or attention, processes that are similarly disrupted following psychostimulant exposure in both humans and rodents [200,308].

Since PL pyramidal neurons project to multiple brain regions, and different projections shape behavior in distinct ways [36,339], I used a projection-specific chemogenetic approach to identify which projection(s) might underlie these behavioral effects. I found that selective excitation of PL pyramidal neurons that project to the VTA, but not the NAc or BLA, recapitulated the hyperlocomotion and fear learning deficits observed with global PL pyramidal neuron excitation. Although stimulation of the PFC can

increase striatal DA release in humans and rodents [340-342], and is reinforcing in preclinical studies [340], the functional roles of specific PFC-to-VTA projections have remained understudied. To my knowledge, my findings are some of the first to directly link the activation of the PL-to-VTA microcircuit to behavioral outcomes. Since this specific projection is also subject to cocaine-induced plasticity [28], my work suggests that hyperexcitability of PL pyramidal neurons, and particularly those that project to the VTA, may contribute to specific cognitive and behavioral impairments associated with chronic cocaine intake.

5.1.2 PL pyramidal neuron GIRK channel activity impacts cocaine-related behaviors

The increase in PL pyramidal neuron excitability following chronic cocaine exposure coincided with a reduction in $GABA_BR$-GIRK signaling, and both plasticity mechanisms were found to durable, lasting for at least 6 wk following the final cocaine treatment [28]. Multiple mechanisms have been proposed to underlie this persistent hyperexcitability [343], including the suppression of $GABA_BR$-GIRK signaling. To model the persistent decrease in $GABA_BR$-GIRK signaling, I employed complementary viral genetic approaches to selectively ablate the GIRK channel or $GABA_BR$ in PL pyramidal neurons in drug-naive mice. I predicted that reduced $GABA_BR$-GIRK signaling would 1) enhance the intrinsic excitability of PL pyramidal neurons and 2) induce cognitive and behavioral impairments associated with chronic cocaine intake. These predictions were tested in **Chapters 2 & 3**.

Impact of $GABA_BR$-GIRK signaling on PL pyramidal neuron physiology

GIRK1 and GB1 are essential subunits that comprise the prototypical GIRK channel and obligate $GABA_BR$ heterodimer [83]. Therefore, I used viral Cre- and CRISPR/Cas9-based approaches to achieve PL pyramidal neuron-selective ablation of GIRK1 and GB1, respectively. Both GIRK1 and GB1 ablation significantly reduced the baclofen-evoked somatodendritic current, similar to what has been described in layer 5/6 PL pyramidal neurons from cocaine-treated mice [28]. As predicted, GIRK1 ablation increased the intrinsic excitability of PL pyramidal neurons, thus emulating the hyperexcitability phenotype. In contrast, GB1 ablation was without effect. The differential impact of GIRK1 or GB1 ablation on intrinsic excitability may reflect the loss of basal (constitutive) GIRK channel activity through Gβγ-dependent and Gβγ-independent mechanisms [171]. Upon confirming that both manipulations were effective in suppressing $GABA_BR$-GIRK signaling, I next assessed the behavioral impact of each manipulation.

Impact of PL pyramidal neuron $GABA_BR$-GIRK signaling on behavior

My behavioral studies focused on several PL-dependent behaviors that have been implicated in aspects of addiction, including acute cocaine-induced locomotion, trace fear conditioning, EPM, FST, and cocaine CPP. Thus, I hypothesized that hypofunctional $GABA_BR$-GIRK signaling in PL pyramidal neurons would enhance behavioral sensitivity to cocaine, promote negative affect, and disrupt cognitive processing.

I first assessed the impact of reduced GIRK channel activity on trace fear conditioning and acute cocaine-induced locomotion. Loss of GIRK1 in PL pyramidal neurons did not impact fear learning, or basal locomotion in the open field test. However, the manipulation potentiated the acute motor-stimulatory effect of cocaine, suggesting that the loss of GIRK channel activity in these neurons induces a “presensitization-like” phenotype. This finding builds on prior studies that have similarly reported an increase in

cocaine-induced locomotion in conditional knockout mice that lack GIRK1 in forebrain pyramidal neurons (i.e., CaMKIICre:*GIRK1*$^{fl/fl}$) [225], as well as in wild-type mice following RNAi-based suppression of *Girk1* and *Girk2* in the PL [28]. Together, these results highlight GIRK channels in PL pyramidal neurons as important regulators of acute cocaine-evoked locomotion, and further suggest that cocaine-induced GIRK plasticity in these neurons may render mice vulnerable to the development of behavioral sensitization.

Since prolonged cocaine exposure has been linked with mood disturbances [303-305], as well as the formation of persistent and recurring drug memories [200,277,278], I next assessed the impact of reduced $GABA_BR$-GIRK signaling on EPM, FST, and the acquisition and extinction of cocaine CPP. Neither GIRK1, nor GB1, ablation impacted behavior in the EPM or FST, which suggests that chronic cocaine exposure induces negative affective behaviors via alternative mechanisms. While reduced $GABA_BR$-GIRK signaling did not affect the acquisition of cocaine CPP, extinction was impaired following GIRK1 ablation in male, but not female, mice. This finding aligned with a previous study that observed cognitive deficits in working memory and behavioral flexibility following GIRK channel ablation in PL pyramidal neurons of male, but not female, mice [296]. These results imply that GIRK channels in PL pyramidal neurons exhibit sex-specific functional roles in regulating distinct cognitive processes. Moreover, these findings raise the intriguing possibility that diminished behavioral flexibility may drive the impairment in extinction, perhaps by disrupting the discrimination between an initial cocaine-related memory and a newer extinction memory. Alternatively, the loss of GIRK channel activity in these neurons may enhance the expression of a cocaine-related memory and/or disrupt the acquisition/expression of an extinction memory.

Given that ablation of GIRK1, but not GB1, increased PL pyramidal neuron excitability and impaired extinction, I hypothesized that hyperexcitability of PL pyramidal

neurons underlies the extinction deficit. However, I found that acute chemogenetic excitation of PL pyramidal neurons during extinction testing did not impair extinction. Although the interpretation of this result may be obfuscated by a hyperactivity phenotype, this finding suggests that elevated PL pyramidal neuron excitability, at least during the extinction test period, does not underlie the extinction impairment. Whether a more persistent increase in PL pyramidal neuronal excitability drives this behavioral phenotype remains an important topic for future research.

Persistent and recurrent drug-related memories are a major obstacle to sustained abstinence in humans and rodents [277,279,315]. Therefore, an impairment in the extinction of drug-related memories may promote continued drug-seeking and relapse after abstinence. Fortunately, emerging evidence suggests that pharmacological and behavioral modulation of extinction learning may represent a promising strategy to weaken drug-related memories and prevent relapse [315]. Since decreased GIRK channel activity in PL pyramidal neurons impaired the extinction of cocaine CPP in male mice, I hypothesized that strengthening GIRK-dependent signaling in these neurons would be sufficient to facilitate extinction. After validating that the viral-mediated overexpression of GIRK2 in PL pyramidal neurons was sufficient to increase $GABA_BR$-GIRK currents and reduce neuronal excitability, I then assessed the behavioral impact of this manipulation. As predicted, GIRK2 overexpression in PL pyramidal neurons enhanced extinction of cocaine CPP in male mice. This finding aligns with clinical and preclinical research to support the notion that postsynaptic inhibitory neurotransmission in PL pyramidal neurons drives extinction learning. For example, GABAergic signaling in the human dorsal anterior cingulate cortex (dACC) [323], as well as the homologous rodent PL [285,286,324], has been suggested to initiate extinction learning in male subjects. Furthermore, systemic delivery of baclofen accelerated extinction of drug-induced CPP in male rodents [310,325,326], intra-

mPFC baclofen restored behavioral flexibility in aged male rats [319], and intra-PL baclofen/muscimol reduced reward-seeking under extinction conditions in male rats [44]. Notably, my results suggest that $GABA_BR$ activity in PL pyramidal neurons is not *necessary* for the extinction of cocaine CPP. When combined with my GIRK overexpression results, however, these findings suggest that $GABA_BR$-GIRK signaling may be *sufficient* for the extinction of cocaine CPP in male mice.

5.1.3 Regulation PL pyramidal neuron GIRK channels by R7 RGS proteins

Despite established links between the dysregulation of $GABA_BR$-GIRK signaling and disease [171], the basic mechanisms underlying the regulation of this signaling pathway in PL pyramidal neurons are not fully understood. In **Chapter 4**, I elucidated the distinct contributions of two RGS proteins, RGS6 and RGS7, to the regulation of $GABA_BR$-GIRK signaling. My multiplexed fluorescence in situ hybridization studies provided initial insight into the expression patterns of RGS6/7 in the PL. Both RGS6/7 were widely expressed throughout the PL, including the primary output regions (layers 5/6), where they were co-expressed in most pyramidal neurons.

To understand the contribution of RGS6/7 to the kinetics of synaptically-evoked $GABA_BR$-GIRK currents, I used a viral optogenetic approach to stimulate local GABA release while recording $GABA_BR$-dependent IPSCs in adjacent PL pyramidal neurons from $RGS6^{-/-}$, $RGS7^{-/-}$, or wild-type mice. I found that loss of RGS7, but not RGS6, delayed the activation and deactivation kinetics of IPSCs. My results aligned with a prior report showing that constitutive ablation of RGS7, but not RGS6, prolonged the activation and deactivation kinetics of electrically-evoked IPSCs in hippocampal pyramidal neurons [166]. Together, these findings demonstrate that RGS7 serves as a critical negative regulator

of synaptic $GABA_BR$-GIRK current kinetics in both PL and hippocampal pyramidal neurons.

I next recorded somatodendritic baclofen-evoked currents to assess sensitivity and maximal amplitude. Loss of RGS7, but not RGS6, increased the sensitivity of $GABA_BR$-GIRK currents, a finding similarly observed in cultured hippocampal pyramidal neurons [160]. In contrast, the ablation of RGS6, but not RGS7, increased the maximal amplitude of $GABA_BR$-GIRK currents. Follow-up studies revealed that this increased amplitude was barium sensitive, consistent with a GIRK current, and was not caused by increased surface expression of the prototypical GIRK channel (i.e., GIRK1/2) – observations that align with a mechanism involving canonical GAP function and enhanced Gβγ-dependent GIRK channel activity. Although I found no prior evidence in the literature that RGS6 can influence GIRK current amplitudes in neurons, the loss of RGS6 in sinoatrial pacemaking cells increased A_1 adenosine receptor-GIRK currents, without impacting GIRK channel expression, deactivation kinetics, or coupling efficiency [337]. These results suggest that RGS6 can selectively suppress GIRK current amplitudes in different cell types, perhaps through GAP activity and reduced steady-state levels of activated $G\alpha_{i/o}$ and Gβγ.

This influence of RGS6 on current amplitude may be specific for somatodendritic recordings, however. Indeed, RGS6 ablation did not impact the amplitude of optically-evoked IPSCs in PL pyramidal neurons. These different outcomes may be explained by differences in the density of $GABA_BRs$ and GIRK channels that were targeted by each manipulation. In other words, it's possible that a lower density of $GABA_BRs$ and GIRK channels were engaged by local GABA release, as compared with saturating concentrations of baclofen, which resulted in smaller currents that may have precluded our ability to detect differences in amplitude. Additionally, RGS6, $GABA_BRs$, and GIRK channels might functionally couple within distinct somatodendritic compartments that are

not sufficiently engaged by local GABA release. Nevertheless, these findings suggest that RGS6/7 exert distinct regulatory influences over $GABA_BR$-GIRK signaling; RGS6 regulates signaling amplitude, while RGS7 regulates signaling kinetics and coupling efficiency. These results represent a novel example of how distinct R7 RGS proteins can differentially regulate the same signaling pathway within a neuron. Altogether, this work informs our understanding of the compartmentalization mechanisms that are critical for ensuring high temporal resolution of neuronal inhibitory G protein-dependent signaling.

5.2 Future directions

This thesis research identified the PL pyramidal neuron GIRK channel as a key regulator of addiction-related behavior. It further identified important regulatory proteins that control the strength, sensitivity, and duration of $GABA_BR$-GIRK signaling in these neurons. Future studies can build on these findings by trying to better understand how pyramidal neuron GIRK channel activity can influence neuronal activity and glutamate release. Additionally, further work should add to our understanding of the impact of GIRK channel activity in subpopulations of PL pyramidal neurons, and in more advanced preclinical models of addiction.

5.2.1 Determine the functional consequences of PL pyramidal neuron GIRK channel activity *in vivo*

The elevated intrinsic excitability observed following selective ablation of GIRK channels in PL pyramidal neurons suggests that GIRK channel activity could influence the regulation of glutamate release *in vivo*. This might especially be true in situations where PL pyramidal neuron $GABA_BR$-GIRK signaling might be engaged, such as during drug-

associated cue exposure or short-term withdrawal following repeated cocaine exposure – timepoints when increased mPFC GABA levels have been observed [292,344]. To determine how PL pyramidal neuron activity and glutamate release are altered *in vivo* when GIRK channel activity is decreased or increased, one could employ genetically encoded calcium indicators and glutamate sensors (iGluSnFr) [345]. Expressing calcium indicators in PL pyramidal neurons would provide a proxy for neuronal activity. Based on my electrophysiological findings, I would predict that ablation or overexpression of GIRK channels would lead to increased or decreased neuronal activity at baseline, respectively, and that these changes would be enhanced when $GABA_B$R-GIRK signaling is engaged. Importantly, the GABA sensor (iGABASnFR) could be simultaneously employed to provide an indication of when GABAergic neurotransmission, and perhaps $GABA_B$R-GIRK activation, occurs in PL pyramidal neurons [346]. If GIRK channel manipulations are sufficient to alter neuronal activity, one could express the glutamate sensor in brain regions that receive dense PL input and that have been implicated in addiction-related behavior (e.g., NAc, VTA). In accordance with the changes in PL pyramidal neuron activity, I would predict that ablation or overexpression of GIRK channels would enhance or reduce downstream glutamate levels, respectively. Together, these *in vivo* studies of PL pyramidal neuron activity and glutamate release could help bridge the gap between the changes I have observed in ex vivo physiology and behavior.

5.2.2 Subpopulation-selective studies of PL pyramidal neuron GIRK channel plasticity

Another future direction to explore is the possibility that behavioral alterations observed following PL pyramidal neuron manipulations might be primarily driven by particular pyramidal neuron subpopulations. Indeed, PL pyramidal neurons are a

heterogenous population that differ with respect to their morphological features, electrophysiological properties, expression of receptors, projection targets, and regulation of behaviors [27]. My work in **Chapter 2** showed that behavioral alterations observed following the global excitation of PL pyramidal neurons could be recapitulated by the selective excitation of PL pyramidal neurons that project to the VTA, but not the NAc or BLA. In **Chapters 2 & 3** I found that global PL pyramidal neuron GIRK channel ablation potentiated cocaine-induced locomotion and impaired the extinction of cocaine CPP. However, whether the loss of GIRK channels in specific PL projections underlies these behavioral outcomes remains unknown. Interestingly, several brain regions that receive PL input (e.g., BLA, PVT, IL, RMTg) have been implicated in similar behaviors, including behavioral sensitivity to cocaine [31], cue-induced reward seeking [36,347], and extinction learning [348,349]. To determine if loss of GIRK channel activity in specific PL projections underlies the aforementioned behavioral abnormalities, one could employ a projection-specific GIRK channel ablation approach. Such an approach would involve the Flp and Cre recombinase systems, and a retrogradely transported vector (AAV2retro) [243]. Specifically, a Flp-dependent Cre (AAV8-CaMKIIα-fDIO-Cre(mCherry)) or control (AAV8-CaMKIIα-fDIO-Cre(mCherry)) vector would be infused into the PL of *GIRK1*$^{fl/fl}$ mice, while AAV2retro-hSyn-Flp(GFP) would be infused into the downstream brain region of interest. In this way, the Cre-driven ablation of GIRK channel activity should occur only in PL pyramidal neurons that specifically project to that brain region. Before examining the behavioral consequences of projection-specific GIRK channel ablation, however, it would be wise to first confirm that cocaine-induced GIRK channel plasticity occurs in that particular PL pyramidal neuron subpopulation. For this, retrobeads or an AAV2retro-based vector expressing a fluorophore could be infused into downstream brain regions of interest to facilitate the targeting of these PL projection neurons during electrophysiological

recordings. Additional studies could also probe for GIRK channel plasticity in D_1R- or D_2R-expressing PL pyramidal neuron subpopulations using D_1R-tdTomato and D_2R-eGFP transgenic mouse lines. Combining D_1R- and D_2R-Cre:Cas9GFP transgenic lines with CaMKIIα-based gRNA vectors could allow one to further examine the contribution of GIRK channels in PL pyramidal neuron subpopulations to behavior. Insights gleaned from these studies could shed light on the role of mesocortical DA release in the PL.

5.2.3 Improved behavioral models of addiction

Work in **Chapter 2** assessing the contribution of acute (chemogenetic) and persistent (GIRK ablation) increases in PL pyramidal neuron excitability relied heavily on the acute locomotor response to cocaine. While this assay is simple to run, relatively easy to interpret, and captures the acute physical and mental status of an animal initially exposed to cocaine, it does not model the change in locomotor response following repeated drug exposure (i.e., locomotor sensitization). Importantly, locomotor sensitization shares some anatomic and neurochemical features with craving- and relapse-like behavior in rodents, and findings from locomotor sensitization studies have led to potential pharmacotherapies that have been tested in animal models of relapse and in human addicts [186]. Future experiments could examine the impact of PL pyramidal neuron-selective chemogenetic and GIRK ablation manipulations on cocaine-induced locomotor sensitization. Since reduced GIRK channel activity potentiated cocaine-induced locomotion, thereby mimicking a “presensitization-like” phenotype, I would predict that the manipulation would preclude the development of locomotor sensitization. Indeed, similar results were observed in wild-type mice following a non cell type-selective knockdown of Girk1 and Girk2 in the PL [28]. Since acute excitation of PL pyramidal neurons evoked baseline hyperactivity, which was additive with the cocaine-induced increase in activity, it

would be interesting to compare locomotor sensitization results with the GIRK channel ablation manipulation. However, one conducting such experiments must consider the potential for ceiling effects with regards to locomotor activity. This concern could be mitigated by using a lower dose of CNO to reduce the level of baseline hyperactivity.

Work in **Chapter 3** examined the impact of reduced GIRK channel activity in PL pyramidal neurons on the acquisition and extinction of cocaine CPP. While loss of GIRK channel activity did not impact the rewarding valence of cocaine, the manipulation impaired extinction of cocaine CPP in male mice. A follow-up experiment found that strengthening GIRK channel activity in these neurons was sufficient to enhance extinction. Although a deficit in extinction could lead to prolonged drug-seeking behavior and a greater propensity for relapse, it's also possible that this reduction in extinction is only temporary. Notably, our study only included a single extinction test after 2 extinction training sessions. Future studies should extend this timeline to determine how long manipulation-induced impairments or enhancements in extinction last. These studies should also assess the impact of GIRK manipulations on cocaine- and/or stress-evoked reinstatement of cocaine CPP, especially considering the critical role of PL pyramidal neuron activity in this process [40]. Additionally, to examine the selectivity of these manipulations for cocaine reward, one might be able to design similar CPP studies that substitute cocaine for natural rewards (e.g., socialization, palatable food) [350,351]. Importantly, these investigations should involve the use of both male and female subjects to probe for sex-specific behavioral impacts of GIRK channel manipulations. Since factors such as the frequency or duration of conditioning or extinction sessions may impact behavioral outcomes [352], it will be important to optimize CPP procedures to help minimize the variability and maximize the reliability of the data.

Cocaine CPP is useful for modeling the rewarding valence of cocaine, but it does not provide much insight into the drug's reinforcing properties. Cocaine self-administration could be used to assess the impact of GIRK manipulations on acquisition, expression, extinction, and reinstatement of self-administration by drug cues, stress, or drug exposure. This model would provide meaningful insight into whether changes in place preference during extinction of cocaine CPP might translate to changes in lever pressing or nose poking. Furthermore, these extinction studies could be conducted over longer time frames to help assess the durability of these behavioral alterations and allow for a better assessment of the GIRK channel's therapeutic potential.

5.3 Concluding thoughts

This dissertation highlights the important contributions of the PL pyramidal neuron GIRK channel to cellular excitability and behavior. My work suggests that cocaine-evoked plasticity of GIRK-dependent signaling in PL pyramidal neurons may contribute to cognitive and behavioral abnormalities associated with chronic cocaine intake. Therefore, manipulations that restore GIRK channel function, or prevent GIRK channel plasticity, might have therapeutic potential for treating or preventing addiction. Interestingly, systemic administration of baclofen facilitated extinction of drug-induced CPP in male rodents [310,325,326], an effect that may involve baclofen's actions in the PL [44,319]. Follow-up studies will be important to determine if drugs that more selectively target GIRK channels, such as the GIRK1-containing GIRK channel activator ML297, can similarly facilitate the extinction process in addiction models. Interestingly, a recent study found that systemic ML297 can restore cognitive flexibility in chronically-stressed male mice [296].

In addition to pharmacological treatments, non-invasive neuromodulation techniques may provide a more targeted therapeutic approach. Indeed, the use of

repetitive transcranial magnetic stimulation (rTMS) in specific PFC subregions has shown promise in the treatment of cocaine-use disorder [353]. For example, repetitive stimulation in the ACC, a brain region that shares homologous features with the rodent PL, has been shown to reduce cocaine craving and consumption in humans [354]. Similar outcomes have been reported in patients with alcohol use disorder that received ACC stimulation via cortical implants [355], which suggests that neuromodulation-based treatments may be amenable to other substance use disorders. Since reductions in drug craving have been correlated with reduced ACC activity following stimulation [354,355], it is tempting to speculate that these therapeutic effects might be partially driven by prolonged reductions in the activity and connectivity of brain circuits that regulate the extinction of drug-related memories. Adjusting the stimulation parameters of neuromodulation techniques may enable selective targeting of specific neuronal subpopulations [356], as well as provide finer control over the neuronal activity patterns and plasticity mechanisms induced by stimulation [353]. Thus, optimizing these conditions may ultimately lead to a more selective and efficacious approach to strengthen the extinction process in addiction.

Bibliography

1 Volkow, N. D., Koob, G. F. & McLellan, A. T. Neurobiologic Advances from the Brain Disease Model of Addiction. *The New England journal of medicine* **374**, 363-371, doi:10.1056/NEJMra1511480 (2016).

2 Derefinko, K. J. *et al.* Addiction Medicine Training Fellowships in North America: A Recent Assessment of Progress and Needs. *Journal of addiction medicine* **14**, e103-e109, doi:10.1097/adm.0000000000000595 (2020).

3 American Psychological Association, APA, (2013).

4 Bell, J. & Strang, J. Medication Treatment of Opioid Use Disorder. *Biol Psychiatry* **87**, 82-88, doi:10.1016/j.biopsych.2019.06.020 (2020).

5 Müller, C. A., Geisel, O., Banas, R. & Heinz, A. Current pharmacological treatment approaches for alcohol dependence. *Expert Opin Pharmacother* **15**, 471-481, doi:10.1517/14656566.2014.876008 (2014).

6 Jackson, S. E., Kotz, D., West, R. & Brown, J. Moderators of real-world effectiveness of smoking cessation aids: a population study. *Addiction* **114**, 1627-1638, doi:10.1111/add.14656 (2019).

7 Douaihy, A. B., Kelly, T. M. & Sullivan, C. Medications for substance use disorders. *Soc Work Public Health* **28**, 264-278, doi:10.1080/19371918.2013.759031 (2013).

8 Kuhn, B. N., Kalivas, P. W. & Bobadilla, A. C. Understanding Addiction Using Animal Models. *Frontiers in behavioral neuroscience* **13**, 262, doi:10.3389/fnbeh.2019.00262 (2019).

9 Volkow, N. D., Michaelides, M. & Baler, R. The Neuroscience of Drug Reward and Addiction. *Physiol Rev* **99**, 2115-2140, doi:10.1152/physrev.00014.2018 (2019).

10 Guo, Q. *et al.* Whole-Brain Mapping of Inputs to Projection Neurons and Cholinergic Interneurons in the Dorsal Striatum. *PloS one* **10**, e0123381, doi:10.1371/journal.pone.0123381 (2015).

11 Ferenczi, E. A. *et al.* Prefrontal cortical regulation of brainwide circuit dynamics and reward-related behavior. *Science* **351**, aac9698, doi:10.1126/science.aac9698 (2016).

12 Carr, D. B. & Sesack, S. R. Projections from the rat prefrontal cortex to the ventral tegmental area: target specificity in the synaptic associations with mesoaccumbens and mesocortical neurons. *J Neurosci* **20**, 3864-3873, doi:10.1523/jneurosci.20-10-03864.2000 (2000).

13 Wise, R. A. Dopamine, learning and motivation. *Nat Rev Neurosci* **5**, 483-494, doi:10.1038/nrn1406 (2004).

14 Pignatelli, M. & Bonci, A. Role of Dopamine Neurons in Reward and Aversion: A Synaptic Plasticity Perspective. *Neuron* **86**, 1145-1157, doi:10.1016/j.neuron.2015.04.015 (2015).

15 Bouarab, C., Thompson, B. & Polter, A. M. VTA GABA Neurons at the Interface of Stress and Reward. *Front Neural Circuits* **13**, 78, doi:10.3389/fncir.2019.00078 (2019).

16 Dobi, A., Margolis, E. B., Wang, H. L., Harvey, B. K. & Morales, M. Glutamatergic and nonglutamatergic neurons of the ventral tegmental area establish local synaptic contacts with dopaminergic and nondopaminergic neurons. *J Neurosci* **30**, 218-229, doi:10.1523/jneurosci.3884-09.2010 (2010).

17 Weele, C. M. V., Siciliano, C. A. & Tye, K. M. Dopamine tunes prefrontal outputs to orchestrate aversive processing. *Brain Res* **1713**, 16-31, doi:10.1016/j.brainres.2018.11.044 (2019).
18 Sesack, S. R. & Grace, A. A. Cortico-Basal Ganglia reward network: microcircuitry. *Neuropsychopharmacology* **35**, 27-47, doi:10.1038/npp.2009.93 (2010).
19 Turner, B. D., Kashima, D. T., Manz, K. M., Grueter, C. A. & Grueter, B. A. Synaptic Plasticity in the Nucleus Accumbens: Lessons Learned from Experience. *ACS chemical neuroscience* **9**, 2114-2126, doi:10.1021/acschemneuro.7b00420 (2018).
20 Xu, L., Nan, J. & Lan, Y. The Nucleus Accumbens: A Common Target in the Comorbidity of Depression and Addiction. *Front Neural Circuits* **14**, 37, doi:10.3389/fncir.2020.00037 (2020).
21 Macpherson, T., Morita, M. & Hikida, T. Striatal direct and indirect pathways control decision-making behavior. *Frontiers in psychology* **5**, 1301, doi:10.3389/fpsyg.2014.01301 (2014).
22 Kupchik, Y. M. *et al.* Coding the direct/indirect pathways by D1 and D2 receptors is not valid for accumbens projections. *Nat Neurosci*, doi:10.1038/nn.4068 (2015).
23 Scofield, M. D. *et al.* The Nucleus Accumbens: Mechanisms of Addiction across Drug Classes Reflect the Importance of Glutamate Homeostasis. *Pharmacol Rev* **68**, 816-871, doi:10.1124/pr.116.012484 (2016).
24 Luscher, C. & Malenka, R. C. Drug-evoked synaptic plasticity in addiction: from molecular changes to circuit remodeling. *Neuron* **69**, 650-663, doi:10.1016/j.neuron.2011.01.017 (2011).
25 Miller, E. K. & Cohen, J. D. An integrative theory of prefrontal cortex function. *Annu Rev Neurosci* **24**, 167-202, doi:10.1146/annurev.neuro.24.1.167 (2001).
26 Hearing, M. C., Zink, A. N. & Wickman, K. Cocaine-induced adaptations in metabotropic inhibitory signaling in the mesocorticolimbic system. *Rev Neurosci* **23**, 325-351, doi:10.1515/revneuro-2012-0045 (2012).
27 Kummer, K. K., Mitrić, M., Kalpachidou, T. & Kress, M. The Medial Prefrontal Cortex as a Central Hub for Mental Comorbidities Associated with Chronic Pain. *International journal of molecular sciences* **21**, doi:10.3390/ijms21103440 (2020).
28 Hearing, M. *et al.* Repeated cocaine weakens GABA(B)-Girk signaling in layer 5/6 pyramidal neurons in the prelimbic cortex. *Neuron* **80**, 159-170, doi:10.1016/j.neuron.2013.07.019 (2013).
29 Muller, J. F., Mascagni, F. & McDonald, A. J. Pyramidal cells of the rat basolateral amygdala: synaptology and innervation by parvalbumin-immunoreactive interneurons. *J Comp Neurol* **494**, 635-650, doi:10.1002/cne.20832 (2006).
30 Lisman, J., Schulman, H. & Cline, H. The molecular basis of CaMKII function in synaptic and behavioural memory. *Nat Rev Neurosci* **3**, 175-190, doi:10.1038/nrn753 (2002).
31 Rose, T. R., Marron Fernandez de Velasco, E., Vo, B. N., Tipps, M. E. & Wickman, K. Impact of Acute and Persistent Excitation of Prelimbic Pyramidal Neurons on Motor Activity and Trace Fear Learning. *J Neurosci* **41**, 960-971, doi:10.1523/JNEUROSCI.2606-20.2020 (2021).
32 Yang, C. R., Seamans, J. K. & Gorelova, N. Electrophysiological and morphological properties of layers V-VI principal pyramidal cells in rat prefrontal cortex in vitro. *J Neurosci* **16**, 1904-1921 (1996).

33 Spruston, N. Pyramidal neurons: dendritic structure and synaptic integration. *Nat Rev Neurosci* **9**, 206-221, doi:10.1038/nrn2286 (2008).
34 Murugan, M. *et al.* Combined Social and Spatial Coding in a Descending Projection from the Prefrontal Cortex. *Cell* **171**, 1663-1677.e1616, doi:10.1016/j.cell.2017.11.002 (2017).
35 Connors, B. W. & Gutnick, M. J. Intrinsic firing patterns of diverse neocortical neurons. *Trends Neurosci* **13**, 99-104 (1990).
36 Otis, J. M. *et al.* Prefrontal cortex output circuits guide reward seeking through divergent cue encoding. *Nature* **543**, 103-107, doi:10.1038/nature21376 (2017).
37 Green, S. M., Nathani, S., Zimmerman, J., Fireman, D. & Urs, N. M. Retrograde Labeling Illuminates Distinct Topographical Organization of D1 and D2 Receptor-Positive Pyramidal Neurons in the Prefrontal Cortex of Mice. *eNeuro* **7**, doi:10.1523/eneuro.0194-20.2020 (2020).
38 Hoover, W. B. & Vertes, R. P. Anatomical analysis of afferent projections to the medial prefrontal cortex in the rat. *Brain Struct Funct* **212**, 149-179, doi:10.1007/s00429-007-0150-4 (2007).
39 Vertes, R. P. Differential projections of the infralimbic and prelimbic cortex in the rat. *Synapse* **51**, 32-58, doi:10.1002/syn.10279 (2004).
40 Goode, T. D. & Maren, S. Common neurocircuitry mediating drug and fear relapse in preclinical models. *Psychopharmacology (Berl)* **236**, 415-437, doi:10.1007/s00213-018-5024-3 (2019).
41 Sharpe, M. J. & Killcross, S. Modulation of attention and action in the medial prefrontal cortex of rats. *Psychol Rev* **125**, 822-843, doi:10.1037/rev0000118 (2018).
42 Giustino, T. F. & Maren, S. The Role of the Medial Prefrontal Cortex in the Conditioning and Extinction of Fear. *Frontiers in behavioral neuroscience* **9**, 298, doi:10.3389/fnbeh.2015.00298 (2015).
43 Riaz, S. *et al.* Prelimbic and infralimbic cortical inactivations attenuate contextually driven discriminative responding for reward. *Scientific reports* **9**, 3982, doi:10.1038/s41598-019-40532-7 (2019).
44 Moorman, D. E. & Aston-Jones, G. Prefrontal neurons encode context-based response execution and inhibition in reward seeking and extinction. *Proc Natl Acad Sci U S A* **112**, 9472-9477, doi:10.1073/pnas.1507611112 (2015).
45 Lui, J. H. *et al.* Differential encoding in prefrontal cortex projection neuron classes across cognitive tasks. *Cell* **184**, 489-506.e426, doi:10.1016/j.cell.2020.11.046 (2021).
46 McFarland, K., Lapish, C. C. & Kalivas, P. W. Prefrontal glutamate release into the core of the nucleus accumbens mediates cocaine-induced reinstatement of drug-seeking behavior. *J Neurosci* **23**, 3531-3537, doi:23/8/3531 [pii] (2003).
47 Rubio, F. J. *et al.* Prelimbic cortex is a common brain area activated during cue-induced reinstatement of cocaine and heroin seeking in a polydrug self-administration rat model. *Eur J Neurosci* **49**, 165-178, doi:10.1111/ejn.14203 (2019).
48 McGlinchey, E. M., James, M. H., Mahler, S. V., Pantazis, C. & Aston-Jones, G. Prelimbic to Accumbens Core Pathway Is Recruited in a Dopamine-Dependent Manner to Drive Cued Reinstatement of Cocaine Seeking. *J Neurosci* **36**, 8700-8711, doi:10.1523/JNEUROSCI.1291-15.2016 (2016).
49 Stefanik, M. T., Kupchik, Y. M. & Kalivas, P. W. Optogenetic inhibition of cortical afferents in the nucleus accumbens simultaneously prevents cue-induced

transient synaptic potentiation and cocaine-seeking behavior. *Brain Struct Funct*, doi:10.1007/s00429-015-0997-8 (2015).
50 Steketee, J. D. Neurotransmitter systems of the medial prefrontal cortex: potential role in sensitization to psychostimulants. *Brain Res Brain Res Rev* **41**, 203-228, doi:10.1016/s0165-0173(02)00233-3 (2003).
51 Pastor, V. & Medina, J. H. Medial prefrontal cortical control of reward- and aversion-based behavioral output: Bottom-up modulation. *Eur J Neurosci* **53**, 3039-3062, doi:10.1111/ejn.15168 (2021).
52 Kawaguchi, Y. & Kubota, Y. GABAergic cell subtypes and their synaptic connections in rat frontal cortex. *Cereb Cortex* **7**, 476-486 (1997).
53 Ferguson, B. R. & Gao, W. J. PV Interneurons: Critical Regulators of E/I Balance for Prefrontal Cortex-Dependent Behavior and Psychiatric Disorders. *Front Neural Circuits* **12**, 37, doi:10.3389/fncir.2018.00037 (2018).
54 Yang, S. S., Mack, N. R., Shu, Y. & Gao, W. J. Prefrontal GABAergic Interneurons Gate Long-Range Afferents to Regulate Prefrontal Cortex-Associated Complex Behaviors. *Front Neural Circuits* **15**, 716408, doi:10.3389/fncir.2021.716408 (2021).
55 Sun, Q. *et al.* A whole-brain map of long-range inputs to GABAergic interneurons in the mouse medial prefrontal cortex. *Nat Neurosci* **22**, 1357-1370, doi:10.1038/s41593-019-0429-9 (2019).
56 Cardin, J. A. Functional flexibility in cortical circuits. *Curr Opin Neurobiol* **58**, 175-180, doi:10.1016/j.conb.2019.09.008 (2019).
57 Chen, R. *et al.* Abolished cocaine reward in mice with a cocaine-insensitive dopamine transporter. *Proc Natl Acad Sci U S A* **103**, 9333-9338, doi:10.1073/pnas.0600905103 (2006).
58 Volkow, N. D. & Morales, M. The Brain on Drugs: From Reward to Addiction. *Cell* **162**, 712-725, doi:10.1016/j.cell.2015.07.046 (2015).
59 Jeffcoat, A. R., Perez-Reyes, M., Hill, J. M., Sadler, B. M. & Cook, C. E. Cocaine disposition in humans after intravenous injection, nasal insufflation (snorting), or smoking. *Drug metabolism and disposition: the biological fate of chemicals* **17**, 153-159 (1989).
60 Kamato, D. *et al.* Structure, Function, Pharmacology, and Therapeutic Potential of the G Protein, Gα/q,11. *Frontiers in cardiovascular medicine* **2**, 14, doi:10.3389/fcvm.2015.00014 (2015).
61 Fan, Q. R., Guo, W. Y., Geng, Y. & Evelyn, M. G. in *G-Protein-Coupled Receptor Dimers* 307-325 (Springer International Publishing, Cham, 2017).
62 Frangaj, A. & Fan, Q. R. Structural biology of GABAB receptor. *Neuropharmacology* **136**, 68-79, doi:10.1016/J.NEUROPHARM.2017.10.011 (2018).
63 Jiang, X. *et al.* GABAB receptor complex as a potential target for tumor therapy. *J Histochem Cytochem* **60**, 269-279, doi:10.1369/0022155412438105 (2012).
64 Bettler, B., Kaupmann, K., Mosbacher, J. & Gassmann, M. Molecular structure and physiological functions of GABA(B) receptors. *Physiol Rev* **84**, 835-867 (2004).
65 Kasten, C. R., Boehm, S. L. & II. Identifying the role of pre-and postsynaptic GABA(B) receptors in behavior. *Neuroscience and biobehavioral reviews* **57**, 70-87, doi:10.1016/j.neubiorev.2015.08.007 (2015).
66 Vigot, R. *et al.* Differential compartmentalization and distinct functions of GABAB receptor variants. *Neuron* **50**, 589-601, doi:10.1016/j.neuron.2006.04.014 (2006).

67 Lee, C., Mayfield, R. D. & Harris, R. A. Intron 4 Containing Novel GABAB1 Isoforms Impair GABAB Receptor Function. *PloS one* **5**, e14044, doi:10.1371/journal.pone.0014044 (2010).
68 Grace, C. R. R. *et al.* NMR structure and peptide hormone binding site of the first extracellular domain of a type B1 G protein-coupled receptor. *Proceedings of the National Academy of Sciences of the United States of America* **101**, 12836-12841, doi:10.1073/pnas.0404702101 (2004).
69 Lehtinen, M. J., Meri, S. & Jokiranta, T. S. Interdomain Contact Regions and Angles Between Adjacent Short Consensus Repeat Domains. *Journal of molecular biology* **344**, 1385-1396, doi:10.1016/J.JMB.2004.10.017 (2004).
70 Blein, S. *et al.* Structural Analysis of the Complement Control Protein (CCP) Modules of GABA _B Receptor 1a. *Journal of Biological Chemistry* **279**, 48292-48306, doi:10.1074/jbc.M406540200 (2004).
71 Schwenk, J. *et al.* Modular composition and dynamics of native GABAB receptors identified by high-resolution proteomics. *Nature Neuroscience* **19**, 233-242, doi:10.1038/nn.4198 (2016).
72 Rice, H. C. *et al.* Secreted amyloid-β precursor protein functions as a GABABR1a ligand to modulate synaptic transmission. **363**, eaao4827 (2019).
73 Hannan, S., Wilkins, M. E. & Smart, T. G. Sushi domains confer distinct trafficking profiles on GABAB receptors. *Proceedings of the National Academy of Sciences of the United States of America* **109**, 12171-12176, doi:10.1073/pnas.1201660109 (2012).
74 Biermann, B. *et al.* The Sushi domains of GABAB receptors function as axonal targeting signals. *The Journal of neuroscience : the official journal of the Society for Neuroscience* **30**, 1385-1394, doi:10.1523/JNEUROSCI.3172-09.2010 (2010).
75 Gassmann, M. & Bettler, B. Regulation of neuronal GABAB receptor functions by subunit composition. *Nature Reviews Neuroscience* **13**, 380-394, doi:10.1038/nrn3249 (2012).
76 Xue, L. *et al.* Rearrangement of the transmembrane domain interfaces associated with the activation of a GPCR hetero-oligomer. *Nature communications* **10**, 2765, doi:10.1038/s41467-019-10834-5 (2019).
77 Comps-Agrar, L. *et al.* The oligomeric state sets GABA _B receptor signalling efficacy. *The EMBO Journal* **30**, 2336-2349, doi:10.1038/emboj.2011.143 (2011).
78 Hammond, C. & Mott, D. The metabotropic GABAB receptors. *Cellular and Molecular Neurophysiology*, 245-267, doi:10.1016/B978-0-12-397032-9.00011-X (2015).
79 Luscher, C. & Slesinger, P. A. Emerging roles for G protein-gated inwardly rectifying potassium (GIRK) channels in health and disease. *Nat Rev Neurosci* **11**, 301-315, doi:10.1038/nrn2834 (2010).
80 Hillenbrand, M., Schori, C., Schöppe, J. & Plückthun, A. Comprehensive analysis of heterotrimeric G-protein complex diversity and their interactions with GPCRs in solution. *Proceedings of the National Academy of Sciences of the United States of America* **112**, E1181-1190, doi:10.1073/pnas.1417573112 (2015).
81 Fritzius, T. & Bettler, B. The organizing principle of GABAB receptor complexes: Physiological and pharmacological implications. *Basic Clin Pharmacol Toxicol*, doi:10.1111/bcpt.13241 (2019).
82 Milligan, G. & Kostenis, E. Heterotrimeric G-proteins: a short history., doi:10.1038/sj.bjp.0706405 (2006).

83 Rose, T. R. & Wickman, K. Mechanisms and Regulation of Neuronal GABAB Receptor-Dependent Signaling. *Current topics in behavioral neurosciences*, doi:10.1007/7854_2020_129 (2020).
84 Schwindinger, W. F. *et al.* Synergistic roles for G-protein gamma3 and gamma7 subtypes in seizure susceptibility as revealed in double knock-out mice. *J Biol Chem* **287**, 7121-7133, doi:10.1074/jbc.M111.308395 (2012).
85 Schwenk, J. *et al.* Modular composition and dynamics of native GABAB receptors identified by high-resolution proteomics. *Nat Neurosci* **19**, 233-242, doi:10.1038/nn.4198 (2016).
86 Halls, M. L. & Cooper, D. M. F. Adenylyl cyclase signalling complexes – Pharmacological challenges and opportunities. *Pharmacology & Therapeutics* **172**, 171-180, doi:10.1016/J.PHARMTHERA.2017.01.001 (2017).
87 Terunuma, M. Diversity of structure and function of GABAB receptors: a complexity of GABAB-mediated signaling. *Proceedings of the Japan Academy. Series B, Physical and biological sciences* **94**, 390-411, doi:10.2183/pjab.94.026 (2018).
88 Knight, A. R. & Bowery, N. G. The pharmacology of adenylyl cyclase modulation by GABAB receptors in rat brain slices. *Neuropharmacology* **35**, 703-712, doi:10.1016/0028-3908(96)84642-9 (1996).
89 Bettler B, K. K., Mosbacher J and Gassmann M. Molecular structure and physiological functions of GABAB receptors. *Physiol Rev* **84**, 835-867 (2004).
90 Bowery N, e. a. Mammalian gamma-aminobutyric acid(B) receptors: structure and function. *Pharmacol Rev* **54**, 247-264 (2002).
91 Hashimoto, T. & Kuriyama, K. In Vivo Evidence that GABAB Receptors Are Negatively Coupled to Adenylate Cyclase in Rat Striatum. *Journal of Neurochemistry* **69**, 365-370, doi:10.1046/j.1471-4159.1997.69010365.x (2002).
92 Rost, B. R. *et al.* Activation of metabotropic GABA receptors increases the energy barrier for vesicle fusion. *Journal of Cell Science* **124**, 3066-3073, doi:10.1242/JCS.074963 (2011).
93 Xiao, Z. *et al.* Noradrenergic depression of neuronal excitability in the entorhinal cortex via activation of TREK-2 K+ channels. *J Biol Chem* **284**, 10980-10991 (2009).
94 Chalifoux, J. R. & Carter, A. G. GABAB Receptors Modulate NMDA Receptor Calcium Signals in Dendritic Spines. *Neuron* **66**, 101-113, doi:10.1016/J.NEURON.2010.03.012 (2010).
95 Connelly, W. M. *et al.* GABAB Receptors Regulate Extrasynaptic GABAA Receptors. *The Journal of neuroscience : the official journal of the Society for Neuroscience* **33**, 3780-3785, doi:10.1523/JNEUROSCI.4989-12.2013 (2013).
96 Ghorbel, M. T., Becker, K. G. & Henley, J. M. Profile of changes in gene expression in cultured hippocampal neurones evoked by the GABAB receptor agonist baclofen. *Physiological genomics* **22**, 93-98, doi:10.1152/physiolgenomics.00202.2004 (2005).
97 Proft, J. & Weiss, N. G protein regulation of neuronal calcium channels: back to the future. **87**, 890-906 (2015).
98 Chalifoux, J. R. & Carter, A. G. GABAB receptor modulation of voltage-sensitive calcium channels in spines and dendrites. *The Journal of neuroscience : the official journal of the Society for Neuroscience* **31**, 4221-4232, doi:10.1523/JNEUROSCI.4561-10.2011 (2011).

99 Burke, K. J. & Bender, K. J. Modulation of Ion Channels in the Axon: Mechanisms and Function. *Frontiers in cellular neuroscience* **13**, 221, doi:10.3389/fncel.2019.00221 (2019).
100 Colecraft, H. M., Patil, P. G. & Yue, D. T. Differential Occurrence of Reluctant Openings in G-Protein–Inhibited N- and P/Q-Type Calcium Channels. *The Journal of General Physiology* **115**, 175-192, doi:10.1085/jgp.115.2.175 (2000).
101 Pérez-Garci, E., Gassmann, M., Bettler, B. & Larkum, M. E. The GABAB1b Isoform Mediates Long-Lasting Inhibition of Dendritic Ca2+ Spikes in Layer 5 Somatosensory Pyramidal Neurons. *Neuron* **50**, 603-616, doi:10.1016/j.neuron.2006.04.019 (2006).
102 Chalifoux, J. R. & Carter, A. G. GABAB receptor modulation of voltage-sensitive calcium channels in spines and dendrites. *J Neurosci* **31**, 4221-4232, doi:10.1523/JNEUROSCI.4561-10.2011 (2011).
103 Booker, S. A. *et al.* Postsynaptic GABABRs Inhibit L-Type Calcium Channels and Abolish Long-Term Potentiation in Hippocampal Somatostatin Interneurons. *Cell reports* **22**, 36-43, doi:10.1016/j.celrep.2017.12.021 (2018).
104 Laviv, T. *et al.* Compartmentalization of the GABAB Receptor Signaling Complex Is Required for Presynaptic Inhibition at Hippocampal Synapses. *Journal of Neuroscience* **31**, 12523-12532, doi:10.1523/JNEUROSCI.1527-11.2011 (2011).
105 Luján, R. *et al.* Differential association of GABAB receptors with their effector ion channels in Purkinje cells. *Brain Structure and Function* **223**, 1565-1587, doi:10.1007/s00429-017-1568-y (2017).
106 Garaycochea, J. & Slaughter, M. M. GABAB receptors enhance excitatory responses in isolated rat retinal ganglion cells. *The Journal of physiology* **594**, 5543-5554, doi:10.1113/JP272374 (2016).
107 Karls, A. & Mynlieff, M. GABAB receptors couple to Gα q to mediate increases in voltage-dependent calcium current during development. *Journal of Neurochemistry* **135**, 88-100, doi:10.1111/jnc.13259 (2015).
108 Workman, E. R., Niere, F. & Raab-Graham, K. F. mTORC1-dependent protein synthesis underlying rapid antidepressant effect requires GABABR signaling. *Neuropharmacology* **73**, 192-203, doi:10.1016/J.NEUROPHARM.2013.05.037 (2013).
109 Zhang, J. *et al.* Presynaptic Excitation via GABA B Receptors in Habenula Cholinergic Neurons Regulates Fear Memory Expression. *Cell* **166**, 716-728, doi:10.1016/j.cell.2016.06.026 (2016).
110 Lujan, R. & Aguado, C. Localization and Targeting of GIRK Channels in Mammalian Central Neurons. *International review of neurobiology* **123**, 161-200, doi:10.1016/bs.irn.2015.05.009 (2015).
111 Karschin, C., Dissmann, E., Stuhmer, W. & Karschin, A. IRK(1-3) and GIRK(1-4) inwardly rectifying K+ channel mRNAs are differentially expressed in the adult rat brain. *J Neurosci* **16**, 3559-3570 (1996).
112 Luján, R., Marron Fernandez de Velasco, E., Aguado, C. & Wickman, K. New insights into the therapeutic potential of Girk channels. *Trends in Neurosciences* **37**, 20-29, doi:10.1016/j.tins.2013.10.006 (2014).
113 Lujan, R., Marron Fernandez de Velasco, E., Aguado, C. & Wickman, K. New insights into the therapeutic potential of Girk channels. *Trends Neurosci* **37**, 20-29, doi:10.1016/j.tins.2013.10.006 (2014).
114 Reuveny, E. *et al.* Activation of the cloned muscarinic potassium channel by G protein beta gamma subunits. *Nature* **370**, 143-146 (1994).

115 Wickman, K. D. *et al.* Recombinant G-protein beta gamma-subunits activate the muscarinic-gated atrial potassium channel. *Nature* **368**, 255-257 (1994).
116 Huang, C. L., Feng, S. & Hilgemann, D. W. Direct activation of inward rectifier potassium channels by PIP2 and its stabilization by Gbetagamma. *Nature* **391**, 803-806 (1998).
117 Nicoll, R. A. My close encounter with GABAB receptors. *Biochemical Pharmacology* **68**, 1667-1674, doi:10.1016/j.bcp.2004.07.024 (2004).
118 Leung, L. S. & Peloquin, P. GABAB receptors inhibit backpropagating dendritic spikes in hippocampal CA1 pyramidal cells in vivo. *Hippocampus* **16**, 388-407, doi:10.1002/hipo.20168 (2006).
119 Blednov, Y. A., Stoffel, M., Chang, S. R. & Harris, R. A. GIRK2 deficient mice. Evidence for hyperactivity and reduced anxiety. *Physiol Behav* **74**, 109-117 (2001).
120 Signorini, S., Liao, Y. J., Duncan, S. A., Jan, L. Y. & Stoffel, M. Normal cerebellar development but susceptibility to seizures in mice lacking G protein-coupled, inwardly rectifying K+ channel GIRK2. *Proc Natl Acad Sci U S A* **94**, 923-927 (1997).
121 Gassmann, M. *et al.* Redistribution of GABAB(1) protein and atypical GABAB responses in GABAB(2)-deficient mice. *J Neurosci* **24**, 6086-6097 (2004).
122 Becher, A., White, J. H. & McIlhinney, R. A. J. The γ-aminobutyric acid receptor B, but not the metabotropic glutamate receptor type-1, associates with lipid rafts in the rat cerebellum. *Journal of Neurochemistry* **79**, 787-795, doi:10.1046/j.1471-4159.2001.00614.x (2008).
123 Koyrakh, L. *et al.* Molecular and cellular diversity of neuronal G-protein-gated potassium channels. *J Neurosci* **25**, 11468-11478 (2005).
124 Fajardo-Serrano, A. *et al.* Association of Rgs7/Gβ5 complexes with GIRK channels and GABAB receptors in hippocampal CA1 pyramidal neurons. *Hippocampus* **23**, 1231-1245, doi:10.1002/hipo.22161 (2013).
125 David, M. *et al.* Interactions between GABA-B1 receptors and Kir 3 inwardly rectifying potassium channels. *Cell Signal* **18**, 2172-2181 (2006).
126 Clancy, S. M. *et al.* Pertussis-toxin-sensitive Galpha subunits selectively bind to C-terminal domain of neuronal GIRK channels: evidence for a heterotrimeric G-protein-channel complex. *Mol Cell Neurosci* **28**, 375-389 (2005).
127 Ciruela, F. *et al.* Evidence for oligomerization between GABAB receptors and GIRK channels containing the GIRK1 and GIRK3 subunits. *Eur J Neurosci* **32**, 1265-1277 (2010).
128 Fowler, C. E., Aryal, P., Suen, K. F. & Slesinger, P. A. Evidence for association of GABA(B) receptors with Kir3 channels and regulators of G protein signalling (RGS4) proteins. *J Physiol* **580**, 51-65 (2007).
129 Kahanovitch, U., Berlin, S. & Dascal, N. Collision coupling in the GABAB receptor-G protein-GIRK signaling cascade. *FEBS Lett* **591**, 2816-2825, doi:10.1002/1873-3468.12756 (2017).
130 Padgett, C. L. *et al.* Methamphetamine-evoked depression of GABA(B) receptor signaling in GABA neurons of the VTA. *Neuron* **73**, 978-989, doi:10.1016/j.neuron.2011.12.031 (2012).
131 Lecca, S. *et al.* Rescue of GABAB and GIRK function in the lateral habenula by protein phosphatase 2A inhibition ameliorates depression-like phenotypes in mice. *Nature Medicine* **22**, 254-261, doi:10.1038/nm.4037 (2016).

132 Gurevich, V. V. & Gurevich, E. V. GPCR Signaling Regulation: The Role of GRKs and Arrestins. *Frontiers in pharmacology* **10**, 125, doi:10.3389/fphar.2019.00125 (2019).
133 Lefkowitz, R. J. Arrestins Come of Age: A Personal Historical Perspective. *Progress in Molecular Biology and Translational Science* **118**, 3-18, doi:10.1016/B978-0-12-394440-5.00001-2 (2013).
134 Benke, D., Zemoura, K. & Maier, P. J. Modulation of cell surface GABAB receptors by desensitization, trafficking and regulated degradation. *World Journal of Biological Chemistry* **3**, 61, doi:10.4331/wjbc.v3.i4.61 (2012).
135 Raveh, A., Turecek, R. & Bettler, B. Mechanisms of Fast Desensitization of GABAB Receptor-Gated Currents. *Advances in Pharmacology* **73**, 145-165, doi:10.1016/BS.APHA.2014.11.004 (2015).
136 Grampp, T., Notz, V., Broll, I., Fischer, N. & Benke, D. Constitutive, agonist-accelerated, recycling and lysosomal degradation of GABAB receptors in cortical neurons. *Molecular and Cellular Neuroscience* **39**, 628-637, doi:10.1016/J.MCN.2008.09.004 (2008).
137 Guetg, N. *et al.* NMDA receptor-dependent GABAB receptor internalization via CaMKII phosphorylation of serine 867 in GABAB1. *Proceedings of the National Academy of Sciences* **107**, 13924-13929, doi:10.1073/pnas.1000909107 (2010).
138 Maier, P. J., Marin, I., Grampp, T., Sommer, A. & Benke, D. Sustained glutamate receptor activation down-regulates GABAB receptors by shifting the balance from recycling to lysosomal degradation. *The Journal of biological chemistry* **285**, 35606-35614, doi:10.1074/jbc.M110.142406 (2010).
139 Kuramoto, N. *et al.* Phospho-Dependent Functional Modulation of GABAB Receptors by the Metabolic Sensor AMP-Dependent Protein Kinase. *Neuron* **53**, 233-247, doi:10.1016/j.neuron.2006.12.015 (2007).
140 Terunuma, M. *et al.* Prolonged activation of NMDA receptors promotes dephosphorylation and alters postendocytic sorting of GABAB receptors. *Proc Natl Acad Sci U S A* **107**, 13918-13923, doi:10.1073/pnas.1000853107 (2010).
141 Couve, A. *et al.* Cyclic AMP–dependent protein kinase phosphorylation facilitates GABAB receptor–effector coupling. *Nature Neuroscience* **5**, 415-424, doi:10.1038/nn833 (2002).
142 Fairfax, B. P. *et al.* Phosphorylation and Chronic Agonist Treatment Atypically Modulate GABA _B Receptor Cell Surface Stability. *Journal of Biological Chemistry* **279**, 12565-12573, doi:10.1074/jbc.M311389200 (2004).
143 Benke, D. Mechanisms of GABAB Receptor Exocytosis, Endocytosis, and Degradation. *Advances in Pharmacology* **58**, 93-111, doi:10.1016/S1054-3589(10)58004-9 (2010).
144 Pontier, S. M. *et al.* Coordinated action of NSF and PKC regulates GABAB receptor signaling efficacy. **25** (2006).
145 Sarker, S., Xiao, K. & Shenoy, S. K. A Tale of Two Sites – How ubiquitination of a G protein-coupled receptor is coupled to its lysosomal trafficking from distinct receptor domains. *Communicative & Integrative Biology* **4**, 528-531, doi:10.4161/cib.16458 (2011).
146 Zemoura, K. *et al.* Endoplasmic Reticulum-associated Degradation Controls Cell Surface Expression of γ-Aminobutyric Acid, Type B Receptors. *Journal of Biological Chemistry* **288**, 34897-34905, doi:10.1074/jbc.M113.514745 (2013).
147 Zemoura, K., Trümpler, C. & Benke, D. Lys-63-linked Ubiquitination of γ-Aminobutyric Acid (GABA), Type B1, at Multiple Sites by the E3 Ligase Mind

Bomb-2 Targets GABAB Receptors to Lysosomal Degradation. *Journal of Biological Chemistry* **291**, 21682-21693, doi:10.1074/jbc.M116.750968 (2016).
148 Zemoura, K., Balakrishnan, K., Grampp, T. & Benke, D. Ca2+/Calmodulin-Dependent Protein Kinase II (CaMKII) β-Dependent Phosphorylation of GABAB1 Triggers Lysosomal Degradation of GABAB Receptors via Mind Bomb-2 (MIB2)-Mediated Lys-63-Linked Ubiquitination. *Molecular Neurobiology* **56**, 1293-1309, doi:10.1007/s12035-018-1142-5 (2019).
149 Lahaie, N., Kralikova, M., Prézeau, L., Blahos, J. & Bouvier, M. Post-endocytotic Deubiquitination and Degradation of the Metabotropic γ-Aminobutyric Acid Receptor by the Ubiquitin-specific Protease 14. **291**, doi:10.1074/jbc.M115.686907 (2016).
150 Schwenk, J. *et al.* Native GABAB receptors are heteromultimers with a family of auxiliary subunits. *Nature* **465**, 231-235, doi:10.1038/nature08964 (2010).
151 Zheng, S., Abreu, N., Levitz, J. & Kruse, A. C. Structural basis for KCTD-mediated rapid desensitization of GABAB signalling. *Nature* **567**, 127-131, doi:10.1038/s41586-019-0990-0 (2019).
152 Adelfinger, L. *et al.* GABAB receptor phosphorylation regulates KCTD12-induced K+ current desensitization. *Biochemical Pharmacology* **91**, 369-379, doi:10.1016/j.bcp.2014.07.013 (2014).
153 Gerber, K. J., Squires, K. E. & Hepler, J. R. Roles for Regulator of G Protein Signaling Proteins in Synaptic Signaling and Plasticity. *Mol Pharmacol* **89**, 273-286, doi:10.1124/mol.115.102210 (2016).
154 Squires, K. E., Montanez-Miranda, C., Pandya, R. R., Torres, M. P. & Hepler, J. R. Genetic Analysis of Rare Human Variants of Regulators of G Protein Signaling Proteins and Their Role in Human Physiology and Disease. *Pharmacol Rev* **70**, 446-474, doi:10.1124/pr.117.015354 (2018).
155 Anderson, G. R., Posokhova, E. & Martemyanov, K. A. The R7 RGS protein family: multi-subunit regulators of neuronal G protein signaling. *Cell biochemistry and biophysics* **54**, 33-46, doi:10.1007/s12013-009-9052-9 (2009).
156 Hollinger, S. & Hepler, J. R. Cellular regulation of RGS proteins: modulators and integrators of G protein signaling. *Pharmacological reviews* **54**, 527-559 (2002).
157 Martemyanov, K. A., Yoo, P. J., Skiba, N. P. & Arshavsky, V. Y. R7BP, a novel neuronal protein interacting with RGS proteins of the R7 family. *J Biol Chem* **280**, 5133-5136 (2005).
158 Jia, L., Linder, M. E. & Blumer, K. J. Gi/o signaling and the palmitoyltransferase DHHC2 regulate palmitate cycling and shuttling of RGS7 family-binding protein. *J Biol Chem* **286**, 13695-13703, doi:10.1074/jbc.M110.193763 (2011).
159 Jia, L. *et al.* A mechanism regulating G protein-coupled receptor signaling that requires cycles of protein palmitoylation and depalmitoylation. *J Biol Chem* **289**, 6249-6257, doi:10.1074/jbc.M113.531475 (2014).
160 Ostrovskaya, O. *et al.* RGS7/Gβ5/R7BP complex regulates synaptic plasticity and memory by modulating hippocampal GABABR-GIRK signaling. *eLife* **3**, e02053, doi:10.7554/eLife.02053 (2014).
161 Xie, K. *et al.* Gβ5 recruits R7 RGS proteins to GIRK channels to regulate the timing of neuronal inhibitory signaling. *Nat Neurosci* **13**, 661-663 (2010).
162 Maity, B. *et al.* Regulator of G protein signaling 6 (RGS6) protein ensures coordination of motor movement by modulating GABAB receptor signaling. *J Biol Chem* **287**, 4972-4981, doi:10.1074/jbc.M111.297218 (2012).
163 Patil, D. N. *et al.* Structural organization of a major neuronal G protein regulator, the RGS7-Gβ5-R7BP complex. *eLife* **7**, doi:10.7554/eLife.42150 (2018).

164 Orlandi, C. *et al.* GPR158/179 regulate G protein signaling by controlling localization and activity of the RGS7 complexes. *J Cell Biol* **197**, 711-719, doi:10.1083/jcb.201202123 (2012).
165 Orlandi, C., Sutton, L. P., Muntean, B. S., Song, C. & Martemyanov, K. A. Homeostatic cAMP regulation by the RGS7 complex controls depression-related behaviors. *Neuropsychopharmacology* **44**, 642-653, doi:10.1038/s41386-018-0238-y (2019).
166 Ostrovskaya, O. I. *et al.* Inhibitory Signaling to Ion Channels in Hippocampal Neurons Is Differentially Regulated by Alternative Macromolecular Complexes of RGS7. *J Neurosci* **38**, 10002-10015, doi:10.1523/JNEUROSCI.1378-18.2018 (2018).
167 Labouebe, G. *et al.* RGS2 modulates coupling between GABAB receptors and GIRK channels in dopamine neurons of the ventral tegmental area. *Nat Neurosci* **10**, 1559-1568 (2007).
168 Kim, G. *et al.* The GABAB receptor associates with regulators of G-protein signaling 4 protein in the mouse prefrontal cortex and hypothalamus. *BMB reports* **47**, 324-329 (2014).
169 Doupnik, C. A., Davidson, N., Lester, H. A. & Kofuji, P. RGS proteins reconstitute the rapid gating kinetics of gbetagamma-activated inwardly rectifying K+ channels. *Proc Natl Acad Sci U S A* **94**, 10461-10466 (1997).
170 Lur, G. & Higley, M. J. Glutamate Receptor Modulation Is Restricted to Synaptic Microdomains. *Cell reports* **12**, 326-334, doi:10.1016/j.celrep.2015.06.029 (2015).
171 Jeremic, D., Sanchez-Rodriguez, I., Jimenez-Diaz, L. & Navarro-Lopez, J. D. Therapeutic potential of targeting G protein-gated inwardly rectifying potassium (GIRK) channels in the central nervous system. *Pharmacol Ther* **223**, 107808, doi:10.1016/j.pharmthera.2021.107808 (2021).
172 Wydeven, N., Young, D., Mirkovic, K. & Wickman, K. Structural elements in the Girk1 subunit that potentiate G protein-gated potassium channel activity. *Proc Natl Acad Sci U S A* **109**, 21492-21497, doi:10.1073/pnas.1212019110 (2012).
173 Rubinstein, M. *et al.* Divergent regulation of GIRK1 and GIRK2 subunits of the neuronal G protein gated K+ channel by GalphaiGDP and Gbetagamma. *J Physiol* **587**, 3473-3491 (2009).
174 Cruz, H. G. *et al.* Bi-directional effects of GABA(B) receptor agonists on the mesolimbic dopamine system. *Nat Neurosci* **7**, 153-159, doi:10.1038/nn1181 (2004).
175 Ma, D. *et al.* Diverse trafficking patterns due to multiple traffic motifs in G protein-activated inwardly rectifying potassium channels from brain and heart. *Neuron* **33**, 715-729 (2002).
176 Munoz, M. B. & Slesinger, P. A. Sorting nexin 27 regulation of G protein-gated inwardly rectifying K(+) channels attenuates in vivo cocaine response. *Neuron* **82**, 659-669, doi:10.1016/j.neuron.2014.03.011 (2014).
177 Tipps, M. E. & Buck, K. J. GIRK Channels: A Potential Link Between Learning and Addiction. *International review of neurobiology* **123**, 239-277, doi:10.1016/bs.irn.2015.05.012 (2015).
178 Chung, H. J., Qian, X., Ehlers, M., Jan, Y. N. & Jan, L. Y. Neuronal activity regulates phosphorylation-dependent surface delivery of G protein-activated inwardly rectifying potassium channels. *Proc Natl Acad Sci U S A* **106**, 629-634, doi:10.1073/pnas.0811615106 (2009).

179 Huang, C. S. *et al.* Common molecular pathways mediate long-term potentiation of synaptic excitation and slow synaptic inhibition. *Cell* **123**, 105-118 (2005).
180 Arora, D. *et al.* Acute cocaine exposure weakens GABA(B) receptor-dependent G-protein-gated inwardly rectifying K+ signaling in dopamine neurons of the ventral tegmental area. *J Neurosci* **31**, 12251-12257, doi:31/34/12251 [pii] 10.1523/JNEUROSCI.0494-11.2011 (2011).
181 Sharpe, A. L., Varela, E., Bettinger, L. & Beckstead, M. J. Methamphetamine self-administration in mice decreases GIRK channel-mediated currents in midbrain dopamine neurons. *Int J Neuropsychopharmacol*, doi:10.1093/ijnp/pyu073 (2014).
182 Xu, P., Chen, A., Li, Y., Xing, X. & Lu, H. Medial prefrontal cortex in neurological diseases. *Physiol Genomics* **51**, 432-442, doi:10.1152/physiolgenomics.00006.2019 (2019).
183 Woon, E. P., Sequeira, M. K., Barbee, B. R. & Gourley, S. L. Involvement of the rodent prelimbic and medial orbitofrontal cortices in goal-directed action: A brief review. *J Neurosci Res* **98**, 1020-1030, doi:10.1002/jnr.24567 (2020).
184 Sesack, S. R., Deutch, A. Y., Roth, R. H. & Bunney, B. S. Topographical organization of the efferent projections of the medial prefrontal cortex in the rat: an anterograde tract-tracing study with Phaseolus vulgaris leucoagglutinin. *J Comp Neurol* **290**, 213-242, doi:10.1002/cne.902900205 (1989).
185 Sesack, S. R. & Pickel, V. M. Prefrontal cortical efferents in the rat synapse on unlabeled neuronal targets of catecholamine terminals in the nucleus accumbens septi and on dopamine neurons in the ventral tegmental area. *J Comp Neurol* **320**, 145-160, doi:10.1002/cne.903200202 (1992).
186 Steketee, J. D. & Kalivas, P. W. Drug wanting: behavioral sensitization and relapse to drug-seeking behavior. *Pharmacol Rev* **63**, 348-365, doi:pr.109.001933 [pii] 10.1124/pr.109.001933 (2011).
187 Kalivas, P. W. The glutamate homeostasis hypothesis of addiction. *Nat Rev Neurosci* **10**, 561-572, doi:nrn2515 [pii] 10.1038/nrn2515 (2009).
188 Li, Y. *et al.* Both glutamate receptor antagonists and prefrontal cortex lesions prevent induction of cocaine sensitization and associated neuroadaptations. *Synapse* **34**, 169-180 (1999).
189 McFarland, K. & Kalivas, P. W. The circuitry mediating cocaine-induced reinstatement of drug-seeking behavior. *J Neurosci* **21**, 8655-8663, doi:21/21/8655 [pii] (2001).
190 Jo, Y. S., Lee, J. & Mizumori, S. J. Y. Effects of Prefrontal Cortical Inactivation on Neural Activity in the Ventral Tegmental Area. *Journal of Neuroscience* **33**, 8159-8171, doi:10.1523/JNEUROSCI.0118-13.2013 (2013).
191 Peters, J., Kalivas, P. W. & Quirk, G. J. Extinction circuits for fear and addiction overlap in prefrontal cortex. *Learn Mem* **16**, 279-288, doi:16/5/279 [pii] 10.1101/lm.1041309 (2009).
192 Gass, J. T. & Chandler, L. J. The Plasticity of Extinction: Contribution of the Prefrontal Cortex in Treating Addiction through Inhibitory Learning. *Front Psychiatry* **4**, 46, doi:10.3389/fpsyt.2013.00046 (2013).
193 Jasinska, A. J., Chen, B. T., Bonci, A. & Stein, E. A. Dorsal medial prefrontal cortex (MPFC) circuitry in rodent models of cocaine use: implications for drug addiction therapies. *Addict Biol* **20**, 215-226, doi:10.1111/adb.12132 (2015).
194 Moorman, D. E., James, M. H., McGlinchey, E. M. & Aston-Jones, G. Differential roles of medial prefrontal subregions in the regulation of drug seeking. *Brain Res* **1628**, 130-146, doi:10.1016/j.brainres.2014.12.024 (2015).

195 Gourley, S. L. & Taylor, J. R. Going and stopping: Dichotomies in behavioral control by the prefrontal cortex. *Nat Neurosci* **19**, 656-664, doi:10.1038/nn.4275 (2016).
196 Pierce, R. C., Reeder, D. C., Hicks, J., Morgan, Z. R. & Kalivas, P. W. Ibotenic acid lesions of the dorsal prefrontal cortex disrupt the expression of behavioral sensitization to cocaine. *Neuroscience* **82**, 1103-1114, doi:S0306452297003667 [pii] (1998).
197 Tzschentke, T. M. & Schmidt, W. J. The development of cocaine-induced behavioral sensitization is affected by discrete quinolinic acid lesions of the prelimbic medial prefrontal cortex. *Brain Res* **795**, 71-76, doi:10.1016/s0006-8993(98)00254-6 (1998).
198 Tzschentke, T. M. & Schmidt, W. J. Differential effects of discrete subarea-specific lesions of the rat medial prefrontal cortex on amphetamine- and cocaine-induced behavioural sensitization. *Cereb Cortex* **10**, 488-498 (2000).
199 Gilmartin, M. R., Balderston, N. L. & Helmstetter, F. J. Prefrontal cortical regulation of fear learning. *Trends Neurosci* **37**, 455-464, doi:10.1016/j.tins.2014.05.004 (2014).
200 Goldstein, R. Z. & Volkow, N. D. Dysfunction of the prefrontal cortex in addiction: neuroimaging findings and clinical implications. *Nat Rev Neurosci* **12**, 652-669, doi:10.1038/nrn3119 (2011).
201 Fuster, J. M. Unit activity in prefrontal cortex during delayed-response performance: neuronal correlates of transient memory. *J Neurophysiol* **36**, 61-78, doi:10.1152/jn.1973.36.1.61 (1973).
202 Funahashi, S., Bruce, C. J. & Goldman-Rakic, P. S. Mnemonic coding of visual space in the monkey's dorsolateral prefrontal cortex. *J Neurophysiol* **61**, 331-349, doi:10.1152/jn.1989.61.2.331 (1989).
203 Baeg, E. H. *et al.* Fast spiking and regular spiking neural correlates of fear conditioning in the medial prefrontal cortex of the rat. *Cereb Cortex* **11**, 441-451, doi:10.1093/cercor/11.5.441 (2001).
204 Compte, A. *et al.* Temporally irregular mnemonic persistent activity in prefrontal neurons of monkeys during a delayed response task. *J Neurophysiol* **90**, 3441-3454, doi:10.1152/jn.00949.2002 (2003).
205 Han, C. J. *et al.* Trace but not delay fear conditioning requires attention and the anterior cingulate cortex. *Proc Natl Acad Sci U S A* **100**, 13087-13092, doi:10.1073/pnas.2132313100 (2003).
206 Runyan, J. D., Moore, A. N. & Dash, P. K. A role for prefrontal cortex in memory storage for trace fear conditioning. *J Neurosci* **24**, 1288-1295, doi:10.1523/JNEUROSCI.4880-03.2004 (2004).
207 Gilmartin, M. R. & McEchron, M. D. Single neurons in the medial prefrontal cortex of the rat exhibit tonic and phasic coding during trace fear conditioning. *Behav Neurosci* **119**, 1496-1510, doi:10.1037/0735-7044.119.6.1496 (2005).
208 Blum, S., Hebert, A. E. & Dash, P. K. A role for the prefrontal cortex in recall of recent and remote memories. *Neuroreport* **17**, 341-344, doi:10.1097/01.wnr.0000201509.53750.bc (2006).
209 Gilmartin, M. R. & Helmstetter, F. J. Trace and contextual fear conditioning require neural activity and NMDA receptor-dependent transmission in the medial prefrontal cortex. *Learn Mem* **17**, 289-296, doi:10.1101/lm.1597410 (2010).
210 Gilmartin, M. R., Miyawaki, H., Helmstetter, F. J. & Diba, K. Prefrontal activity links nonoverlapping events in memory. *J Neurosci* **33**, 10910-10914, doi:10.1523/JNEUROSCI.0144-13.2013 (2013).

211 Kawaguchi, Y. Groupings of nonpyramidal and pyramidal cells with specific physiological and morphological characteristics in rat frontal cortex. *J Neurophysiol* **69**, 416-431 (1993).
212 Kvitsiani, D. *et al.* Distinct behavioural and network correlates of two interneuron types in prefrontal cortex. *Nature* **498**, 363-366, doi:10.1038/nature12176 (2013).
213 Slaker, M. L. *et al.* Cocaine Exposure Modulates Perineuronal Nets and Synaptic Excitability of Fast-Spiking Interneurons in the Medial Prefrontal Cortex. *eNeuro* **5**, doi:10.1523/ENEURO.0221-18.2018 (2018).
214 Ferguson, B. R. & Gao, W. J. Thalamic Control of Cognition and Social Behavior Via Regulation of Gamma-Aminobutyric Acidergic Signaling and Excitation/Inhibition Balance in the Medial Prefrontal Cortex. *Biol Psychiatry* **83**, 657-669, doi:10.1016/j.biopsych.2017.11.033 (2018).
215 Dong, Y. *et al.* Cocaine-induced plasticity of intrinsic membrane properties in prefrontal cortex pyramidal neurons: adaptations in potassium currents. *J Neurosci* **25**, 936-940, doi:10.1523/jneurosci.4715-04.2005 (2005).
216 Nasif, F. J., Sidiropoulou, K., Hu, X. T. & White, F. J. Repeated cocaine administration increases membrane excitability of pyramidal neurons in the rat medial prefrontal cortex. *J Pharmacol Exp Ther* **312**, 1305-1313, doi:10.1124/jpet.104.075184 (2005).
217 Huang, C. C., Lin, H. J. & Hsu, K. S. Repeated cocaine administration promotes long-term potentiation induction in rat medial prefrontal cortex. *Cereb Cortex* **17**, 1877-1888, doi:10.1093/cercor/bhl096 (2007).
218 Lu, H., Cheng, P. L., Lim, B. K., Khoshnevisrad, N. & Poo, M. M. Elevated BDNF after cocaine withdrawal facilitates LTP in medial prefrontal cortex by suppressing GABA inhibition. *Neuron* **67**, 821-833, doi:10.1016/j.neuron.2010.08.012 (2010).
219 Nasif, F. J., Hu, X. T., Ramirez, O. A. & Perez, M. F. Inhibition of neuronal nitric oxide synthase prevents alterations in medial prefrontal cortex excitability induced by repeated cocaine administration. *Psychopharmacology (Berl)* **218**, 323-330, doi:10.1007/s00213-010-2105-3 (2011).
220 Otis, J. M. *et al.* Prefrontal Neuronal Excitability Maintains Cocaine-Associated Memory During Retrieval. *Frontiers in behavioral neuroscience* **12**, 119, doi:10.3389/fnbeh.2018.00119 (2018).
221 Sepulveda-Orengo, M. T. *et al.* Riluzole Impairs Cocaine Reinstatement and Restores Adaptations in Intrinsic Excitability and GLT-1 Expression. *Neuropsychopharmacology* **43**, 1212-1223, doi:10.1038/npp.2017.244 (2018).
222 Slaker, M. *et al.* Removal of perineuronal nets in the medial prefrontal cortex impairs the acquisition and reconsolidation of a cocaine-induced conditioned place preference memory. *J Neurosci* **35**, 4190-4202, doi:10.1523/jneurosci.3592-14.2015 (2015).
223 Torrecilla, M. *et al.* G-protein-gated potassium channels containing Kir3.2 and Kir3.3 subunits mediate the acute inhibitory effects of opioids on locus ceruleus neurons. *J Neurosci* **22**, 4328-4334 (2002).
224 Bettahi, I., Marker, C. L., Roman, M. I. & Wickman, K. Contribution of the Kir3.1 subunit to the muscarinic-gated atrial potassium channel IKACh. *J Biol Chem* **277**, 48282-48288 (2002).
225 Marron Fernandez de Velasco, E., Carlblom, N., Xia, Z. & Wickman, K. Suppression of inhibitory G protein signaling in forebrain pyramidal neurons triggers plasticity of glutamatergic neurotransmission in the nucleus accumbens

core. *Neuropharmacology* **117**, 33-40, doi:10.1016/j.neuropharm.2017.01.021 (2017).
226 Tamamaki, N. *et al.* Green fluorescent protein expression and colocalization with calretinin, parvalbumin, and somatostatin in the GAD67-GFP knock-in mouse. *J Comp Neurol* **467**, 60-79, doi:10.1002/cne.10905 (2003).
227 Tipps, M., Marron Fernandez de Velasco, E., Schaeffer, A. & Wickman, K. Inhibition of Pyramidal Neurons in the Basal Amygdala Promotes Fear Learning. *eNeuro* **5**, doi:10.1523/ENEURO.0272-18.2018 (2018).
228 Lein, E. S. *et al.* Genome-wide atlas of gene expression in the adult mouse brain. *Nature* **445**, 168-176, doi:10.1038/nature05453 (2007).
229 Schneider, C. A., Rasband, W. S. & Eliceiri, K. W. NIH Image to ImageJ: 25 years of image analysis. *Nature methods* **9**, 671-675, doi:10.1038/nmeth.2089 (2012).
230 Marron Fernandez de Velasco, E. *et al.* Sex differences in GABA(B)R-GIRK signaling in layer 5/6 pyramidal neurons of the mouse prelimbic cortex. *Neuropharmacology* **95**, 353-360, doi:10.1016/j.neuropharm.2015.03.029 (2015).
231 Warthen, D. M. *et al.* Activation of Pyramidal Neurons in Mouse Medial Prefrontal Cortex Enhances Food-Seeking Behavior While Reducing Impulsivity in the Absence of an Effect on Food Intake. *Frontiers in behavioral neuroscience* **10**, 63, doi:10.3389/fnbeh.2016.00063 (2016).
232 Volle, J. *et al.* Enhancing Prefrontal Neuron Activity Enables Associative Learning of Temporally Disparate Events. *Cell reports* **15**, 2400-2410, doi:10.1016/j.celrep.2016.05.021 (2016).
233 Pati, S., Sood, A., Mukhopadhyay, S. & Vaidya, V. A. Acute pharmacogenetic activation of medial prefrontal cortex excitatory neurons regulates anxiety-like behaviour. *J Biosci* **43**, 85-95 (2018).
234 Zhang, T. *et al.* Glutamatergic neurons in the medial prefrontal cortex mediate the formation and retrieval of cocaine-associated memories in mice. *Addict Biol* **25**, e12723, doi:10.1111/adb.12723 (2020).
235 Dimidschstein, J. *et al.* A viral strategy for targeting and manipulating interneurons across vertebrate species. *Nat Neurosci* **19**, 1743-1749, doi:10.1038/nn.4430 (2016).
236 Brinley-Reed, M., Mascagni, F. & McDonald, A. J. Synaptology of prefrontal cortical projections to the basolateral amygdala: an electron microscopic study in the rat. *Neurosci Lett* **202**, 45-48, doi:10.1016/0304-3940(95)12212-5 (1995).
237 Herzig, V. & Schmidt, W. J. Amygdala cannulation alters expression of cocaine conditioned place preference and locomotion in rats. *Addict Biol* **12**, 478-481, doi:10.1111/j.1369-1600.2007.00060.x (2007).
238 Abraham, A. D., Neve, K. A. & Lattal, K. M. Dopamine and extinction: a convergence of theory with fear and reward circuitry. *Neurobiol Learn Mem* **108**, 65-77, doi:10.1016/j.nlm.2013.11.007 (2014).
239 Wendler, E. *et al.* The roles of the nucleus accumbens core, dorsomedial striatum, and dorsolateral striatum in learning: performance and extinction of Pavlovian fear-conditioned responses and instrumental avoidance responses. *Neurobiol Learn Mem* **109**, 27-36, doi:10.1016/j.nlm.2013.11.009 (2014).
240 Kochli, D. E., Thompson, E. C., Fricke, E. A., Postle, A. F. & Quinn, J. J. The amygdala is critical for trace, delay, and contextual fear conditioning. *Learn Mem* **22**, 92-100, doi:10.1101/lm.034918.114 (2015).

241 Runegaard, A. H. *et al.* Modulating Dopamine Signaling and Behavior with Chemogenetics: Concepts, Progress, and Challenges. *Pharmacol Rev* **71**, 123-156, doi:10.1124/pr.117.013995 (2019).
242 Kirry, A. J., Twining, R. C. & Gilmartin, M. R. Prelimbic input to basolateral amygdala facilitates the acquisition of trace cued fear memory under weak training conditions. *Neurobiol Learn Mem* **172**, 107249, doi:10.1016/j.nlm.2020.107249 (2020).
243 Tervo, D. G. *et al.* A Designer AAV Variant Permits Efficient Retrograde Access to Projection Neurons. *Neuron* **92**, 372-382, doi:10.1016/j.neuron.2016.09.021 (2016).
244 Campanac, E. & Hoffman, D. A. Repeated cocaine exposure increases fast-spiking interneuron excitability in the rat medial prefrontal cortex. *J Neurophysiol* **109**, 2781-2792, doi:10.1152/jn.00596.2012 (2013).
245 Steketee, J. D. & Beyer, C. E. Injections of baclofen into the ventral medial prefrontal cortex block the initiation, but not the expression, of cocaine sensitization in rats. *Psychopharmacology (Berl)* **180**, 352-358, doi:10.1007/s00213-005-2149-y (2005).
246 Simon, S. L. *et al.* Cognitive performance of current methamphetamine and cocaine abusers. *J Addict Dis* **21**, 61-74, doi:10.1300/j069v21n01_06 (2002).
247 Lundqvist, T. Cognitive consequences of cannabis use: comparison with abuse of stimulants and heroin with regard to attention, memory and executive functions. *Pharmacol Biochem Behav* **81**, 319-330, doi:10.1016/j.pbb.2005.02.017 (2005).
248 Gould, T. J. Addiction and cognition. *Addict Sci Clin Pract* **5**, 4-14 (2010).
249 Porter, J. N. *et al.* Chronic cocaine self-administration in rhesus monkeys: impact on associative learning, cognitive control, and working memory. *J Neurosci* **31**, 4926-4934, doi:10.1523/JNEUROSCI.5426-10.2011 (2011).
250 Briand, L. A. *et al.* Persistent alterations in cognitive function and prefrontal dopamine D2 receptors following extended, but not limited, access to self-administered cocaine. *Neuropsychopharmacology* **33**, 2969-2980, doi:10.1038/npp.2008.18 (2008).
251 George, O., Mandyam, C. D., Wee, S. & Koob, G. F. Extended access to cocaine self-administration produces long-lasting prefrontal cortex-dependent working memory impairments. *Neuropsychopharmacology* **33**, 2474-2482, doi:10.1038/sj.npp.1301626 (2008).
252 Rizzo, V. *et al.* Encoding of contextual fear memory requires de novo proteins in the prelimbic cortex. *Biol Psychiatry Cogn Neurosci Neuroimaging* **2**, 158-169, doi:10.1016/j.bpsc.2016.10.002 (2017).
253 McIlwain, K. L., Merriweather, M. Y., Yuva-Paylor, L. A. & Paylor, R. The use of behavioral test batteries: effects of training history. *Physiol Behav* **73**, 705-717, doi:10.1016/s0031-9384(01)00528-5 (2001).
254 Enomoto, T., Tse, M. T. & Floresco, S. B. Reducing prefrontal gamma-aminobutyric acid activity induces cognitive, behavioral, and dopaminergic abnormalities that resemble schizophrenia. *Biol Psychiatry* **69**, 432-441, doi:10.1016/j.biopsych.2010.09.038 (2011).
255 Asinof, S. K. & Paine, T. A. Inhibition of GABA synthesis in the prefrontal cortex increases locomotor activity but does not affect attention in the 5-choice serial reaction time task. *Neuropharmacology* **65**, 39-47, doi:10.1016/j.neuropharm.2012.09.009 (2013).

256 Luscher, C., Jan, L. Y., Stoffel, M., Malenka, R. C. & Nicoll, R. A. G protein-coupled inwardly rectifying K+ channels (GIRKs) mediate postsynaptic but not presynaptic transmitter actions in hippocampal neurons. *Neuron* **19**, 687-695 (1997).
257 Smith, K. S., Bucci, D. J., Luikart, B. W. & Mahler, S. V. DREADDS: Use and application in behavioral neuroscience. *Behav Neurosci* **130**, 137-155, doi:10.1037/bne0000135 (2016).
258 Ito, R., Robbins, T. W. & Everitt, B. J. Differential control over cocaine-seeking behavior by nucleus accumbens core and shell. *Nat Neurosci* **7**, 389-397, doi:10.1038/nn1217 (2004).
259 Adhikari, A. *et al.* Basomedial amygdala mediates top-down control of anxiety and fear. *Nature* **527**, 179-185, doi:10.1038/nature15698 (2015).
260 Murugan, M. *et al.* Combined Social and Spatial Coding in a Descending Projection from the Prefrontal Cortex. *Cell* **171**, 1663-1677 e1616, doi:10.1016/j.cell.2017.11.002 (2017).
261 Woods, V. E. & Ettenberg, A. Increased amphetamine-induced locomotion during inactivation of the basolateral amygdala. *Behav Brain Res* **149**, 33-39, doi:10.1016/s0166-4328(03)00212-2 (2004).
262 Degoulet, M. F., Rostain, J. C., David, H. N. & Abraini, J. H. Repeated administration of amphetamine induces a shift of the prefrontal cortex and basolateral amygdala motor function. *Int J Neuropsychopharmacol* **12**, 965-974, doi:10.1017/S1461145709009973 (2009).
263 Runegaard, A. H. *et al.* Locomotor- and Reward-Enhancing Effects of Cocaine Are Differentially Regulated by Chemogenetic Stimulation of Gi-Signaling in Dopaminergic Neurons. *eNeuro* **5**, doi:10.1523/ENEURO.0345-17.2018 (2018).
264 Boekhoudt, L. *et al.* Chemogenetic activation of dopamine neurons in the ventral tegmental area, but not substantia nigra, induces hyperactivity in rats. *Eur Neuropsychopharmacol* **26**, 1784-1793, doi:10.1016/j.euroneuro.2016.09.003 (2016).
265 Mahler, S. V. *et al.* Chemogenetic Manipulations of Ventral Tegmental Area Dopamine Neurons Reveal Multifaceted Roles in Cocaine Abuse. *J Neurosci* **39**, 503-518, doi:10.1523/JNEUROSCI.0537-18.2018 (2019).
266 Jing, M. Y. *et al.* Re-examining the role of ventral tegmental area dopaminergic neurons in motor activity and reinforcement by chemogenetic and optogenetic manipulation in mice. *Metab Brain Dis* **34**, 1421-1430, doi:10.1007/s11011-019-00442-z (2019).
267 Sesack, S. R., Carr, D. B., Omelchenko, N. & Pinto, A. Anatomical substrates for glutamate-dopamine interactions: evidence for specificity of connections and extrasynaptic actions. *Ann N Y Acad Sci* **1003**, 36-52 (2003).
268 Geisler, S. & Wise, R. A. Functional implications of glutamatergic projections to the ventral tegmental area. *Rev Neurosci* **19**, 227-244 (2008).
269 Murase, S., Grenhoff, J., Chouvet, G., Gonon, F. G. & Svensson, T. H. Prefrontal cortex regulates burst firing and transmitter release in rat mesolimbic dopamine neurons studied in vivo. *Neurosci Lett* **157**, 53-56 (1993).
270 Tong, Z. Y., Overton, P. G. & Clark, D. Stimulation of the prefrontal cortex in the rat induces patterns of activity in midbrain dopaminergic neurons which resemble natural burst events. *Synapse* **22**, 195-208, doi:10.1002/(SICI)1098-2396(199603)22:3<195::AID-SYN1>3.0.CO;2-7 (1996).

271 Johnson, S. W., Seutin, V. & North, R. A. Burst firing in dopamine neurons induced by N-methyl-D-aspartate: role of electrogenic sodium pump. *Science* **258**, 665-667 (1992).
272 Chergui, K. *et al.* Tonic activation of NMDA receptors causes spontaneous burst discharge of rat midbrain dopamine neurons in vivo. *Eur J Neurosci* **5**, 137-144 (1993).
273 Taber, M. T. & Fibiger, H. C. Electrical stimulation of the prefrontal cortex increases dopamine release in the nucleus accumbens of the rat: modulation by metabotropic glutamate receptors. *J Neurosci* **15**, 3896-3904 (1995).
274 Karreman, M. & Moghaddam, B. The prefrontal cortex regulates the basal release of dopamine in the limbic striatum: an effect mediated by ventral tegmental area. *J Neurochem* **66**, 589-598 (1996).
275 Beier, K. T. *et al.* Circuit Architecture of VTA Dopamine Neurons Revealed by Systematic Input-Output Mapping. *Cell* **162**, 622-634, doi:10.1016/j.cell.2015.07.015 (2015).
276 Luo, R. *et al.* A dopaminergic switch for fear to safety transitions. *Nature communications* **9**, 2483, doi:10.1038/s41467-018-04784-7 (2018).
277 Kauer, J. A. & Malenka, R. C. Synaptic plasticity and addiction. *Nat Rev Neurosci* **8**, 844-858 (2007).
278 Koob, G. F. & Volkow, N. D. Neurobiology of addiction: a neurocircuitry analysis. *Lancet Psychiatry* **3**, 760-773, doi:10.1016/S2215-0366(16)00104-8 (2016).
279 Rich, M. T. & Torregrossa, M. M. Molecular and synaptic mechanisms regulating drug-associated memories: Towards a bidirectional treatment strategy. *Brain Res Bull* **141**, 58-71, doi:10.1016/j.brainresbull.2017.09.003 (2018).
280 Torregrossa, M. M. & Taylor, J. R. Learning to forget: manipulating extinction and reconsolidation processes to treat addiction. *Psychopharmacology (Berl)* **226**, 659-672, doi:10.1007/s00213-012-2750-9 (2013).
281 Robinson, T. E. & Kolb, B. Structural plasticity associated with exposure to drugs of abuse. *Neuropharmacology* **47 Suppl 1**, 33-46, doi:10.1016/j.neuropharm.2004.06.025 (2004).
282 Muñoz-Cuevas, F. J., Athilingam, J., Piscopo, D. & Wilbrecht, L. Cocaine-induced structural plasticity in frontal cortex correlates with conditioned place preference. *Nat Neurosci* **16**, 1367-1369, doi:10.1038/nn.3498 (2013).
283 Hare, B. D. & Duman, R. S. Prefrontal cortex circuits in depression and anxiety: contribution of discrete neuronal populations and target regions. *Mol Psychiatry* **25**, 2742-2758, doi:10.1038/s41380-020-0685-9 (2020).
284 Riga, D. *et al.* Optogenetic dissection of medial prefrontal cortex circuitry. *Front Syst Neurosci* **8**, 230, doi:10.3389/fnsys.2014.00230 (2014).
285 Visser, E. *et al.* Extinction of Cocaine Memory Depends on a Feed-Forward Inhibition Circuit Within the Medial Prefrontal Cortex. *Biol Psychiatry*, doi:10.1016/j.biopsych.2021.08.008 (2021).
286 Sparta, D. R. *et al.* Activation of prefrontal cortical parvalbumin interneurons facilitates extinction of reward-seeking behavior. *J Neurosci* **34**, 3699-3705, doi:10.1523/jneurosci.0235-13.2014 (2014).
287 Nasif, F. J., Hu, X. T. & White, F. J. Repeated cocaine administration increases voltage-sensitive calcium currents in response to membrane depolarization in medial prefrontal cortex pyramidal neurons. *J Neurosci* **25**, 3674-3679, doi:10.1523/jneurosci.0010-05.2005 (2005).
288 Napier, T. C., Chen, L., Kashanchi, F. & Hu, X. T. Repeated cocaine treatment enhances HIV-1 Tat-induced cortical excitability via over-activation of L-type

calcium channels. *J Neuroimmune Pharmacol* **9**, 354-368, doi:10.1007/s11481-014-9524-6 (2014).
289 Fogaça, M. V. & Duman, R. S. Cortical GABAergic Dysfunction in Stress and Depression: New Insights for Therapeutic Interventions. *Frontiers in cellular neuroscience* **13**, 87, doi:10.3389/fncel.2019.00087 (2019).
290 Perova, Z., Delevich, K. & Li, B. Depression of excitatory synapses onto parvalbumin interneurons in the medial prefrontal cortex in susceptibility to stress. *J Neurosci* **35**, 3201-3206, doi:10.1523/jneurosci.2670-14.2015 (2015).
291 Soumier, A. & Sibille, E. Opposing effects of acute versus chronic blockade of frontal cortex somatostatin-positive inhibitory neurons on behavioral emotionality in mice. *Neuropsychopharmacology* **39**, 2252-2262, doi:10.1038/npp.2014.76 (2014).
292 Miller, C. A. & Marshall, J. F. Altered prelimbic cortex output during cue-elicited drug seeking. *J Neurosci* **24**, 6889-6897, doi:10.1523/jneurosci.1685-04.2004 (2004).
293 Platt, R. J. *et al.* CRISPR-Cas9 knockin mice for genome editing and cancer modeling. *Cell* **159**, 440-455, doi:10.1016/j.cell.2014.09.014 (2014).
294 Marron Fernandez de Velasco, E. *et al.* GIRK2 splice variants and neuronal G protein-gated K+ channels: implications for channel function and behavior. *Scientific reports* **7**, 1639, doi:10.1038/s41598-017-01820-2 (2017).
295 Marron Fernandez de Velasco, E. *et al.* Sex differences in GABA(B)R-GIRK signaling in layer 5/6 pyramidal neurons of the mouse prelimbic cortex. *Neuropharmacology* **95**, 353-360, doi:10.1016/j.neuropharm.2015.03.029 (2015).
296 Anderson, E. M. *et al.* Suppression of pyramidal neuron G protein-gated inwardly rectifying K+ channel signaling impairs prelimbic cortical function and underlies stress-induced deficits in cognitive flexibility in male, but not female, mice. *Neuropsychopharmacology* **46**, 2158-2169, doi:10.1038/s41386-021-01063-w (2021).
297 Doncheck, E. M. *et al.* Estradiol Regulation of the Prelimbic Cortex and the Reinstatement of Cocaine Seeking in Female Rats. *J Neurosci* **41**, 5303-5314, doi:10.1523/jneurosci.3086-20.2021 (2021).
298 Clare, K. *et al.* Cocaine Reduces the Neuronal Population While Upregulating Dopamine D2-Receptor-Expressing Neurons in Brain Reward Regions: Sex-Effects. *Frontiers in pharmacology* **12**, 624127, doi:10.3389/fphar.2021.624127 (2021).
299 Anderson, E. M., Engelhardt, A., Demis, S., Porath, E. & Hearing, M. C. Remifentanil self-administration in mice promotes sex-specific prefrontal cortex dysfunction underlying deficits in cognitive flexibility. *Neuropsychopharmacology* **46**, 1734-1745, doi:10.1038/s41386-021-01028-z (2021).
300 Warden, M. R. *et al.* A prefrontal cortex-brainstem neuronal projection that controls response to behavioural challenge. *Nature* **492**, 428-432, doi:10.1038/nature11617 (2012).
301 Adhikari, A., Topiwala, M. A. & Gordon, J. A. Single units in the medial prefrontal cortex with anxiety-related firing patterns are preferentially influenced by ventral hippocampal activity. *Neuron* **71**, 898-910, doi:10.1016/j.neuron.2011.07.027 (2011).
302 Yang, W. *et al.* Cocaine Withdrawal Reduces Gamma-Aminobutyric Acid-Ergic Transmission and Gephyrin Expression at Medial Prefrontal Cortex in Cocaine-Conditioned Place-Preference Rats, Which Shows Increased Cocaine Seeking. *European addiction research* **23**, 28-36, doi:10.1159/000452657 (2017).

303 Perrine, S. A., Sheikh, I. S., Nwaneshiudu, C. A., Schroeder, J. A. & Unterwald, E. M. Withdrawal from chronic administration of cocaine decreases delta opioid receptor signaling and increases anxiety- and depression-like behaviors in the rat. *Neuropharmacology* **54**, 355-364, doi:10.1016/j.neuropharm.2007.10.007 (2008).
304 Filip, M. *et al.* Alterations in BDNF and trkB mRNAs following acute or sensitizing cocaine treatments and withdrawal. *Brain Res* **1071**, 218-225, doi:10.1016/j.brainres.2005.11.099 (2006).
305 Hall, B. J., Pearson, L. S. & Buccafusco, J. J. Effect of the use-dependent, nicotinic receptor antagonist BTMPS in the forced swim test and elevated plus maze after cocaine discontinuation in rats. *Neurosci Lett* **474**, 84-87, doi:10.1016/j.neulet.2010.03.011 (2010).
306 El Hage, C. *et al.* Enhanced anxiety observed in cocaine withdrawn rats is associated with altered reactivity of the dorsomedial prefrontal cortex. *PloS one* **7**, e43535, doi:10.1371/journal.pone.0043535 (2012).
307 Biselli, T., Lange, S. S., Sablottny, L., Steffen, J. & Walther, A. Optogenetic and chemogenetic insights into the neurocircuitry of depression-like behaviour: A systematic review. *Eur J Neurosci* **53**, 9-38, doi:10.1111/ejn.14603 (2021).
308 Krueger, D. D. *et al.* Prior chronic cocaine exposure in mice induces persistent alterations in cognitive function. *Behav Pharmacol* **20**, 695-704, doi:10.1097/FBP.0b013e328333a2bb (2009).
309 Burke, K. A., Franz, T. M., Gugsa, N. & Schoenbaum, G. Prior cocaine exposure disrupts extinction of fear conditioning. *Learn Mem* **13**, 416-421, doi:10.1101/lm.216206 (2006).
310 Meng, S., Quan, W., Qi, X., Su, Z. & Yang, S. Effect of baclofen on morphine-induced conditioned place preference, extinction, and stress-induced reinstatement in chronically stressed mice. *Psychopharmacology (Berl)* **231**, 27-36, doi:10.1007/s00213-013-3204-8 (2014).
311 Leão, R. M., Cruz, F. C., & Planeta, C. S. Prior exposure to stress delays extinction but does not modify reinstatement of nicotine-induced conditioned place preference. *Psychology & Neuroscience* **3**, 53-57, doi:10.3922/j.psns.2010.1.006 (2010).
312 Czéh, B. *et al.* Long-Term Stress Disrupts the Structural and Functional Integrity of GABAergic Neuronal Networks in the Medial Prefrontal Cortex of Rats. *Frontiers in cellular neuroscience* **12**, 148, doi:10.3389/fncel.2018.00148 (2018).
313 Fenton, G. E. *et al.* Persistent prelimbic cortex activity contributes to enhanced learned fear expression in females. *Learn Mem* **21**, 55-60, doi:10.1101/lm.033514.113 (2014).
314 Baran, S. E., Armstrong, C. E., Niren, D. C. & Conrad, C. D. Prefrontal cortex lesions and sex differences in fear extinction and perseveration. *Learn Mem* **17**, 267-278, doi:10.1101/lm.1778010 (2010).
315 Liu, J. F., Tian, J. & Li, J. X. Modulating reconsolidation and extinction to regulate drug reward memory. *Eur J Neurosci* **50**, 2503-2512, doi:10.1111/ejn.14072 (2019).
316 Laricchiuta, D. *et al.* Optogenetic Stimulation of Prelimbic Pyramidal Neurons Maintains Fear Memories and Modulates Amygdala Pyramidal Neuron Transcriptome. *International journal of molecular sciences* **22**, doi:10.3390/ijms22020810 (2021).

317 Shaban, H. *et al.* Generalization of amygdala LTP and conditioned fear in the absence of presynaptic inhibition. *Nat Neurosci* **9**, 1028-1035, doi:10.1038/nn1732 (2006).
318 Jacobson, L. H., Kelly, P. H., Bettler, B., Kaupmann, K. & Cryan, J. F. GABAB1 receptor isoforms differentially mediate the acquisition and extinction of aversive taste memories. *J Neurosci* **26**, 8800-8803 (2006).
319 Beas, B. S., McQuail, J. A., Ban Uelos, C., Setlow, B. & Bizon, J. L. Prefrontal cortical GABAergic signaling and impaired behavioral flexibility in aged F344 rats. *Neuroscience* **345**, 274-286, doi:10.1016/j.neuroscience.2016.02.014 (2017).
320 Huston, J. P., Silva, M. A., Topic, B. & Müller, C. P. What's conditioned in conditioned place preference? *Trends Pharmacol Sci* **34**, 162-166, doi:10.1016/j.tips.2013.01.004 (2013).
321 McKendrick, G. & Graziane, N. M. Drug-Induced Conditioned Place Preference and Its Practical Use in Substance Use Disorder Research. *Frontiers in behavioral neuroscience* **14**, 582147, doi:10.3389/fnbeh.2020.582147 (2020).
322 Mustroph, M. L., Stobaugh, D. J., Miller, D. S., DeYoung, E. K. & Rhodes, J. S. Wheel running can accelerate or delay extinction of conditioned place preference for cocaine in male C57BL/6J mice, depending on timing of wheel access. *Eur J Neurosci* **34**, 1161-1169, doi:10.1111/j.1460-9568.2011.07828.x (2011).
323 Levar, N., van Leeuwen, J. M. C., Puts, N. A. J., Denys, D. & van Wingen, G. A. GABA Concentrations in the Anterior Cingulate Cortex Are Associated with Fear Network Function and Fear Recovery in Humans. *Frontiers in human neuroscience* **11**, 202, doi:10.3389/fnhum.2017.00202 (2017).
324 Courtin, J. *et al.* Prefrontal parvalbumin interneurons shape neuronal activity to drive fear expression. *Nature* **505**, 92-96, doi:10.1038/nature12755 (2014).
325 Voigt, R. M., Herrold, A. A. & Napier, T. C. Baclofen facilitates the extinction of methamphetamine-induced conditioned place preference in rats. *Behav Neurosci* **125**, 261-267, doi:10.1037/a0022893 (2011).
326 Heinrichs, S. C., Leite-Morris, K. A., Carey, R. J. & Kaplan, G. B. Baclofen enhances extinction of opiate conditioned place preference. *Behav Brain Res* **207**, 353-359, doi:10.1016/j.bbr.2009.10.013 (2010).
327 Lecca, S., Trusel, M. & Mameli, M. Footshock-induced plasticity of GABA(B) signalling in the lateral habenula requires dopamine and glucocorticoid receptors. *Synapse* **71**, doi:10.1002/syn.21948 (2017).
328 Lemos, J. C. *et al.* Repeated stress dysregulates kappa-opioid receptor signaling in the dorsal raphe through a p38alpha MAPK-dependent mechanism. *J Neurosci* **32**, 12325-12336, doi:10.1523/jneurosci.2053-12.2012 (2012).
329 Anderson, G. R., Posokhova, E. & Martemyanov, K. A. The R7 RGS protein family: multi-subunit regulators of neuronal G protein signaling. *Cell Biochem Biophys* **54**, 33-46, doi:10.1007/s12013-009-9052-9 (2009).
330 Gold, S. J., Ni, Y. G., Dohlman, H. G. & Nestler, E. J. Regulators of G-protein signaling (RGS) proteins: region-specific expression of nine subtypes in rat brain. *J Neurosci* **17**, 8024-8037, doi:10.1523/jneurosci.17-20-08024.1997 (1997).
331 Stewart, A. *et al.* Regulator of G protein signaling 6 is a critical mediator of both reward-related behavioral and pathological responses to alcohol. *Proc Natl Acad Sci U S A* **112**, E786-795, doi:10.1073/pnas.1418795112 (2015).
332 Luessen, D. J., Sun, H., McGinnis, M. M., McCool, B. A. & Chen, R. Chronic intermittent ethanol exposure selectively alters the expression of Gα subunit isoforms and RGS subtypes in rat prefrontal cortex. *Brain Res* **1672**, 106-112, doi:10.1016/j.brainres.2017.07.014 (2017).

333 Posokhova, E., Wydeven, N., Allen, K. L., Wickman, K. & Martemyanov, K. A. RGS6/Gβ5 complex accelerates IKACh gating kinetics in atrial myocytes and modulates parasympathetic regulation of heart rate. *Circ Res* **107**, 1350-1354, doi:10.1161/circresaha.110.224212 (2010).
334 Cao, Y. *et al.* Regulators of G protein signaling RGS7 and RGS11 determine the onset of the light response in ON bipolar neurons. *Proc Natl Acad Sci U S A* **109**, 7905-7910, doi:10.1073/pnas.1202332109 (2012).
335 Vo, B. N. *et al.* Bidirectional influence of limbic GIRK channel activation on innate avoidance behavior. *J Neurosci*, doi:10.1523/JNEUROSCI.2787-20.2021 (2021).
336 Wydeven, N. *et al.* Mechanisms underlying the activation of G-protein-gated inwardly rectifying K+ (GIRK) channels by the novel anxiolytic drug, ML297. *Proc Natl Acad Sci U S A* **111**, 10755-10760, doi:10.1073/pnas.1405190111 (2014).
337 Anderson, A. *et al.* GPCR-dependent biasing of GIRK channel signaling dynamics by RGS6 in mouse sinoatrial nodal cells. *Proc Natl Acad Sci U S A* **117**, 14522-14531, doi:10.1073/pnas.2001270117 (2020).
338 Kubota, Y., Karube, F., Nomura, M. & Kawaguchi, Y. The Diversity of Cortical Inhibitory Synapses. *Front Neural Circuits* **10**, 27, doi:10.3389/fncir.2016.00027 (2016).
339 Diehl, M. M. *et al.* Divergent projections of the prelimbic cortex bidirectionally regulate active avoidance. *eLife* **9**, doi:10.7554/eLife.59281 (2020).
340 Wise, R. A. Forebrain substrates of reward and motivation. *The Journal of comparative neurology* **493**, 115-121, doi:10.1002/cne.20689 (2005).
341 Hill, D. F., Parent, K. L., Atcherley, C. W., Cowen, S. L. & Heien, M. L. Differential release of dopamine in the nucleus accumbens evoked by low-versus high-frequency medial prefrontal cortex stimulation. *Brain stimulation* **11**, 426-434, doi:10.1016/j.brs.2017.11.010 (2018).
342 Strafella, A. P., Paus, T., Barrett, J. & Dagher, A. Repetitive transcranial magnetic stimulation of the human prefrontal cortex induces dopamine release in the caudate nucleus. *J Neurosci* **21**, Rc157, doi:10.1523/JNEUROSCI.21-15-j0003.2001 (2001).
343 Porter, J. T. & Sepulveda-Orengo, M. T. Learning-induced intrinsic and synaptic plasticity in the rodent medial prefrontal cortex. *Neurobiol Learn Mem* **169**, 107117, doi:10.1016/j.nlm.2019.107117 (2020).
344 Torregrossa, M. M. & Kalivas, P. W. Microdialysis and the neurochemistry of addiction. *Pharmacology, biochemistry, and behavior* **90**, 261-272, doi:10.1016/j.pbb.2007.09.001 (2008).
345 Marvin, J. S. *et al.* Stability, affinity, and chromatic variants of the glutamate sensor iGluSnFR. *Nature methods* **15**, 936-939, doi:10.1038/s41592-018-0171-3 (2018).
346 Marvin, J. S. *et al.* A genetically encoded fluorescent sensor for in vivo imaging of GABA. *Nature methods* **16**, 763-770, doi:10.1038/s41592-019-0471-2 (2019).
347 Yu, L. *et al.* Activity in projection neurons from prelimbic cortex to the PVT is necessary for retrieval of morphine withdrawal memory. *Cell reports* **35**, 108958, doi:10.1016/j.celrep.2021.108958 (2021).
348 Cruz, A. M., Spencer, H. F., Kim, T. H., Jhou, T. C. & Smith, R. J. Prelimbic cortical projections to rostromedial tegmental nucleus play a suppressive role in cue-induced reinstatement of cocaine seeking. *Neuropsychopharmacology* **46**, 1399-1406, doi:10.1038/s41386-020-00909-z (2021).
349 Marek, R., Xu, L., Sullivan, R. K. P. & Sah, P. Excitatory connections between the prelimbic and infralimbic medial prefrontal cortex show a role for the prelimbic

cortex in fear extinction. *Nat Neurosci* **21**, 654-658, doi:10.1038/s41593-018-0137-x (2018).
350 Trezza, V., Damsteegt, R. & Vanderschuren, L. J. Conditioned place preference induced by social play behavior: parametrics, extinction, reinstatement and disruption by methylphenidate. *Eur Neuropsychopharmacol* **19**, 659-669, doi:10.1016/j.euroneuro.2009.03.006 (2009).
351 Velázquez-Sánchez, C. *et al.* Seeking behavior, place conditioning, and resistance to conditioned suppression of feeding in rats intermittently exposed to palatable food. *Behav Neurosci* **129**, 219-224, doi:10.1037/bne0000042 (2015).
352 Cunningham, C. L., Gremel, C. M. & Groblewski, P. A. Drug-induced conditioned place preference and aversion in mice. *Nature protocols* **1**, 1662-1670, doi:10.1038/nprot.2006.279 (2006).
353 Torres-Castaño, A. *et al.* Transcranial Magnetic Stimulation for the Treatment of Cocaine Addiction: A Systematic Review. *Journal of clinical medicine* **10**, doi:10.3390/jcm10235595 (2021).
354 Zhao, Y. *et al.* Anterior Cingulate Cortex in Addiction: New Insights for Neuromodulation. *Neuromodulation*, doi:10.1111/ner.13291 (2020).
355 Leong, S. L. *et al.* Anterior Cingulate Cortex Implants for Alcohol Addiction: A Feasibility Study. *Neurotherapeutics : the journal of the American Society for Experimental NeuroTherapeutics* **17**, 1287-1299, doi:10.1007/s13311-020-00851-4 (2020).
356 Yu, K., Niu, X., Krook-Magnuson, E. & He, B. Intrinsic functional neuron-type selectivity of transcranial focused ultrasound neuromodulation. *Nature communications* **12**, 2519, doi:10.1038/s41467-021-22743-7 (2021).